RSP-413.9

Final Report

R413.9 Evaluation of Safety Assessment Codes for Used Fuel Disposal Facilities

Canadian Nuclear Safety Commission (CNSC)

Paula Osborne, Ph.D.

December 18, 2015

Acknowledgements

The author would like to acknowledge the significant help supplied by the United States Nuclear Regulatory Commission (US NRC). The US NRC supplied the SOAR model for application to this project at no charge. Also, the US NRC staff, especially Drs. James Rubenstone, Jin-Ping Gwo, and Christopher Markley, who provided valuable time in training and discussion on the general application of SOAR as well as more specific information towards this current project.

The author would also like to express thanks to the CNSC for the opportunity to work on the contract for this project, R413.9 Evaluation of Safety Assessment Codes for Used Fuel Disposal Facilities. Also, to the staff, especially Dr. Shizhong Lei, for the accommodations, understanding and aid provided throughout the duration of this contract.

Abstract

The Fifth Case Study report by the Nuclear Waste Management Organization (NWMO) (2011) documents the post-closure safety assessment of a generic deep geological repository for nuclear fuel wastes in sedimentary rocks. This involves modelling the groundwater flow and transport of radionuclides to predict the total dose to humans over a period of one million years. One dimensional modelling was conducted at the Site Scale using SYVAC3-CC4 which contains a biosphere component.

The author was retained by the Canadian Nuclear Safety Commission to independently model the NWMO's Fifth Case Study dose calculations using the SOAR (Scoping of Options and Analyzing Risk) model, which was developed by the US NRC as a prediction tool in assessing different disposal options of nuclear waste.

This report summarizes the independent modelling work in which the SOAR model was applied to the Reference Case presented in the Fifth Case Study report by the NWMO. The SYVAC3-CC4 model results from NWMO were compared against those obtained from the SOAR model, using both deterministic and probabilistic approaches. The deterministic model results compared well. The sensitivity analysis conducted using both SOAR and SYVAC3-CC4 showed that the total dose rate was most sensitive to the values of the diffusion coefficient. Probabilistic modelling results from SOAR were lower than those generated by SYVAC3-CC4 as a result of differing methods of release from bound waste form and exposure pathways. None of the total dose rates from the SOAR or SYVAC3-CC4 model exceeded the dose acceptance criterion at any time for any of the simulations. For SOAR, the highest maximum total dose rate as predicted by SOAR was more than four orders of magnitude below the acceptance criterion. Overall the results between the two models agreed well providing additional confidence in their use as scoping tools. This report also presents a general review of the licensing status and of the models and codes used internationally for the assessment of deep disposal of nuclear waste.

Table of Contents

List of Figures

List of Tables

1.0 Introduction

Nuclear power plants have been generating electricity in Canada since the first commercial CANDU reactor became operational in Pickering, Ontario in 1971. Nuclear power plants contribute approximately 15% of Canada's electricity production (World Nuclear Association, 2014a). Once removed from the nuclear reactor, the spent fuel rods are highly radioactive and the disposal of this waste needs to be conducted in order to protect people or the environment, now and in the future.

The international consensus is that the high-level waste (HLW) produced from nuclear reactors should be buried underground in deep geological repositories (DGR). Extensive research in numerous countries, such as Sweden, Finland, France and Switzerland, has been conducted to ensure that these DGR facilities will be designed, constructed, operated and maintained in a safe manner.

Internationally, many countries are performing extensive research to select and characterize sites for a DGR and to design and demonstrate the long-term performance of the engineered barriers. Spent nuclear fuel needs to be disposed of within the country it was generated. Therefore, the challenge facing many countries is a proper location of a DGR with satisfactory geological properties as well as other considerations. Many years of research have been conducted including testing, modelling and other analyses. Countries are at different stages in terms of determining a site for the DGR and the stages of achieving licensing (See Section 2).

The Nuclear Waste Management Organization (NWMO) in Canada was formed in 2002 and is responsible for determining methods to manage Canada's nuclear waste generated from electricity production. If not managed properly, the nuclear waste will pose a risk to the public and the environment. The NWMO recommended the Adaptive Phased Management Method (APM) to the government in 2006, and that method was accepted. The APM would ultimately result in a DGR in a site located in either crystalline rocks of the Canadian Shield or in a sedimentary rock formation. The NWMO is currently going through a site selection process among volunteer communities in both types of rocks. At the same time, the NWMO continues with advancing knowledge through a research program and through the conduction of generic safety assessment in both types of rocks.

The NWMO has submitted a report on a generic site for a DGR, known as the Fifth Case Study (NWMO, 2013a and b) to the CNSC for review. The NWMO's Fifth Case Study illustrates a postclosure safety assessment of a hypothetical site with the repository at 500 m depth within sedimentary rock. As part of the NWMO research, numerical modelling was conducted to evaluate groundwater flow, contaminant transport and the dose to humans. As part of the modelling exercise, NWMO examined the hypothetical site at three different scales: Regional Scale; Site Scale; and Repository Scale. The scale of interest for this current project is the Site Scale which the NWMO modelled in both one and three dimensions. The NWMO used a numerical code called SYVAC3-CC4 for the one-dimensional modelling exercise as it considered the groundwater flow and transport as well as calculated the total dose to humans via several different exposure pathways.

The Scoping of Options and Analyzing Risk (SOAR) model was developed by the US Nuclear Regulatory Commission (US NRC) to provide insights into different disposal options of nuclear waste. The SOAR model is coded within the GoldSim environment and uses the contaminant transport module. This contaminant transport module in GoldSim provides different coding elements for modelling movement of contaminants through a prescribed system. SOAR contains a one-dimensional flow and transport code that assumes steady state flow. The user can input the quantity and age of waste at time of disposal, the package properties, modes of package failure and information on the buffer material, geosphere and biosphere. The user can examine results at different stages along the path to the biosphere as well as the ultimate dose. The dose calculated with SOAR only considers ingestion through water and no other exposure pathways.

The purpose of this project is to independently model groundwater flow, contaminant transport and dose calculations presented in the NWMO's Fifth Case Study using SOAR. The objective was to independently assess the one-dimensional modelling of the Site Scale conducted by the NWMO and to consider the applicability of SOAR in evaluating nuclear waste disposal options. The report presents in Section 2 the status at the international stage of deep geological repositories. Section 3 describes the development of the Fifth Case Study within SOAR as well as comparison with the SYVAC3-CC4 model results as presented by NWMO. The total dose predicted by SOAR using deterministic parameters is presented in Section 4. These total dose rates are compared against those predicted by SYVAC3-CC4. The total dose rate predicted with probabilistic modelling is presented in Section 5. These results present the range of possible outcomes. The overall results between SOAR and SYVAC-CC4 are compared.

2.0 International Status of DGR

This section discusses the current status of different countries in terms of DGR research, determination of appropriate sites and where if applicable they are in the stage of licensing.

2.1 Sweden

In Sweden, the organisation in charge of managing nuclear waste is the Swedish Nuclear Fuel and Waste Management Company (SKB). The SKB was established by the nuclear power companies in Sweden to manage and dispose of the nuclear waste (www.skb.se).

Currently, the SKB manages and operates an interim storage facility, CLAB, for spent nuclear fuel near Oskarshamn. A final repository for short-lived radioactive waste is operational in Forsmark. Also, the safe transportation of waste from the power plant to the disposal facilities is carried out using a vessel named M/S Sigrid (www.skb.se).

The final repository for HLW has yet to be built and on-going research has been conducted for over 30 years in this regard. Based on this research it was decided to put spent fuel in copper canisters that are placed in crystalline rock at 500 m depth and embedded in clay. In June, 2009, the final site for the DGR was chosen to be in Forsmark. An application was submitted by SKB to the Swedish Radiation Authority and the Land and Environmental Court in regards to obtaining the required permissions to construct this DGR in Forsmark (www.skb.se). If accepted, the facility would be expected to receive the first waste sometime in the 2030's.

Simultaneously, a second application was submitted to construct an encapsulation plant that would be used to encapsulate the spent nuclear fuel prior to transportation to the DGR. It is forecasted that the DGR will receive approximately 12,000 tonnes of spent nuclear fuel, corresponding to approximately 6000 canisters.

The technical reports prepared as part of the application demonstrates the research and analyses that were conducted and discusses the numerous modelling codes utilized as part of the scientific backing for the DGR (Kärnbränslehantering AB, 2011a, b and c). A summary of the various codes used by SKB in these reports are presented in Table A.1 in Appendix A.

DarcyTools is a groundwater flow and particle tracking model that was developed collaboratively by SKB, MFRDC (Michel Ferry, R&D Consulting) and CFE AB (Computer-aided Fluid Engineering AB). In groundwater flow modelling, two basic approaches can be taken. The first approach is an equivalent continuous-porous media (ECPM) and the second is discrete fracture network (DFN). In the DarcyTools code, both of these methods are combined. First, a fracture network is generated for the geological system and then using the GEOHYCO module within DarcyTools, the DFN is translated into an ECPM (Svensson et al., 2010).

ConnectFlow is a groundwater flow and transport modelling code that considers ECPM, DFN or combined (AMEC, 2012). For the SKB research, three different studies were conducted to model bedrock flow (Kärnbränslehantering, 2011b). The first two studies were conducted using DarcyTools (Svensson and Follin, 2010; Vidstrand et al., 2010) and the third was conducted using ConnectFlow (Joyce et al., 2010).

The biosphere modelling was conducted with several codes, including Ecolego, MIKE SHE and Pandora (Avila et al., 2010). Pandora was developed by Facilia AB and has been used by SKB and Posiva Oy (See Section 2.2 Finland). It is a biosphere modelling code that can be used in assessment of HLW repositories. Pandora has been tested and verified against other similar tools and has been proven to provide reliable solutions (Ekström, 2011). Ecolego is a code to model radionuclide movement in the near-field, geosphere and biosphere. The Ecolego software was used to perform probabilistic simulations, as well as for comparison with the Pandora results. MIKE-SHE was a code used to model radionuclides that reached the surface water (Bosson et al., 2010). COMSOL Multiphysics (COMSOL, 2012) was used for near-field flow modelling inside the repository. PHREEQC was used for aqueous geochemical reactions.

2.2 Finland

In Finland, the regulation of nuclear energy is by the Radiation and Nuclear Safety Authority (STUK). STUK establishes safety requirements and regulates the use of nuclear power plants in Finland (www.stuk.fi).

In 2013, a total of 70.9 TWh of electricity was produced in Finland, of which 23.6 TWh was produced by nuclear power. Currently, there are four operational reactors in Finland and a fifth is currently under construction. Finland's existing reactors are very efficient, of which two are boiling water reactors and are operated by Teollisuuden Voima Oy (TVO). The other two reactors are pressurized water reactors and are operated by Fortum Corporation. The fifth reactor is expected to be operational in 2018 (World Nuclear Association, 2014b).

In Finland, it is the responsibility of the power companies to responsibly manage the resulting waste. Posiva Oy is jointly owned by TVO and Fortum and is responsible for developing management schemes for the disposal of nuclear waste from the four existing reactors. Posiva Oy is in charge of the research and development that is required for determining final disposal options. Posiva Oy and SKB have a five-year cooperation agreement to share research information so that efforts are not duplicated (www.posiva.fi).

Currently, Posiva Oy manages a surface pool storage for spent fuel that has been in operation since 1987 at Olkiluoto. Also at Olkiluoto, an underground repository for low- and intermediate-level waste has been in operation since 1992. For HLW, deep geological disposal in bedrock is the chosen waste management method and is currently under investigation (World Nuclear Association, 2014b).

In 2001, the Parliament of Finland endorsed the principle of a geological repository at the Olkiluoto, Emajoki site (POSIVA, 2013). In 2011, two deep boreholes were drilled at the site, for extensive analysis of geology and Posiva Oy submitted an application for construction of the DGR in late 2012. In 2015, the Finnish Government granted licence to Posiva Oy to commence construction of the final disposal facility for spent nuclear fuel (www.posiva.fi). The site will consist of two components with the first being an encapsulation plant where the spent fuel will be encapsulated in copper canisters that are water-and gas-tight. The second component is the final repository in which the canisters will be disposed at a minimum of 400 m depth in Finnish bedrock. There will be a buffer between the host rock and the canisters and the projected start of disposal is in the early 2020's. This DGR project is the first to be granted licence for construction world-wide.

As part of the research and development to determine the site of the DGR, Posiva Oy conducted numerical modelling to predict possible outcomes due to radionuclide transport (POSIVA, 2012). Several different codes were used in this modelling effort (see Table A.2, Appendix A). ConnectFlow was used to model flow and transport of the Olkiluoto site (POSIVA, 2013). ConnectFlow allowed for variable density, heat transport, radionuclide transport and ECPM, DFN or combined concept. The flow and transport were also modelled using FEFTRA-FEM and this code allows for flow, transport and heat transfer as coupled or separate processes.

GoldSim was used to model the near-field radionuclide movement, as well as for probabilistic analysis with the Monte Carlo technique. MARFA was used to analyze geosphere retention and transport of radionuclides in most deterministic cases. SHYD was used for surface and near-surface hydrogeological modelling. Ecolego was used to model movement of radionuclides in the biosphere. Pandora was used for the landscape model for radionuclide fate and transport modelling (POSIVA, 2012). Geochemical analyses were conducted using PHREEQC.

2.3 France

In France, the management of nuclear waste is conducted by the Agence nationale pour la gestion des déchets radioactifs (Andra). This organization was created in 1979 and was established in the December 1991 Waste Act as the organization in charge of the long-term management of nuclear waste (www.andra.fr).

In France, a very-low-level waste repository is located in the Morvillers in the Aube district. This repository was commissioned in August, 2003, has an overall capacity of 650,000 m^3 and at the end of 2012 had received 227,400 m^3. The repository has waste disposed in vaults within a clay formation and protected by a synthetic membrane. It is planned to have a future clay cover.

Low- and intermediate- level short lived wastes are disposed in a facility located in the La Hague district. This facility is now in the post-closure monitoring phase. As the disposal at this site was not conducted with current quality assurance procedures, the inventory is not well known, and includes some long-lived radionuclides. Therefore, this site will be monitored for 500 years.

In 2007, HLW consisted of 0.2% of France's total volume of radioactive waste, with 94.98% of the total radioactivity (www.andra.fr). Currently, HLW is stored at production sites in La Hague, Marcoule and Cadarache. The HLW is temporarily stored in tanks prior to being calcined into a powder and then incorporated into molten glass. The molten glass mixture is then encapsulated in stainless steel containers (www.andra.fr).

The long-term disposal facility for HLW is currently in the planning/licensing phase. The proposed repository will be located in Bure, to the east of Paris in the Meuse/Haute Marne area (World Nuclear Association, 2013). The Centre Industriel de Stockage Géologique (Cigéo) facility was contracted in 2012 for the development of a storage facility at 500 m depth. The waste will be disposed within the Bure clay formation. The design will be for permanent disposal however French law states that the disposal must be reversible for the first 100 years. If granted licence by the French Nuclear Safety Authority (ASN), Andra plans to begin construction of Cigéo in 2019, with operation commencing in 2025.

As part of the application for licence to ASN, Andra prepared numerous reports illustrating research and analyses for the proposed repository (Andra, 2005). As part of the research, Andra conducted numerical modelling to ascertain and predict the future risk over a one million year period (See Table A.3, Appendix A). For groundwater flow modelling within both ECPM and DFN, ConnectFlow was used. Geoan and Porflow codes were also used to evaluate the flow regime considering ECPM and both are three-dimensional finite difference codes. For additional flow modelling considering DFN, FracMan/MAFIC codes were also applied. FracMan/MAFIC codes have been developed by the Golder Associates' FracMan Technology Group using an advanced DFN simulator.

For modelling the transport of radionuclides using an ECPM approach, PROPER, GoldSim and Porflow were used. For a DFN approach, PROPER, PathPipe and GoldSim were used to predict the radionuclide movement.

2.4 Switzerland

In Switzerland, there are five nuclear reactors producing approximately 40% of the country's electricity (World Nuclear Association, 2015). Zwilag, a company owned by four Swiss nuclear utilities, handles the radioactive waste. Currently, there is an interim storage facility for HLW in Würenlingen.

A national co-operative for disposal of radioactive wastes (Nagra) was established in 1972 by the power plant operators and the federal government (World Nuclear Association, 2015). In 1983, Nagra began the operation of an underground research laboratory in Grimsel for HLW, located in granite. A second underground research facility in a sedimentary rock formation at Mont Terri, has been operated since by a consortium of international partners, that includes NAGRA.

In Switzerland, the Nuclear Energy Law stipulates that the disposal of nuclear waste be in deep geological repositories (Nagra, 2014). Nagra is proposing two types of repositories, the first for

HLW, spent fuel and long-lived intermediate-level waste. The second repository would be for low- and intermediate-level waste.

The procedure to determine a site for these repositories is set forth within the Sectoral Plan for Deep Geological Repositories (SGT). The process is established over three stages. The first stage required Nagra to propose different potential regions based on long-term safety and engineering feasibility (Nagra, 2014). Nagra proposed six different regions at this stage.

The second stage is based on further research to reduce the number of proposed sites to two possibilities. In 2014, Nagra conducted further investigation of the six possible regions and two sites were short-listed in January, 2015 (World Nuclear Association, 2015). The two sites are in Jura Ost and Zurich Nordost.

The third stage of the process will involve further research that will be conducted on these two sites to perform a formal safety-related comparison (Nagra, 2014).

As part of the investigations to determine future risk associated with the repositories, Nagra performed numerical modelling to predict flow and transport of radionuclides (Nagra, 2014). A summary of the codes used is presented in Appendix A, Table A.4. All codes used are in-house that have been produced by Nagra.

The near-field was modelled using VPAC 1.1 (Holocher et al., 2008) and STMAN 5.9 (Robinson, 2013). VPAC 1.1 is a versatile performance assessment code that simulates groundwater flow and radionuclide transport in either two or three dimensions from the waste and one dimension through the engineered barrier. STMAN 5.9 is a family of three codes that models transport from the waste through the engineered barrier.

The geosphere was modelled using PICNIC-TD 1.4 (Robinson and Watson, 2013), which models the transport of radionuclides along a one-dimensional transport path.

For the biosphere model, Swi BAC 1.2 (Walke and Keesmann, 2013) was used to evaluate the distribution of radionuclides and determine the dose. A newly developed code, NC14M v3, was used for the biosphere model in the consideration of C-14 (Nagra, 2013).

3.0 Model Development

The NWMO is responsible for proposing permanent disposal options for Canada's spent nuclear waste. As part of this mandate, the NWMO has conducted several case studies for the safety assessment of hypothetical disposal options. Currently, the NWMO has presented a Fifth Case Study for the safety assessment of the deep geological disposal of Canada's nuclear waste within sedimentary rock (NWMO, 2013a).

3.1 NWMO Fifth Case Study Overview

The Fifth Case Study evaluates the deep geological disposal of nuclear fuel waste. It was assumed that the waste will be placed in a repository at approximately 500 m depth in the Cobourg Formation in the Michigan Basin in Southwestern Ontario. The Cobourg Formation is a massive limestone formation overlain by thick shale units and then thinner limestone and shale units. All units through which the contaminants will travel are assumed to be free of fractures. The scenario assumed that radionuclide release was through undetected defects in the waste package and that it would require 10,000 years for sufficient water to be present to transport radionuclides.

Overlying the units above the repository is a more permeable unit, an aquifer, within the Guelph Formation. Within this aquifer, the NWMO assumed a pumping-well would be installed in the future. The NWMO assumed that the well would be used by a self-sufficient farming family for all their water requirements and would pump at a constant rate of 1307 m^3/yr. This assumption provides a conservative approach in that the family will receive all water from this source.

The hypothetical case study was evaluated at several different scales, including the Regional Scale, Site Scale and Repository Scale by the NWMO. The Regional Scale model was used to examine flow patterns and the effects of total dissolved solids (TDS). The results from this scale were used to establish boundary conditions for the Site Scale. The Site Scale was examined to model movement of contaminants from the repository to the biosphere and to calculate the dose to humans. The Repository Scale was used to investigate the package components and movement of radionuclides out of the package at a closer scale.

The scale of interest for the current report is the Site Scale model which encompasses the entire repository and some of the surrounding geosphere (see Figure 3.1). In NWMO's analysis several different numerical codes were used (NWMO, 2013a, b). For the Site Scale, NWMO used SYVAC3-CC4 and FRAC3DVS-OPG for modelling purposes. SYVAC3-CC4 is a one-dimensional flow and transport code that allows for modelling the package, mode of failure, linear decay chains, movement through the geosphere and a biosphere model to calculate the dose. FRAC3DVS-OPG is a commercially available three-dimensional finite element and finite difference groundwater flow and contaminant transport code that supports both equivalent porous media and dual porosity representations of the geologic media (Therrien et al., 2010).

The model considers variable density flow and can be used to predict movement through the geosphere but does not have a biosphere model to calculate dose.

Figure 3.1 – Site-Scale model for NWMO's Fifth Case Study (NWMO, 2013a)

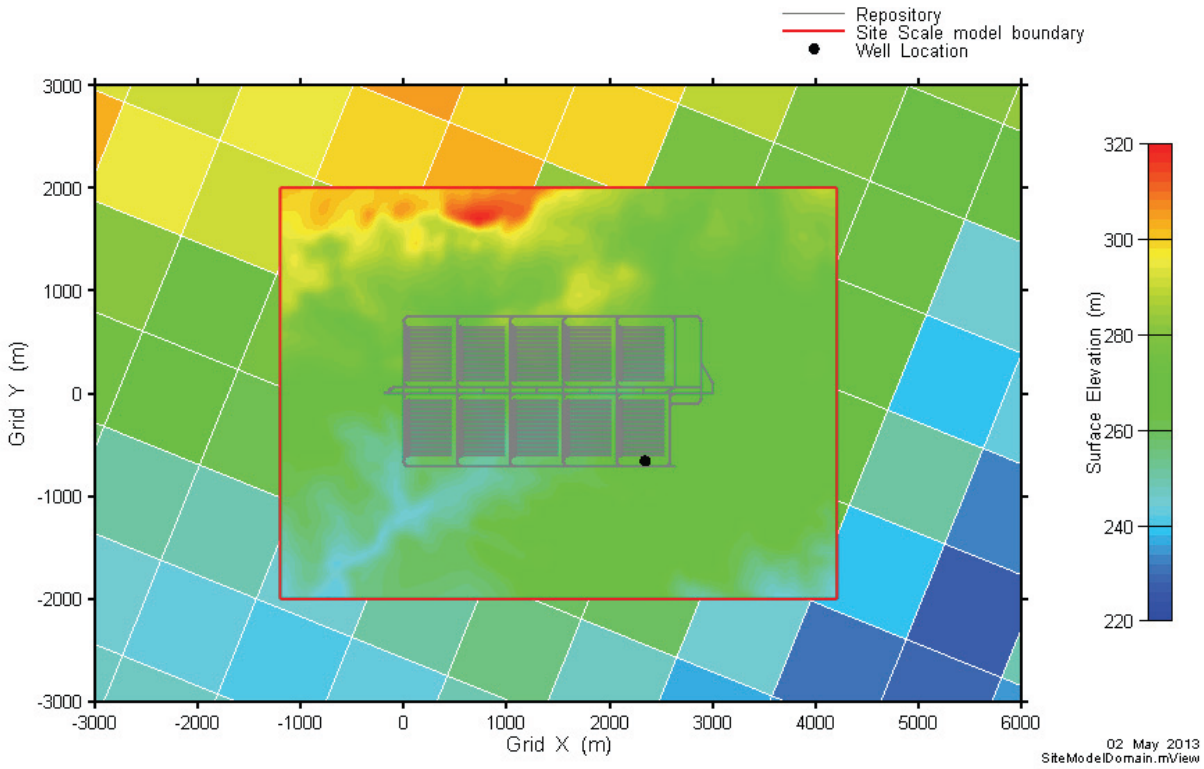

For the Site Scale model, the release of contaminants from the waste packages was modelled using SYVAC3-CC4. This release from the package was then used as a source term for both the three-dimensional modelling using FRAC3DVS and also for the one-dimensional modelling using SYVAC3-CC4. The modelled releases at different points in the geosphere were compared between FRAC3DVS-OPG and SYVAC3-CC4 (NWMO, 2013a). As FRAC3DVS-OPG does not contain biosphere calculations, only the one-dimensional modelling using SYVAC3-CC4 was used to calculate the dose.

The objective of the current project was to independently model the groundwater flow, contaminant transport and dose calculations presented in NWMO's Fifth Case Study using SOAR. SOAR contains a one-dimensional groundwater flow and contaminant transport code and therefore the one-dimensional modelling using SYVAC3-CC4 will be the focus of this discussion.

The SYVAC3-CC4 model diagram that was generated by NWMO to model the Fifth Case Study in one dimension is presented in Appendix B. For the NWMO analysis, the repository was

divided into five waste vaults. The model determined the amount of waste leaving the vaults based on waste package failure and then through the buffer, geosphere and to the biosphere. NWMO considered two separate pathways from the waste vaults to the well. One pathway is through the natural geosphere of limestone and shale units and the other through the backfilled shaft. The times to reach the biosphere and ultimate dose were calculated. On the diagram, there is a lake as the SYVAC3-CC4 code required a second discharge. However, the lake was positioned sufficiently far away to not affect results and can be neglected in the current study.

3.2 SOAR Overview

SOAR is a model that was developed and coded within the GoldSim platform by the US NRC (GoldSim Version 10.50). The purpose of the model is to provide a flexible platform to provide insight into various options for the disposal of nuclear waste. The SOAR model is modular and has five main components: The Waste Form Component; The Waste Package Component; The Near Field Component; The Far Field Component; and The Biosphere Component (see Figure 3.2). The modular format of SOAR allows for changes to one component without affecting others. Outputs from one component are inputted to others as required.

Figure 3.2 – SOAR model configuration (taken from SOAR, 2011)

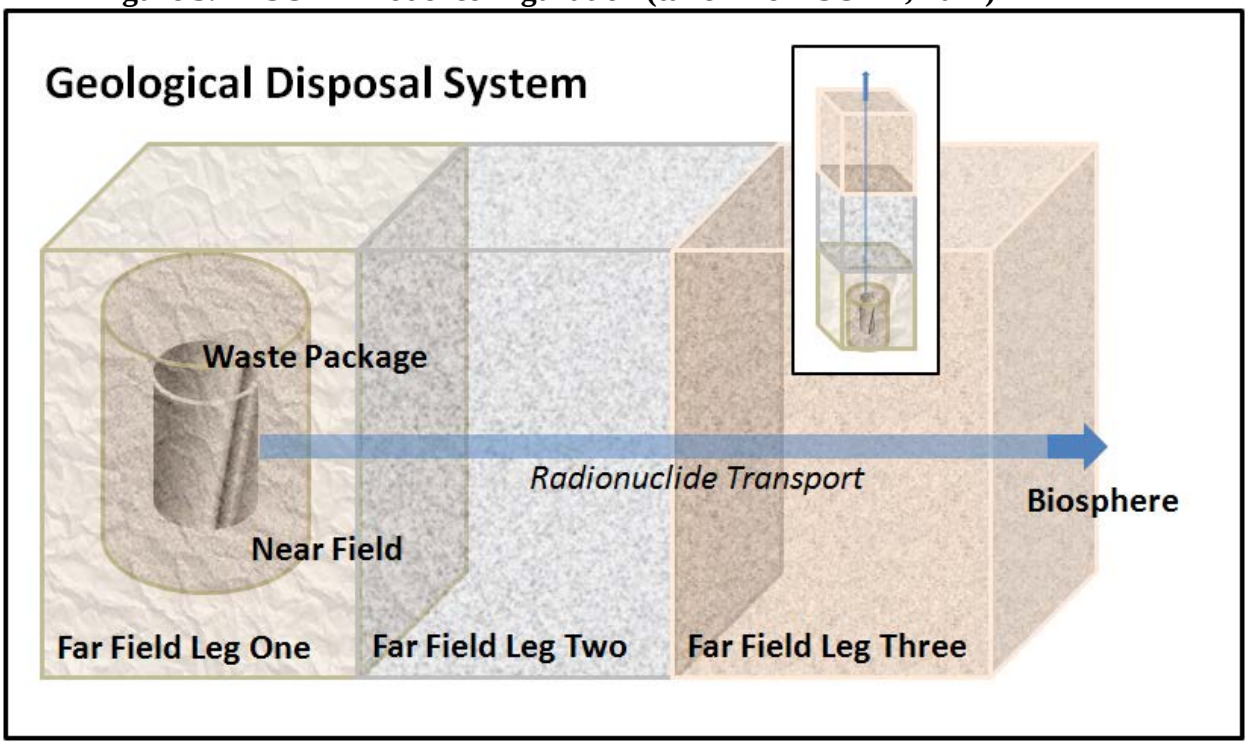

The SOAR model has several limitations in the current version (SOAR, 2011) that is used in this study. A summary of these restrictions as well as how some parameters that were accounted for

differently in SYVAC3-CC4 are presented in Table 3.1. The potential effects of these differences are also presented. Each of these limitations will be further discussed in the appropriate sections.

Table 3.1 – Restriction and differences in application of SOAR

Limitation/Difference	Comment
Waste package configuration not explicitly modelled in SOAR	In the SYVAC3-CC4 model, the repository was divided into 5 waste vaults and had 5 pathways through limestone of Cobourg Formation to a single path through remaining natural geosphere units. In SOAR, the waste package is treated as one unit and one pathway is provided through all geosphere units.
Only ingestion of drinking water considered in dose calculation	SYVAC3-CC4 considered multiple exposure pathways. Therefore, dose calculation in SOAR could possibly be underestimated.
SOAR only considers 16 radionuclides	NWMO considered 37 radionuclides, and 14 of those are considered in SOAR. As will be discussed further in this report, I-129 (which is accounted for in SOAR) is the dominant contributor to total dose for the Reference Case. Exclusion of other radionuclides does not affect the total dose significantly.
Method of defining waste form degradation from bound waste in SOAR	NWMO used a dissolution model in SYVAC3-CC4 that was defined by numerous parameters, of which eight were defined by a PDF. SOAR is modelled within GoldSim and uses a coding element called a “Source Property” to account for the release of bound and unbound inventories. Within this element, GoldSim allows for the bound inventory to be released according to “Lifetime”, “Degradation Rate” or “Congruent dissolution” settings. The congruent dissolution setting within GoldSim is different than that used in SYVAC3-CC4. SOAR utilizes the lifetime setting equal to 1/degradation rate. The degradation rates were calculated from the dissolution model. For further explanation please refer to Section 3.4.1.3.

The original version of the SOAR model from US NRC was obtained for this current project. The original version is linked to a Microsoft Access database containing typical values of the parameters required by the SOAR model. The model also has different dashboards in which general information can be inputted by the user. There are three different levels by which SOAR can be used. The first level is changing values on the various dashboards, running the model and viewing the results using the free GoldSim player. The second level is by altering parameters

within the database and linking to the model to run and view results. The third level of using SOAR is by making alterations, additions or deletions of model elements within the code itself. The second and third levels both require the purchase of GoldSim Pro.

For this project, the third level of SOAR was applied in order to model the NWMO's Fifth Case Study. In the original version of SOAR, many parameters were inputted to the model through a Microsoft Access database called fpa-soar.mdb. Changing values of the parameter within the database was possible and then could be uploaded to the SOAR model. However, changing the probability distribution type proved more difficult and through discussion with US NRC, it was decided to change the parameters required for the NWMO's Fifth Case Study directly within the code rather than through the database.

Changes were also made to the code in terms of how parameters were assigned in different portions of the model. These changes will be discussed in the appropriate sections and it should be noted that any changes made to the code do not affect how the code itself functions. The changes are in how several parameters are assigned and the addition of a few parameters as will be discussed.

3.3 Governing Equations used in SOAR and SYVAC3-CC4

The SOAR and SYVAC3-CC4 models are both one-dimensional models that assume steady state flow. The SOAR model was developed in a coding environment called GoldSim. GoldSim is a Monte Carlo simulation software that can be used for dynamically modelling of various business, engineering and science problems. GoldSim has numerous elements contained within the software that are used to code the problem in question. An add-on Contaminant Transport module is available and was used by the US NRC in creating the SOAR model. This Contaminant Transport module makes it possible to model mass transport processes within engineered and/or natural systems. The elements within this module make it possible to have a source that releases mass over time, and mass movement through the defined system based on hydrogeological properties. The governing equations of both the SYVAC3-CC4 and SOAR models are presented in Table 3.2. The initial condition used for both models is that the concentration of nuclides was set to zero.

A further description of the GoldSim elements used within SOAR with equations is presented in the following sections. For a more detailed description of all equations used by GoldSim in the different components used within the SOAR model see the GoldSim Contaminant Transport Module User's Guide, Appendix B (GoldSim Technology Group, 2014) available on the GoldSim website (www.goldsim.com).

Table 3.2 – Model governing equations

	SYVAC3-CC4	SOAR
Source Term	Uses instant and bound form releases with solubility limits and information on water volume to calculate radionuclide concentration that are released to buffer.	Uses a GoldSim element called a "Source". This element defines information on sources and based on the properties GoldSim calculates rates of release of mass from source(s) to specified pathways. Mass transport controlled by partitioning, solubility constraints and mass transfer. See Section 3.3.2.1 for more information.
Near Field (or Buffer)	Calculated with response function approach. Concentration is obtained from source term.	Represented by a series of GoldSim "Cell pathways" which is essentially a finite difference representation of the diffusion equation. The concentration from the Source element is the boundary condition for the first Cell pathway in the series. See Section 3.3.2.2 for more information on Cell pathways.
Far Field (or Geosphere)	Transport in each segment calculated using 1D advection-diffusion equation using semi-analytical equations. Advection is neglected as the hydraulic conductivity is low.	Represented by a series of GoldSim "Pipe pathways". See Section 3.3.2.3 for more information. The release from the Near Field is the boundary condition at the entrance of the first pipe. The mass then travels along the remaining pipes through mass flux link. The mass exiting the final Pipe pathways in the series is used in the Biosphere model calculations.
Biosphere	The well is defined as an analytical solution to provide drawdown and capture envelope. Assumes a constant head boundary condition at discharge end of a non-leaky aquifer.	Uses equations presented in Section 4.1 of this report using the mass of contaminants released from the final Far Field Pipe Pathways.

3.3.1 SYVAC3-CC4

The subsequent sections present a small portion of the equations and numerical methods used within the SYVAC3-CC4 model. The reader is referred to NWMO, 2012 for a more detailed presentation of the governing equations and methodologies used in SYVAC3-CC4.

3.3.1.1 Transport through buffer

To model the transport of contaminants through the buffer material, SYVAC3-CC4 applies a response function approach for transport of a decay chain member nuclide i.

$$F_j(t) = \sum_j \int_0^t J_j(t) \cdot G_{ij}(t-\tau)d\tau \qquad \textbf{3.1}$$

The input flow rate $J_j(t)$ is the flow rate of precursor nuclide j out of container defect $F_j^{out}(t)$ from the source. The response functions were derived from a Boundary Integral Model for mass transport developed for case of point defect in a container.

The advection-dispersion mass balance equation for a single decaying nuclide in a cylindrically symmetric system that was used in SYVAC3-CC4 is as follows:

$$\frac{\partial C}{\partial t} - \frac{D_r}{K}\frac{\partial^2 C}{\partial r^2} - \frac{D_r}{Kr}\frac{\partial C}{\partial r} - \frac{D_z}{K}\frac{\partial^2 C}{\partial z^2} + \frac{V_z}{K}\frac{\partial C}{\partial z} + \frac{\emptyset}{Kr}\frac{\partial C}{\partial r} + \lambda C = 0 \qquad \textbf{3.2}$$

Where:

V_z = Axial Darcy velocity

ϕ = product of radial Darcy velocity and radius

C = concentration in pore water

D_r = radial intrinsic dispersion coefficient

D_z = axial intrinsic dispersion coefficient

K = capacity factor

λ = decay constant

The boundary conditions at the end of the rooms are that contaminant flux is proportional to the axial Darcy velocity of groundwater.

3.3.1.2 Transport through Geosphere

Within the SYVAC3-CC4 model the transport through the geosphere units was defined using the following one-dimensional mass balance partial differential equation for a decay chain of length n.

$$R_q \frac{\partial C_q}{\partial t} = D\frac{\partial^2 C_q}{\partial^2 \zeta^2} - U\frac{\partial C_q}{\partial \zeta} - R_q\lambda_q C_q + R_{q-1}\lambda_{q-1}C_{q-1} for\ q = 1.n \qquad \textbf{3.3}$$

Where:

U = average linear groundwater flow velocity [m/yr]

D = dispersion coefficient [m^2/yr]

R_q = retardation factor for nuclide q[]

λ_q = radioactive decay constant for nuclide q [1/yr]

C_q = concentration in groundwater of nuclide q [mol/m^3]

t = time

ζ = linear spatial coordinate

The term on the left hand side accounts for sorption to the rock matrix and the terms on the right hand side represent diffusive transport, advective transport, radioactive decayof nuclide q and ingrowth of nuclide q from decay of its precursor nuclide q-1.

The expression of contaminant flow rate out of a transport segment in response to an impulse input of contaminant into a segment is called a response function. Analytical solutions are available and for the NWMO's Fifth Case Study, the case assuming a semi-infinite domain with impulse source was used.

3.3.2 GoldSim and SOAR

The following is a general description of the equations and numerical methods used within GoldSim Source, Cell Pathways and Pipe Pathways that were used within the coding of the SOAR model.

3.3.2.1 Sources in GoldSim

Within the SOAR model, a Source element was used to define the time and quantity for release of contaminants from the repository. A Source is an element within GoldSim that can be used to define contaminants that have barriers, different inventories of contaminants and contaminants that break down or degrade over time. The Source element calculates the concentration of the different contaminants and is used as a boundary condition to the first Cell Pathway representing the transport through the buffer material. Within the Source element it is possible to provide information on how and when a barrier fails, the inventory, the waste matrix, mass transfer and connection to a pathway network.

3.3.2.2 Cell Pathways in GoldSim

Cell pathways were used in SOAR to represent the transport through the buffer material from the interior of the package to the geosphere or Far Field. This section of buffer material was defined by a series of connecting Cells. The basic mass balance equation for Cell Pathway i is as follows:

$$m'_{is} = -m_{is}\lambda_s + \sum_{p=1}^{NP_s} m_{ip}\lambda_p f_{ps} R_{sp}\left(\frac{A_s}{A_p}\right) + \sum_{c=1}^{NF_i} f_{cs} + S_{is} \qquad \textbf{3.4}$$

Where:

m'_{is} = rate of increase of mass of species s in Cell i [M/T];
m_{is} = mass of species s in Cell i [M];
λ_s = decay rate for species s [T^{-1}]
NP_s = number of direct parents for species s;
f_{ps} = fraction of parent p which decays into species s;
R_{sp} = stoichiometric ratio of moles of species s produced per mole of species p decayed;
A_s = molecular (or atomic) weight of species s [M/mol]
A_p = molecular (or atomic) weight of species p [M/mol]
NF_i = number of mass flux links from/to Cell i;
f_{cs} = influx rate of species s (into cell i) through mass flux link c [M/T]; and
S_{is} = rate of direct input of species s to Cell i from "external" sources [M/T].

Looking at the terms on the right hand side, the first term represents decay, the second represents ingrowth, the third term represents mass transfer in or out of cell and fourth represents direct input from other sources. There are numerous equations defining different components of this equation such as advective mass flux link and precipitate removal mass flux link amongst others. The reader is referred to GoldSim Contaminant Transport Module User's Guide, Appendix B (GoldSim Technology Group, 2014) available on the GoldSim website (www.goldsim.com) for further explanation of these equations.

For the NWMO's Fifth Case Study, the transport is diffusion dominated and as such the equation/rationale for this mass flux link as used within GoldSim will be presented here. The diffusive mass flux is governed by a concentration gradient.

$$DiffusiveMassRate = (DiffusiveConductance) \times (ConcentrationDifference) \qquad \textbf{3.5}$$

If it is assumed that the contaminants are diffusing through a single fluid, then the Diffusive Conductance term (D) can be calculated using the following equation:

$$D = (A\ d\ t\ n\ r)/L \qquad \textbf{3.6}$$

Where:

A = mean cross-sectional are of the connection [L^2]
D = Diffusivity Conductance [L^3/T]
d = diffusivity in the fluid [L^2/T]
n = porosity of the porous medium
t = tortuosity of the porous medium
r = reduction factor that varies with saturation (1 if saturated)
L = diffusive length [L]

The diffusive flux, f_s, from pathway i to pathway j is computed using the following equation:

$$f_{s,i\to j} = D_s\left(c_{ims} - \frac{c_{jns}}{K_{nms}}\right) + \sum_{t=1}^{NPT_{im}} PF_t \cdot D_t\left(c_{its} \cdot cp_{imt} - c_{jts} \cdot cp_{jnt}\right) \qquad \textbf{3.7}$$

Where:

D_s = diffusive conductance for species s in the mass flux link [L^3/T]
c_{ims} = the dissolved concentration of species s in medium m within Cell i [M/L^3]
c_{jns} = the dissolved concentration of species s in medium n within Cell j [M/L^3]
K_{nms} = partition coefficient between fluid medium n (in Cell j) and fluid medium m (in Cell i) for species s [L^3 medium m/L^3 medium n]
NPT_{im} = the number of particulate solid media in fluid m within Cell i
PF_t = Boolean flag (0 or 1) which indicates whether diffusion of solid t suspended in the fluid is allowed for the mass flux link
D_t = diffusive conductance for particulate t in the mass flux link [L^3/T]
c_{its} = the sorbed concentration of species s associated with solid t within Cell i [M/M]
cp_{imt} = the concentration of solid particulate t within fluid m in Cell i [M/L^3]
c_{jts} = the sorbed concentration of species s associated with solid t within Cell j [M/M]
cp_{jnt} = concentration of solid particulate t within fluid n in Cell j [M/L^3]

The first term in the equation accounts for diffusion of the dissolved species and the second term accounts for diffusion of particulates suspended in the fluid. From the above equations, a matrix equation was developed to solve the equations numerically using a backward difference approach. GoldSim used a customized version of the Iterative Methods Library IML++, version 1.2a, available from the National Institute of Standards web site http://math.nist.gov/iml++/.

For a more detailed explanation the numerous equations and numerical procedures used in GoldSim for the Cell Pathway element please refer to the GoldSim Contaminant Transport Module User's Guide, Appendix B (GoldSim Technology Group, 2014).

3.3.2.3 Pipe Pathways in GoldSim

The Pipe Pathway element is used within SOAR to represent the transport through the Far Field or geosphere. The objective within a Pipe Pathway in GoldSim is to compute the flux of each contaminant leaving the pathway over time, calculated using the following equation.

$$Flux_s = Q \cdot SV_s \cdot c_{m,s} - (A_m D_s + \alpha \cdot Q \cdot SV_s) \frac{\delta c_{m,s}}{\delta x}\Big|_{x=L} \quad \textbf{3.8}$$

Where:

$Flux_s$ = flux of species s leaving the pathway [M/T]
Q = volumetric flow rate of fluid in the pathway [L^3/T]
SV_s = suspended solid velocity magnification factor for species s
$c_{m,s}$ = mean mobile concentration of species s in available fraction of saturated pore space in mobile zone of pathway [M/L^3]
A_m = cross-sectional area of the mobile zone [L^2]
D_s = effective diffusivity of species s in the mobile zone = $n_{m,s} \cdot t_m \cdot d_{m,r} \cdot d_{m,s}$
$n_{m,s}$ = available porosity of the porous medium in the mobile zone for species s
t_m = tortuosity of the infill material
$d_{m,r}$ = reference diffusivity for the reference fluid
$d_{m,s}$ = relative diffusivity for species s in the reference fluid
α = dispersivity of the pathway [L]
L = length of the pathway [L]
x = distance into the pathway [L]

The governing equation of the concentration within the mobile zone of the pipe is defined through the following equation, which is an expanded version of the one-dimensional advection-dispersion equation.

$$\frac{\delta c_{m,s}}{\delta t} = -\left[\left(\frac{Q \cdot SV_s}{n_{m,s} \cdot A_m \cdot R_{m,s}}\right)\frac{\partial c_{m,s}}{\partial x} - \left(\frac{A_m \cdot D_s + \alpha \cdot Q \cdot SV_s}{n_{m,s} \cdot A_m \cdot R_{m,s}}\right)\frac{\partial^2 c_{m,s}}{\partial x^2}\right] + \left[-c_{m,s}\lambda_s + \sum_{p=1}^{NP_s} c_{m,p} \cdot \lambda_p \cdot f_{ps} \cdot S_{ps}\left(\frac{AW_s}{AW_p}\right)\left(\frac{R_{m,p}}{R_{m,s}}\right)\left(\frac{n_{m,p}SF_p}{n_{m,s}SF_s}\right)\right] - \left[\frac{F_{st,s}}{n_{m,s}A_m R_{m,s}}\right] \quad \textbf{3.9}$$

Where:

A_m = cross-sectional are of the mobile zone [L^2]
$R_{m,s}$ = retardation factor for species s in the mobile zone

$R_{m,p}$ = retardation factor for parent species p in the mobile zone
λ_s = decay rate for species s [T^{-1}]
λ_p = decay rate for parent species p [T^{-1}]
f_{ps} = fraction of parent p which decays into species s
NP_s = number of direct parents of species s
S_{ps} = stoichiometric ratio of moles of species s produced per mole of species p which decays
AW_s = molecular (or atomic) weight of species s [M/mole]
AW_p = molecular (or atomic) weight of parent species p [M/mole]
$n_{m,p}$ = available porosity of the porous medium in the mobile zone for species p
$n_{m,s}$ = available porosity of the porous medium in the mobile zone for species s
$c_{m,p}$ = dissolved concentration of parent species p in mobile zone of pathway [M/L^3]
$F_{st,s}$ = flux of species s from the mobile zone to storage zones per unit length of pathway [M/T/L]
SF_p = Suspended solid storage factor for species p
SF_s = Suspended solid storage factor for species s

For the above advection-dispersion equation, the first term on the right-hand side represents the rate of change due to advective and dispersive fluxes, the second term represents rate of change due to decay and ingrowth, the third term represents changes due to exchanges with storage zones. The boundary conditions for this equation are:

- $c_{m,s} \rightarrow 0$ as $x \rightarrow \infty$
- at x = 0, a flux boundary condition is applied such that:

$$Q \cdot SV_s c_{m,s} - (A_m D_s + \alpha \cdot Q \cdot SV_s) \left.\frac{\partial c_{m,s}}{\partial x}\right|_{x=0} = \delta(t) M_{init,s} + F_{bc,s} + F_{paths,s}$$

Where:

$M_{init,s}$ = user-specified initial mass of species s applied to the pathway [M]

$F_{bc,s}$ = user-specified boundary flux for species s [M/T]

$F_{paths,s}$ = flux of species s into pathway from other GoldSim pathways [M/T]

$\delta(t)$ = the Dirac delta function [T^{-1}]

For use in the SOAR model, the mass exiting the final Cell Pathway representing the transport through the buffer material is inputted as the boundary condition to the first leg of the Far Field. The method by which GoldSim solves the resulting set of Pipe Pathway equations is by using Laplace transforms. For a more detailed discussion and further equation for each parameter in the Pipe Pathway representation, please refer to the GoldSim Contaminant Transport Module User's Guide, Appendix B (GoldSim Technology Group, 2014).

3.4 Model Creation in SOAR

The following sections discuss the development of the NWMO's Fifth Case Study within SOAR. The model creation description is divided into the different components of SOAR.

3.4.1 Waste Form Component

In SOAR, the Waste Form Component requires information related to the type and amount of waste being disposed, so that initial inventories can be determined. The initial inventory is then divided into both bound and unbound inventories. The unbound inventory is the amount of radionuclides that will be released instantaneously once the waste comes in contact with water. The bound inventory is the remaining radionuclides that are bound to the solid matrix and will release slowly over time according to congruent dissolution, which SOAR defines through a degradation rate.

3.4.1.1 Inventory

The used fuel waste form that the NWMO used for the Fifth Case Study is an irradiated natural-uranium UO_2 CANDU fuel bundle (NWMO, 2013b). The NWMO assumed that the standard 37-element (Bruce) fuel bundle should be used to determine inventories as it is the most abundant, and that the fuel age at placement in the repository is 30 years. For the repository, the design is for 4.6×10^6 bundles, located in waste packages that will hold approximately 360 bundles. Table 3.3 summarizes the general information in regards to the waste form.

Table 3.3 – Used Fuel Parameters

Parameter	Value
Number of bundles	4.6×10^6
Mass U/bundle	19.25 kg
Number of bundles/package	360
Number of packages	12,778
Fuel age at placement	30 years
Total U initial	8.86×10^7 kg

Within the Waste Component of SOAR, four types of waste can be inputted: spent nuclear fuel (SNF), spent mixed-oxide (sMOX), high-level waste glass (HLWg) and/or high-level waste

ceramic (HLWc). Through discussion with developers of SOAR at US NRC, it was decided that for this project the waste should be inputted through the sMOX inputs as these inputs are the most appropriate for the waste type being considered in this case.

In the NWMO's assessment, a screening analysis was conducted to determine which radionuclides are of concern. Short-lived radionuclides, for example, were screened out. A final list of 38 elements was used for analysis by the NWMO as follows:

C-14	**Tc-99**	**Pu-242**	**U-236**	*Th-232*	*Ac-225*
I-129	*Am-241*	*Pb-210*	**U-238**	*Th-234*	*Ac-227*
Cl-36	**Np-237**	*Bi-210*	*Th-227*	*Ra-223*	*Rn-222*
Cs-135	*Pa-231*	*Po-210*	*Th-228*	*Ra-224*	
Pd-107	*Pa-233*	**U-233**	*Th-229*	*Ra-225*	
Se-79	**Pu-239**	**U-234**	*Th-230*	*Ra-226*	
Sm-147	**Pu-240**	**U-235**	*Th-231*	*Ra-228*	

Note: Those elements in bold are considered by SOAR and those italics are not.

SOAR as previously discussed only considers 16 radionuclides (14 of which are used in NWMO analysis). Table 3.4 provides the inventory of the 16 radionuclides considered by SOAR, and their respective half-lives as presented by NWMO (2013b). The NWMO presented the inventory in terms of moles/kg U initial however SOAR requires the inventory in terms of mass. Therefore, the SOAR code was modified so that the inventory was inputted using the data in Table 3.4 and then appropriate calculations were conducted within the SOAR model to obtain the initial inventory in grams.

3.4.1.2 Instant Release Fractions

Radionuclides are released from the waste form in two ways: instant release; and waste-form degradation. The instant release fraction is that portion which is rapidly released once in contact with water. The instant release fractions for the elements considered in SOAR are presented in Table 3.5 and were taken from NWMO (2013b). The instant release fractions were inputted directly into the code and for the results in this section a deterministic value of the mean is used. The probability density function (PDF) was inputted for the subsequent probabilistic simulations.

The instant release fraction is multiplied by the initial inventory in SOAR to determine the amount of radionuclides released once the package fails and the waste comes in contact with water, known as the unbound inventory in SOAR. The remaining mass is contained in the bound inventory. The initial bound and unbound inventories as calculated by SOAR using deterministic values of the instant release are presented in Table 3.6.

Table 3.4 – Inventories of radionuclides used in SOAR

Radionuclide	Half-life [yr]	Inventory [moles/kg U Initial]	Initial Inventory [g]
C-14	5.700×10^{3}	5.60×10^{-6}	6.94×10^{3}
Cs-135	2.300×10^{6}	2.675×10^{-4}	3.20×10^{6}
I-129	1.570×10^{7}	4.228×10^{-4}	4.83×10^{6}
Np-237	2.144×10^{6}	1.708×10^{-4}	3.58×10^{6}
Pu-238	-	-	-
Pu-239	2.411×10^{4}	1.123×10^{-2}	2.38×10^{8}
Pu-240	6.561×10^{3}	5.339×10^{-3}	1.13×10^{8}
Pu-242	3.735×10^{5}	4.257×10^{-4}	9.12×10^{6}
Se-79	2.950×10^{5}	1.762×10^{-5}	1.23×10^{5}
Tc-99	2.111×10^{5}	2.409×10^{-3}	2.11×10^{7}
U-232	-	-	-
U-233	1.592×10^{5}	3.608×10^{-5}	7.44×10^{5}
U-234	2.455×10^{5}	2.089×10^{-4}	4.33×10^{6}
U-235	7.038×10^{8}	7.238×10^{-3}	1.51×10^{8}
U-236	2.342×10^{7}	3.501×10^{-3}	7.32×10^{7}
U-238	4.468×10^{9}	4.125	8.69×10^{10}

Note: ´-` represents those radionuclides not considered in NWMO analysis

Table 3.5 – Instant Release Fractions

Radionuclide	PDF Type	PDF Attributes (mean, st. dev.)	PDF Bounds
C	Normal	(0.027, 0.016)	0.0005, 0.075
Cs	Normal	(0.04, 0.01)	0.015, 0.20
I	Normal	(0.04, 0.01)	0.015, 0.20
Np	Constant	0	
Pu	Constant	0	
Se	Normal	(0.006, 0.0015)	0.0023, 0.03
Tc	Lognormal	(0.01, 2)	0.0005, 0.05
U	Constant	0	

Table 3.6 – Initial bound and unbound inventory

Element	Unbound inventory [g]	Bound inventory [g]
C-14	1.87×10^{2}	6.75×10^{3}
Cs-135	1.28×10^{5}	3.07×10^{6}
I-129	1.93×10^{5}	4.64×10^{6}
Np-237	0	3.58×10^{6}
Pu-239	0	2.38×10^{8}
Pu-240	0	1.13×10^{8}
Pu-242	0	9.12×10^{6}
Se-79	7.40×10^{2}	1.23×10^{5}
Tc-99	2.11×10^{5}	2.09×10^{7}
U-233	0	7.44×10^{5}
U-234	0	4.33×10^{6}
U-235	0	1.51×10^{8}
U-236	0	7.32×10^{7}
U-238	0	8.69×10^{10}

3.4.1.3 Waste-Form Degradation

The radionuclides within the waste that were not released instantaneously will be released slowly over time from the bound waste form. Within the SOAR model, the waste is released over time according to a degradation rate in units [1/yr]. The degradation rate can be specified within SOAR as a constant, PDF or changing over time.

In NWMO (2013a and b), the following dissolution model was used to describe the release of radionuclides from the waste form. The dissolution rate due to α-, β- and γ- radiolysis (R_α, R_β and R_γ) were calculated according to Equations 3.10, 3.11 and 3.12.

$$\boldsymbol{R_\alpha = A_{cont} G_\alpha f_\alpha [D_\alpha (t + t_c)]^{a\alpha}} \quad \textbf{3.10}$$

$$\boldsymbol{R_\beta = A_{cont} G_\beta f_\beta \left[D_\beta (t + t_c)\right]^{a\beta}} \quad \textbf{3.11}$$

$$\boldsymbol{R_\gamma = A_{cont} G_\gamma f_\gamma \left[D_\gamma (t + t_c)\right]^{a\gamma}} \quad \textbf{3.12}$$

With $a\alpha = a\beta = a\gamma = 1$. The total dissolution rate (R_{tot} [mol/yr]) is then calculated according to equation 3.13.

$$\boldsymbol{R_{tot} = R_\alpha + R_\beta + R_\gamma + R_{CH} \times A_{cont}} \quad \textbf{3.13}$$

Where:

R_{CH} is the chemical dissolution rate [mol/m^2·yr]

$D_\alpha(t+t_c)$, $D_\beta(t+t_c)$ and $D_\gamma(t+t_c)$ are time-dependent dose rates and are presented in Table 3.7 [Gy/yr]

t is the time after placement in the repository [yr]

t_c is the age of fuel at time of placement [yr]

G_α, G_β and G_γ are constants presented in Table 3.8 [mol/m^2·yr]

f_α, f_β and f_γ are alpha, beta and gamma dose variability factors presented in Table 3.8

A_{cont} is the effective surface area of dissolving fuel per container [m^2]

Table 3.7 – Radiation Doses at Fuel Surface (taken from NWMO (2013b))

Time After Fuel Discharge (years)	Alpha Dose Rate [Gy/yr]	Beta Dose Rate [Gy/yr]	Gamma Dose Rate [Gy/yr]
10	1.42E6	3.77E6	7.11E5
20	1.72E6	2.82E6	5.30E5
30	1.89E6	2.20E6	3.95E5
40	1.99E6	1.72E6	2.95E5
50	2.03E6	1.35E6	2.20E5
60	2.05E6	1.06E6	1.74E5
75	2.04E6	7.38E5	1.23E5
100	2.00E6	4.04E5	6.87E4
150	1.88E6	1.24E5	2.16E4
200	1.77E6	3.96E4	6.80E3
300	1.58E6	6.66E3	1.02E3
500	1.30E6	2.69E3	22.8
1,000	9.03E5	1.53E3	15.5
10,000	3.21E5	3.78E2	16.5
100,000	1.80E4	1.68E2	28.4
1,000,000	6.24E3	1.49E2	38.4
10,000,000	4.19E3	1.15E2	35.8

Table 3.8 – Used Fuel Dissolution Rate (taken from NWMO (2013b))

Parameter	Value	PDF
Fuel surface area per container	1570 m^2	Lognormal PDF with GM = 1570 m^2, GSD = 3, bounds of 340 and 7860 m^2
Alpha, beta and gamma dose rates	Table 3.6	Variability included separately through the f_α, f_β and f_γ factors
Alpha dose rate variability factor, f_α	1.0	Triangular PDF with bounds of 0.80 and 1.20
Beta dose rate variability factor, f_β	1.0	Triangular PDF with bounds of 0.80 and 1.20
Gamma dose rate variability factor, f_γ	1.0	Triangular PDF with bounds of 0.80 and 1.20
Age of fuel at time of placement, t_c	30 years	Design basis
G_α	1.4×10^{-10} $mol \cdot m^{-2} \cdot Gy^{-1}$	Lognormal PDF with GM = 1.4×10^{-10} $mol \cdot m^{-2} \cdot Gy^{-1}$, GSD = 6.0, bounds of 3.5×10^{-12} and 2.1×10^{-9} $mol \cdot m^{-2} \cdot Gy^{-1}$
G_β and G_γ	1.1×10^{-9} $mol \cdot m^{-2} \cdot Gy^{-1}$	Loguniform PDF with bound of 3.7×10^{-11} and 3.3×10^{-8} $mol \cdot m^{-2} \cdot Gy^{-1}$
Chemical dissolution rate	4.0×10^{-7} $mol \cdot m^{-2} \cdot yr^{-1}$	Loguniform PDF with bounds of 4.0×10^{-8} and 4.0×10^{-6} $mol \cdot m^{-2} \cdot yr^{-1}$

The values of total dissolution rate (R_T) were calculated over time as described by the dissolution model in NWMO (2013b) (see Table 3.9). Within the SOAR model, the bound and unbound inventories were managed through a GoldSim element called a Source Property. Within this element the bound form was released at a specified rate. GoldSim allows for three different methods of defining the release rate, which are through the Lifetime, Degradation Rate and Congruent Dissolution. Congruent dissolution is a method defined by Gold Sim and differs from the dissolution model used by NWMO.

The basic equation describing the degradation rate of matrix materials is $\boldsymbol{r = -dM/dt}$, where $\boldsymbol{M}$ [kg] is the mass of the matrix materials and $\boldsymbol{r}$ [kg/yr] is the degradation rate, considered constant in SOAR. The dissolution rates of matrix-bound radionuclides away from the waste matrix are computed by GoldSim source elements by assuming congruent dissolution with the waste form matrix. The degradation rate can also be expressed as $\boldsymbol{dM/dt = -r = -gM_0 = -RAM_0}$, where $\boldsymbol{M_0}$ is the initial mass of the waste form matrix and $\boldsymbol{g\ (=R\ A)}$ is the initial fractional degradation rate**.** $\boldsymbol{R}$ [$g/cm^2/yr$] is the matrix dissolution rate, and $\boldsymbol{A}$ [cm^2/g] is the initial specific area of the waste

form exposed to an aqueous environment. Experimental values for the dissolution rate, ***R***, and initial specific area, ***A***, reported in the literature for various waste forms were considered to compute initial fractional degradation rates, ***g***, which are inputs to the Waste Form model component. From the fractional degradation rates, the waste form lifetime is computed as ***1/g***. The waste form lifetime is a direct input to the GoldSim source element. The dissolution rate of each radionuclide is determined by the fraction of each radionuclide in the waste form based on congruent dissolution (US NRC and CNWRA, 2011). Fractional degradation rates are called degradation rate for short hereafter.

To calculate the corresponding degradation rates for SOAR, several calculations from the dissolution model were conducted. The degradation rates in [1/yr] over time were calculated by dividing the dissolution rate [mol/yr] by the total number of moles initially present. The total number of moles was determined by using several values from NWMO's dissolution model. At 1 year, the dissolution rate was 4.9 mol/yr (see Table 3.9) and the cumulative dissolution rate was 0.01% (see Figure 3.3). From these values, the total number of moles was calculated as 4.9 x 10^4 moles. The degradation rate was then calculated at selected times by dividing the dissolution rate in [mol/yr] by the total number of moles and is presented in Table 3.9.

Table 3.9 – Calculation of degradation rates used in SOAR

t [yr]	R_T [mol/yr]	Degradation Rate [1/yr]	Lifetime [yr]
1	4.90	1.00E-4	1.00E+4
10	3.92	8.00E-5	1.25E+4
20	3.16	6.45E-5	1.55E+4
30	3.51	7.18E-5	1.39E+4
45	1.94	3.95E-5	2.53E+4
70	1.26	2.57E-5	3.90E+4
120	0.67	1.36E-5	7.36E+4
170	0.47	9.59E-6	1.04E+5
270	0.36	7.37E-6	1.36E+5
470	0.29	5.94E-6	1.68E+5
970	0.20	4.12E-6	2.43E+5
9970	0.072	1.47E-6	6.82E+5
99,970	0.0049	1.01E-7	9.95E+6
999,970	0.0023	4.74E-8	2.11E+7
9,999,970	0.0018	3.69E-8	2.71E+7

The degradation rates vary from 10^{-4} 1/yr to 10^{-8} 1/yr and could be inputted to SOAR in different manners such as a constant value, as a PDF or varying over time. To observe the effects of the waste degradation rate it was inputted to SOAR in different manners. The results of these changes in waste form degradation will be discussed in Section 3.4.

The SYVAC3-CC4 model used the aforementioned dissolution model that results in a dissolution rate decreasing over time. The SOAR model used the degradation rate (or lifetime) to define how the waste released from the bound waste form. The NWMO assumes that 10,000 years are required prior to sufficient water being present for transport through the undetected defects. As will be discussed in the waste package section, the manner in which this scenario was modelled in SOAR was by setting the waste package breach to 10,000 years. GoldSim does not consider the degradation rates until waste package breach (10,000 years) and as such, SOAR does not consider any of the higher degradation rates that occur before this time, which are in the 10^{-4} to 10^{-6} 1/yr range (see Table 3.9). Therefore, once SOAR began utilizing the degradation rates, the values were much lower resulting in lower amount of radionuclides being released from the bound form. If degradation rates decreasing over time were used in this model it would be expected to predict lower releases as the higher degradation rates were not applied. The releases with respect to degradation rates will be discussed in Section 3.5.

Figure 3.3 – Fuel Dissolution Rate (taken from NWMO (2013a))

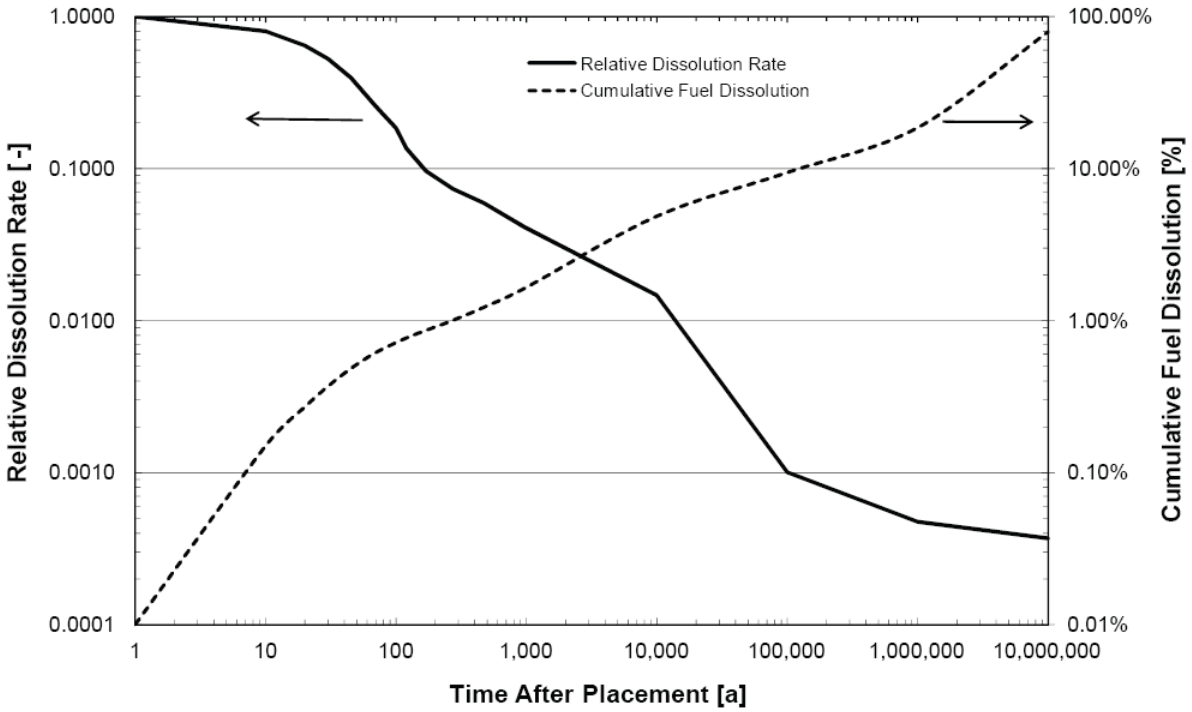

3.4.2 Waste Package Component

Within SOAR, the Waste Package Component is where package information such as container material type and thicknesses are inputted and depicts how and when waste packages fail. The failure may be due to localized or general corrosion or specified through what is called the Disruptive Event Component. The Disruptive Event Component allows the user different methods of setting package failure.

One of the limitations of SOAR is that the waste package configuration is not explicitly modelled. In NWMO's analyses, the waste was divided into five waste vaults. Representing the waste in this manner was not possible within SOAR.

The waste package configuration that was presented by the NWMO in the Fifth Case Study was that 360 fuel bundles were held in steel baskets. The bundles are then encompassed by an inner carbon steel shell to provide strength to the package. Finally the package would be encased by an outer copper shell to reduce the effects of corrosion. The dimensions of the waste package as described by NWMO (2013b) are presented in Table 3.10 and Figure 3.4.

Table 3.10 – Waste Package Dimensions

Parameter	Value
Carbon steel shell thickness	10.25 cm
Copper shell thickness	2.5 cm
Internal void volume	1.58 m^3

In the NWMO's conceptual model, the inner carbon steel shell was not specifically modelled (NWMO, 2013a). In other words, the corrosion of the carbon steel would occur rapidly once in contact with water and therefore could be ignored. The corrosion of copper was assumed to be sufficiently slow that it could be ignored.

The waste package failure was assumed to occur through undetected defects in the copper outer shell. Through probabilistic calculations, the NWMO assumed for the Reference Case that 3 packages would be placed in the repository with defects. The containers with defects were randomly assigned to one of the five waste vaults. The defects were assumed to have a radius of 1 mm and in the initial model were inputted as a discrete value. For the subsequent probabilistic modelling, the defect radius was defined by a triangular PDF from 0.2 to 2 mm. Through simulations, the NWMO (2013a) determined that it would take approximately 10,000 years for sufficient water to be present to create a transport pathway for radionuclides to exit the waste package and enter the Near Field.

3.4.2.1 Free-Water Diffusivity

The transport pathway by which contaminants escape from the interior to exterior of the waste package through any defects is via diffusion. NWMO in their analyses assumed higher values for free-water diffusivity as this would cause the contaminants to leave the package faster, providing conservative results. The free-water diffusivities that were used by NWMO are presented in Table 3.11. Initially for the deterministic modelling the discrete values equal to the reference value were used. Once the probabilistic modelling was conducted, a log uniform distribution was used with an upper and lower bound equal to a factor of 10 higher and lower, respectively.

Figure 3.4 – Waste package configuration (taken from NWMO (2013b))

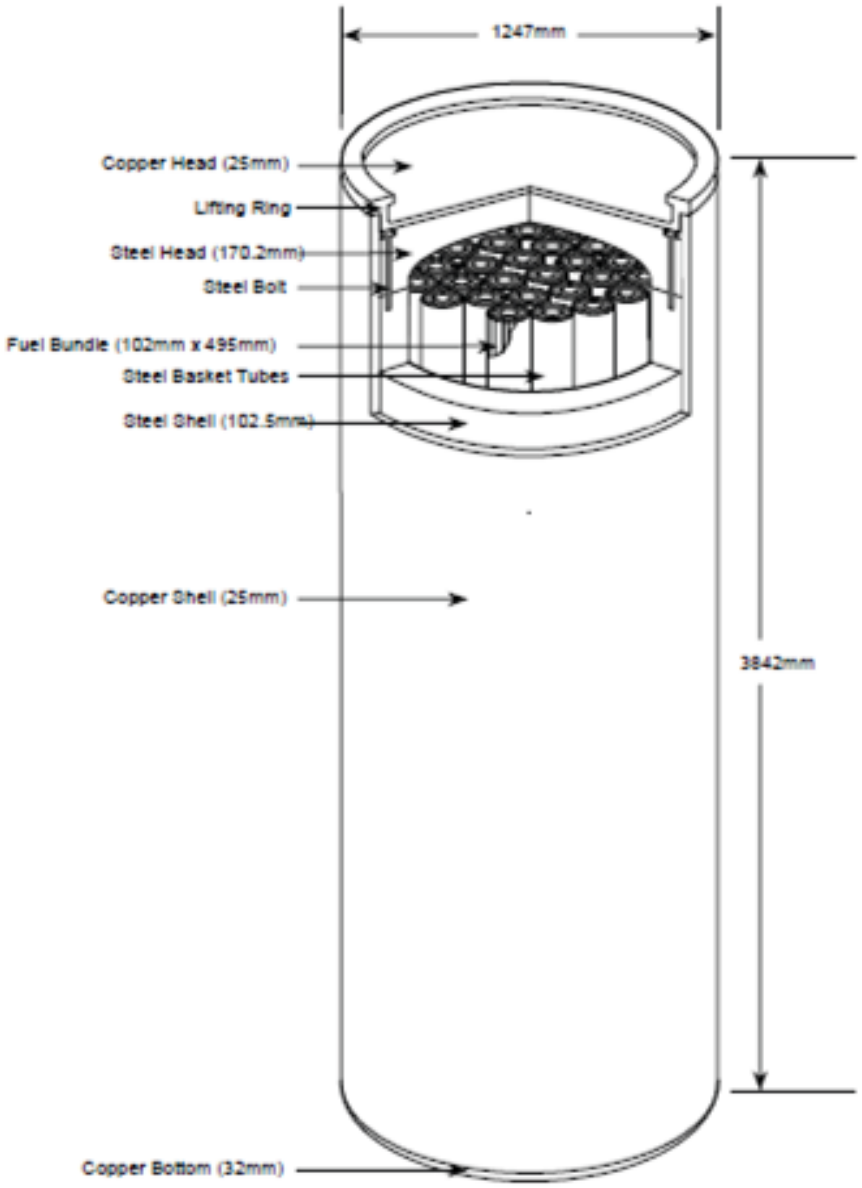

Table 3.11 – Free-Water Diffusivity

Ion	Reference Value [m^2/yr]
Cs	0.1572
Other species	0.0524

3.4.2.2 Defects

The mode of failure assumed by the NWMO is through undetected defects in 3 waste packages. The radius of the defect was 1 mm and it would take 10,000 years for enough water to be present for transport out of the waste package.

In order to model this failure using SOAR the best method to incorporate it was to use the Disruptive Event Component. Even though this is not a "disruptive event", this component allowed for setting the time of failure to occur at the specified time of 10,000 years. The settings used on the Disruptive Event Dashboard within SOAR are presented in Table 3.12. All other parameters on the dashboard are not used within the SOAR code and therefore do not need to be changed and do not affect results.

Table 3.12 – Disruptive Event Dashboard Settings

Parameter	Setting
Type of Disruptive Event	Waste Package Failure Rate
Start Time of Waste Package Failure (yr)	9999
End Time of Waste Package Failure (yr)	10,000
Disable Localized Corrosion	Checked
Disable General Corrosion	Checked

The main outputs from the Waste Package Component are the breach area fraction and number of waste packages failed. In order to calculate these parameters for the current mode of failure of three defects, changes within the original version of SOAR were made. Within the code, a new element for the defect radius was created. For the deterministic modelling, the breach area and fraction breach area were calculated from distinct values of the defect radius and other geometry (see Figure 3.5). The number of packages that fail was set to a constant value of 3 within the code and then used to calculate the fraction of packages that fail (see Figure 3.6). The outputs of breach area and number of waste packages failed from the Disruptive Components are sent to the Waste Package Component.

For the probabilistic simulations, the PDF for the radius was inputted as triangular PDF from 0.2 mm to 2 mm as defined by NWMO (2013b). The number of defective containers was defined by a binomial distribution characterized by the probability of a container having a defect and the total number of packages. The probability of a container having a defect was defined through a lognormal distribution with geometric mean equal to 2×10^{-4}, a geometric standard deviation equal to 2 and bounds set as 10^{-4} and 10^{-3} (NWMO, 2013a). For each simulation, the number of defective containers was determined and randomly placed within a waste vault in the repository.

Figure 3.5 – Fraction breached area with deterministic values used in SOAR

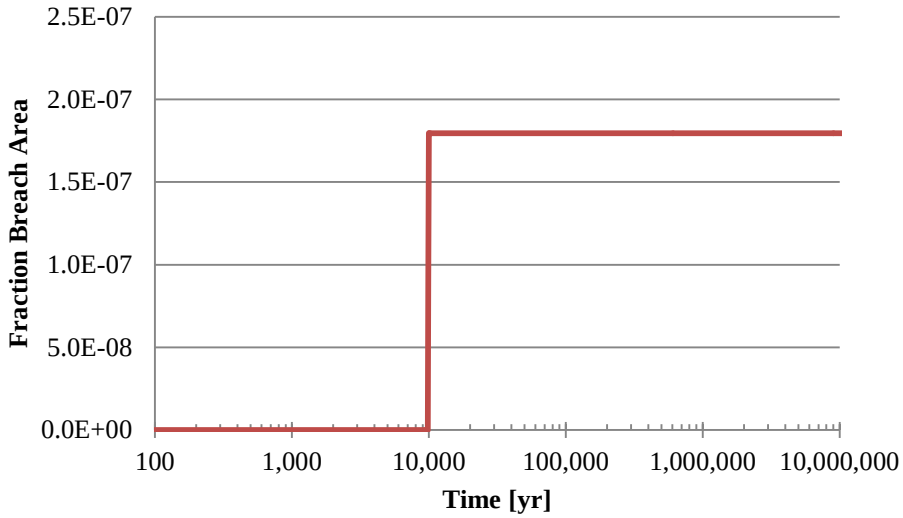

Figure 3.6 – Fraction waste packages breached with deterministic values used in SOAR

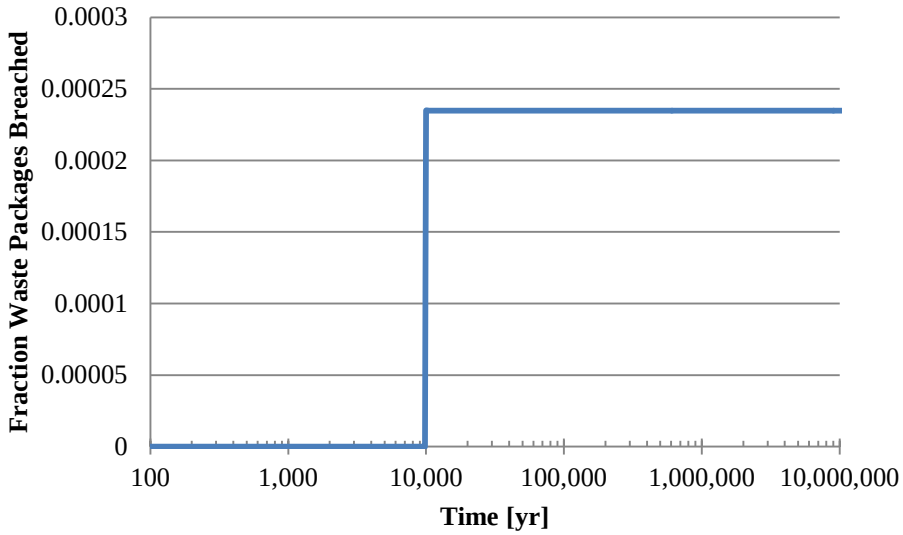

3.4.3 Near Field Component

The Near Field Component is the transport of radionuclides from the interior of the package, through the buffer material and to the geosphere. In SOAR this is broken into three zones. Zone 1 is the transport from the waste package interior to the waste package surface. The next zone is the transport through the buffer material. And the final zone is the transition from the buffer material to the closest fracture in the geosphere. In this case, the geosphere is not fractured and therefore Zone 3 was automatically neglected within SOAR.

The Near Field as presented by the NWMO (2013b) has the waste package placed on a highly compacted bentonite pedestal and surrounded by bentonite pellets (see Figure 3.7). For modelling purposes, it was assumed in the NWMO analysis that the pedestal and bentonite pellets form a homogeneous unit (NWMO, 2013b).

Figure 3.7 – Cross-sectional view of placement room (taken from NWMO (2013b))

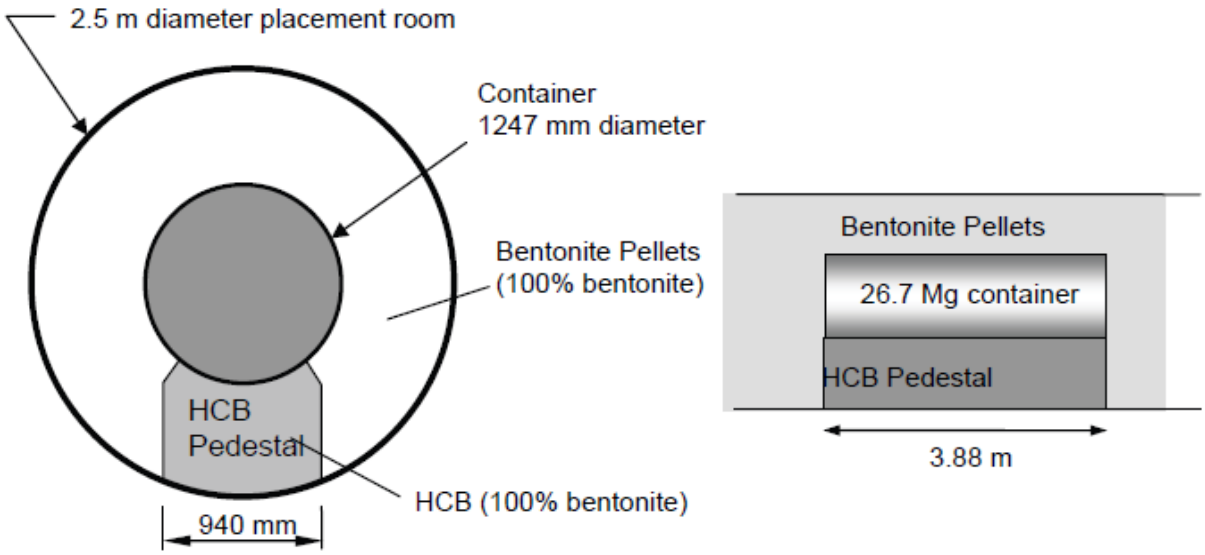

On the Near Field Component dashboard, the settings were configured as shown in Table 3.13. The parameters that are not listed in the table were left at the default settings as these do not affect the SOAR model for this scenario. The water volume inside the waste package was taken from the void space within the waste package (see Table 3.10). The transport length was calculated from the dimensions of the waste package and buffer. Buffer degradation was not considered within SOAR for this scenario.

Table 3.13 – Near Field Component Dashboard Settings

Parameter	Setting
Water Volume inside the waste package (m^3)	1.58
Transport Length (m)	0.627

3.4.3.1 Near Field Diffusivities

The Near Field effective diffusivities were obtained from NWMO (2013b) and are presented in Table 3.14. For the deterministic modelling, the diffusivities within SOAR are set as a constant value equal to the reference value. The probabilistic modelling was conducted with the diffusivities set as a triangular distribution with the values in the table. The diffusivity values were inputted directly into the SOAR code itself under the User-Defined Diffusivities.

Table 3.14 – Effective diffusivity values for buffer material in SOAR

Radionuclide	Reference Value [m^2/yr]	Lower Bound [m^2/yr]	Upper Bound [m^2/yr]
Cs	1.3×10^{-2}	3.0×10^{-3}	1.3×10^{-2}
Other species	4.4×10^{-3}	2.9×10^{-3}	6.6×10^{-3}

3.4.3.2 Near Field Sorption Parameters

The sorption parameters for the buffer material were obtained from NWMO (2013b) (see Table 3.15). The values were inputted directly into the SOAR code for the reducing condition parameters. SOAR assumes the REDOX conditions for the Near Field are the same as those assigned to the first leg in the Far Field. As will be discussed in the subsequent Far Field section, the legs of the Far Field were reducing. For the deterministic model runs, the sorption for each radionuclide was set to the Reference Value in the table. The PDF for each element was assigned for the subsequent probabilistic modelling.

Table 3.15 – Sorption Coefficients for Buffer

Element	Reference Value [m^3/kg]	Distribution	Lower Bound [m^3/kg]	Upper Bound [m^3/kg]
Cs	0.004	Log uniform	0.0007	0.024
Np	4.3	Log uniform	0.8	23
Pu	0.5(3.2)[1]	Lognormal	0.05	5
U	40	Triangular	2.3	700
Other	0	Constant	-	-

1. The value is the geometric mean and the value in () is the geometric standard deviation for lognormal distributions.

3.4.3.3 Near Field Soil Properties

Within the SOAR code, an element called the Backfill soil property was defined and used in the simulation. The sorption values previously described were inputted to this soil property. The model also required the dry density and porosity of the buffer material, which were obtained from NWMO (2013b) and are presented in Table 3.16.

Table 3.16 – Buffer soil properties

Property	Value
Dry Density	1423 kg/m^3
Porosity	0.48

3.4.3.4 Near Field Solubilities

The element solubilities were taken from NWMO (2013b) and are presented in Table 3.17. Within the NWMO report, it was stated that the solubility used was ten times higher than reported in NWMO (2013b) to account for uncertainties, therefore, the values in Table 3.17 reflect this increase. The SOAR code requires the solubilities in mg/L and those from the NWMO report are in mol/L. The values in mg/L were calculated using the molecular weight and inputted to SOAR in the user-defined solubilities. For those elements with no solubility limit a value of "-1" was assigned, which indicates to SOAR to treat these values as having no limit.

For the initial deterministic model the values were set as constant and given the mean value. The PDF was inputted when conducting the probabilistic simulations.

Table 3.17 – Element Solubilities

Element	Value		GSD	PDF Type
	mol/m^3	mg/m^3		
C	$2.2x10^{1}$	$2.64x10^{2}$	3.2	Lognormal
Np	$1.7x10^{-5}$	$4.03x10^{-3}$	3.2	Lognormal
Se	$3.4x10^{-5}$	$2.69x10^{-3}$	3.2	Lognormal
Tc	$4.4x10^{-5}$	$4.31x10^{-3}$	3.2	Lognormal
U	$4.5x10^{-5}$	$1.07x10^{-2}$	3.2	Lognormal
Other	-1	-1	-	Constant

3.4.4 Far Field Component

The Far Field Component within the original version of SOAR allowed for three different legs in the geosphere. Within the SOAR code, each leg was defined by a GoldSim Pipe Pathway and the original scenario had three Pipe Pathways in series that exited to the Biosphere Component. A GoldSim Pipe Pathway is a coding element used in the GoldSim contaminant transport module, as described in Section 3.3. For each Pipe Pathway the flow and transport parameters are inputted including tube length, hydraulic conductivity, flow rate and sorption. GoldSim calculates the transport through the Pipe Pathway considering advection, diffusion and dispersion. The output from one Pipe Pathway can be inputted to another in which different geosphere properties can be defined. Several Pipe Pathways connected in series can be used to define different layers within the geosphere. Within the SOAR code, the hydraulic conductivity, sorption (Kd) value, length and gradient could be defined for each leg and were allowed to vary from leg to leg.

For the current scenario, NWMO considered two pathways from the repository to the biosphere as discussed in Section 3.1 and Appendix B. One pathway is through the natural geosphere of shale and limestone units and the second is through the shaft materials. As stated previously, the NWMO divided the repository into five waste vaults. The NWMO in their one-dimensional modelling assumed that 0.015% of the release from the fifth waste vault went through the shaft pathway (NWMO, 2013a). As SOAR does not allow for multiple waste vaults it was assumed that the release to the shaft path was 0.015% of the total Near Field Release. A second option would have been to set the release to shaft as one fifth of the Near Field Release to represent release from only the fifth waste vault. As will be discussed later, the shaft release only represents 0.31% of the contribution to the total dose and therefore applying the first assumption does not greatly impact the prediction. It was stated in the NWMO analyses that all formations within the modelling domain were reducing.

From the geology, the natural geosphere pathway was through six different formations and therefore would require six different legs or Pipe Pathways in series within SOAR (See

Appendix B). For each of these legs, different values of the hydraulic conductivity, length, gradient, porosity, density and sorption parameters were required.

The shaft pathway would also be through six different legs including layers of bentonite/sand, degraded concrete and asphalt. Similar to the geosphere pathway, the parameters for the shaft pathway vary from leg to leg.

In order to model the two different pathways with varying parameters, changes needed to be conducted to the original SOAR code. A series of six GoldSim Pipe Pathways were coded into SOAR to represent the six legs of the natural geosphere (see Figure 3.8). To account for the shaft pathway, a second series of Pipe Pathways was coded in parallel to the first series, with an input of 0.015% of the Near Field Release. All parameters required by the model, including sorption and tortuosity were allowed to vary from leg to leg.

Figure 3.8 – Schematic of Far Field changes in SOAR

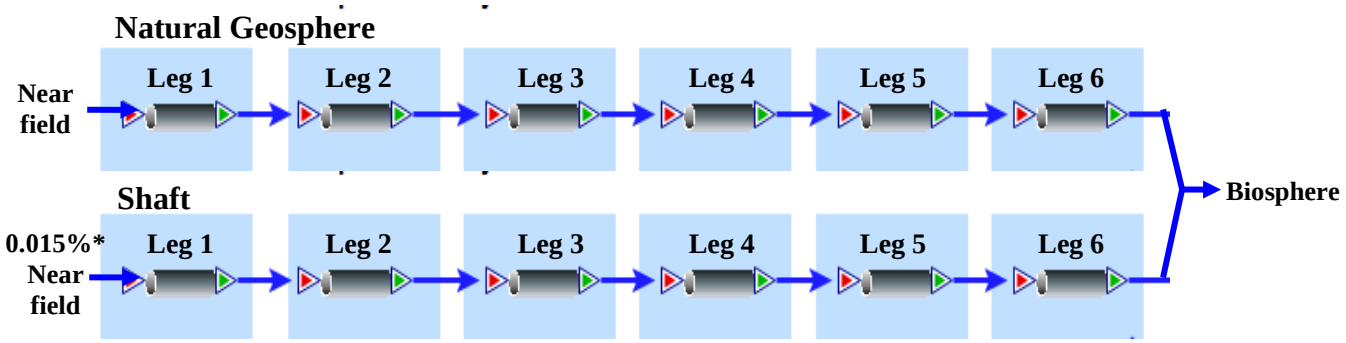

The parameters for each leg were inputted directly into the code and were allowed to vary from leg to leg. Those parameters for the geosphere pathway are presented in Table 3.18. The sorption parameters for limestone and shale are presented in Table 3.19. The dispersivity fraction assumed by NWMO (2013b) for all legs was 0.15 and was applied to SOAR.

The parameters for the shaft pathway are presented in Table 3.20. The sorption parameters for all legs in the shaft pathway are set to zero as this was the assumption made by the NWMO (2013a).

For the SYVAC3-CC4 modelling conducted by NWMO, the diffusion coefficients were inputted directly using the values presented in Table 3.20. However, the diffusion coefficient (D_e) is calculated within SOAR from the free-water diffusivity (D_0), porosity (φ) and tortuosity (τ) according to equation 3.5. The values of free-water diffusivity were presented in Table 3.11 and porosity in Table 3.18 and Table 3.20. Tortuosity values were calculated using the NWMO diffusion coefficients (NWMO, 2013a) and inputted to SOAR (see Table 3.21).

$$D_e = D_0 \cdot \varphi \cdot \tau \qquad \textbf{(3.5)}$$

For the probabilistic modelling conducted using SYVAC3-CC4, the diffusion coefficients in the geosphere were defined according to a loguniform distribution with limits set at 10x and 0.1x the mean value (NWMO, 2013a). Within the SOAR model, the diffusion was calculated using inputs of the tortuosity, porosity and free-water diffusivity according to equation 3.5. Therefore to account for the uncertainty within SOAR, the free-water diffusivity was assigned a log-uniform PDF with the aforementioned limits to result in the same PDF for diffusion in the geosphere.

Table 3.18 – Parameters for the geosphere pathway

Leg	Formation	Medium	K [m/s]	Length [m]	Gradient	Porosity	Density [kg/m^3]
6	Fossil Hill	Limestone	$5.0\text{x}10^{-13}$	6.65	$1.5\text{x}10^{-4}$	0.031	2710
5	Cabot Head	Shale	$9.0\text{x}10^{-15}$	15.89	$1.7\text{x}10^{-3}$	0.116	2765
4	Manitoulin	Limestone	$9.0\text{x}10^{-15}$	15.54	$1.7\text{x}10^{-3}$	0.028	2710
3	Queenston	Shale	$2.0\text{x}10^{-15}$	77.58	$7.6\text{x}10^{-3}$	0.073	2765
2	Georgian Bay	Shale	$3.0\text{x}10^{-15}$	154.49	$4.9\text{x}10^{-3}$	0.07	2765
1	Cobourg	Limestone	$2.0\text{x}10^{-15}$	23.61	$1.5\text{x}10^{-2}$	0.015	2710

Table 3.19 – Sorption parameters for limestone and shale

Element	Limestone		Shale	
	K_d [m^3/kg]	PDF	K_d [m^3/kg]	PDF
Cs	$3.6\text{x}10^{-4}$	Log uniform ($4.0\text{x}10^{-5}$, $3.3\text{x}10^{-3}$)	0.06	Log uniform (0.0092, 0.38)
Np	2.6	Log uniform (0.7, 10)	1.2	Log uniform (0.15, 9)
Pu	0.02	Lognormal (3.2, 0.002, 0.2)	0.2	Lognormal (3.2, 0.02, 2)
U	2.6	Log uniform (0.7, 10)	1.2	Log uniform (0.15, 9)
Other	0	Constant	0	Constant

Table 3.20 – Parameters for the shaft pathway

Leg	Medium	K [m/s]	Length [m]	Gradient	Porosity	Density [kg/m^3]
6	Degraded Concrete	$1.0x10^{-10}$	7.28	$1.4x10^{-4}$	0.100	2491
5	Bentonite/Sand	$1.6x10^{-11}$	142.7	$5.0x10^{-3}$	0.411	1600
4	Asphalt	$1.0x10^{-12}$	40	$7.3x10^{-3}$	0.020	1960
3	Bentonite/Sand	$1.6x10^{-11}$	80	$4.4x10^{-3}$	0.411	1600
2	Degraded Concrete	$1.0x10^{-10}$	12	$6.7x10^{-4}$	0.100	2491
1	Bentonite/Sand	$1.6x10^{-11}$	222	$1.2x10^{-3}$	0.411	1600

Table 3.21 – Diffusion coefficient and tortuosity

Formation	$D_{e,v}$ [m^2/yr]		Tortuosity
	Cs	All other species	
Natural Geosphere			
Fossil Hill	$4.07x10^{-6}$	$1.36x10^{-6}$	0.0017
Cabot Head	$2.94x10^{-4}$	$9.80x10^{-5}$	0.032
Manitoulin	$1.42x10^{-5}$	$4.74x10^{-6}$	0.0065
Queenston	$9.45x10^{-5}$	$3.16x10^{-5}$	0.016
Georgian Bay	$7.75x10^{-5}$	$2.59x10^{-5}$	0.014
Cobourg	$3.51x10^{-5}$	$1.17x10^{-5}$	0.03
Shaft Materials			
Degraded Concrete	$1.18x10^{-2}$	$3.94x10^{-3}$	0.75
Asphalt	$9.47x10^{-6}$	$3.16x10^{-5}$	0.003
Bentonite/Sand	$2.37x10^{-2}$	$7.89x10^{-3}$	0.44

3.4.5 Biosphere Component

The Biosphere Component in SOAR determines the dose to humans through the ingestion of water alone. Other exposure pathways that would affect the dose are not considered by SOAR. When making comparisons of the dose with those reported by NWMO, the method by which SOAR calculates the dose should be considered. As will be discussed later in this report, the results from the SYVAC3-CC4 prediction showed that the dominant contribution to total dose was through I-129. The dose due to I-129 had approximately equal input through exposure of

ingestion of water and food. As SOAR only considers ingestion of water, it would be expected that the total dose rate should be approximately half that predicted by SYVAC3-CC4.

Within the Biosphere Component, the user defines the well capture fraction, which is the percentage of water released from the geosphere that flows to the well rather than downstream in the Biosphere. Through the three-dimensional modelling conducted by NWMO using FRAC3DVS-OPG, they determined that the well capture fraction was 93.7% (NWMO, 2013a).

The ingestion dose coefficients were also defined to determine the ultimate dose. Those dose coefficients already specified within SOAR were the same as those specified by NWMO (2013b) and were therefore not changed.

The well pumping rate defined by NWMO (2013a) is 1307 m^3/yr and was inputted to SOAR as the water flow rate to the biosphere.

3.4.6 Excavated Damage Zone (EDZ)

During construction of the repository, different blasting and drilling methods would be used to create the required shafts and placement rooms. By creating these openings, an excavated damage zone (EDZ) in the natural formations will be created. The EDZ is a small zone in which the hydraulic conductivity is increased, possibly creating preferential pathway for transport. Different keys would be placed along these preferential pathways to impede the movement. The EDZ is an important consideration as the radionuclides could preferentially travel along these zones of increased hydraulic conductivity.

Within the SOAR model, two pathways were considered from the Near Field to the Biosphere. One pathway was through the natural geosphere of limestone and shale units. The other pathway was through the seal material within the main shaft. These two pathways are discussed further below.

For the first pathway through the natural geosphere the radionuclides would exit the buffer material of the Near Field and then pass through the Inner and Outer EDZ and subsequently into the Far Field units (see Figure 3.9). As the SOAR model is one-dimensional, the radionuclides would be transported through the EDZ to the limestone unit of the Cobourg Formation in the Far Field. In a three-dimensional flow and transport code, the radionuclides would preferentially travel along the plane of the EDZ. For this reason, the NWMO in their design have keyed in blocks to stop preferential movement along these pathways.

Figure 3.9 – Conceptualized EDZ for natural geosphere pathway (Not to scale)

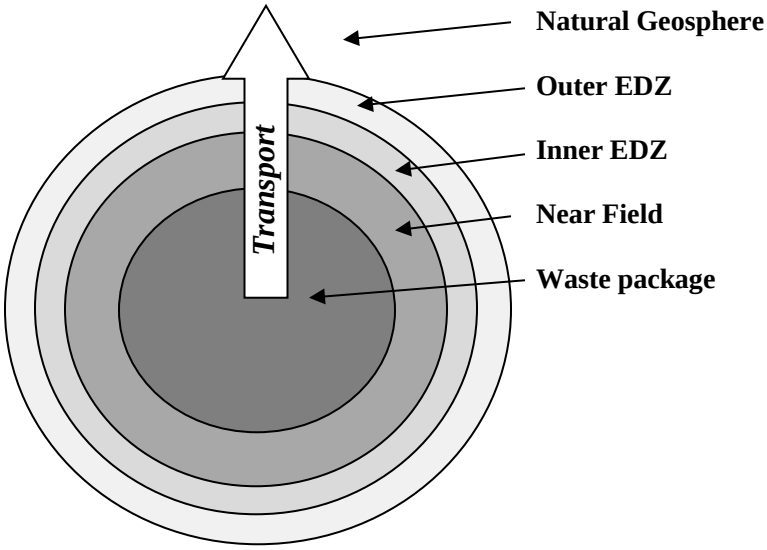

In order to model the EDZ within SOAR, two legs were added to the Far Field to represent the Inner EDZ and the Outer EDZ. The parameters of these two additional legs are presented in Table 3.22. The hydraulic conductivity, porosity, tortuosity and thickness are as specified in the NWMO analysis (NWMO, 2013a). The hydraulic conductivity for Inner EDZ is 10^3 x K and for outer EDZ is 10^2 x K in which K was that from the Cobourg Formation. Porosity and tortuosity of the EDZ is twice that of the original host rock.

Table 3.22 – SOAR parameters for Inner and Outer EDZ

Leg	Thickness	K [m/s]	Gradient	Porosity	Tortuosity
Inner EDZ	0.3 m	2×10^{-11}	0.015	0.03	0.06
Outer EDZ	0.5 m	2×10^{-12}	0.015	0.03	0.06

For the shaft pathway, the EDZ transport direction would be parallel to that within the backfilled shaft materials (see Figure 3.10). Water could preferentially travel along the planes with higher hydraulic conductivity. Therefore, the water would tend to travel along the Inner and Outer EDZ. In the design presented by the NWMO, different blocks would be keyed in to prevent radionuclides moving long distances along the EDZ. However, for modelling purposes a conservative approach was taken in assuming the radionuclides could travel freely along the EDZ. In order to model the EDZ in the shaft pathway, the hydraulic conductivity was increased by 10^3 of that of the surrounding limestone and shale units along the side of the shaft pathway.

By representing the EDZ in this manner, it was assumed that the flow would be preferentially along the inner EDZ which has the higher hydraulic conductivity than the outer EDZ.

Figure 3.10 – Conceptualized EDZ for shaft pathway (Not to scale)

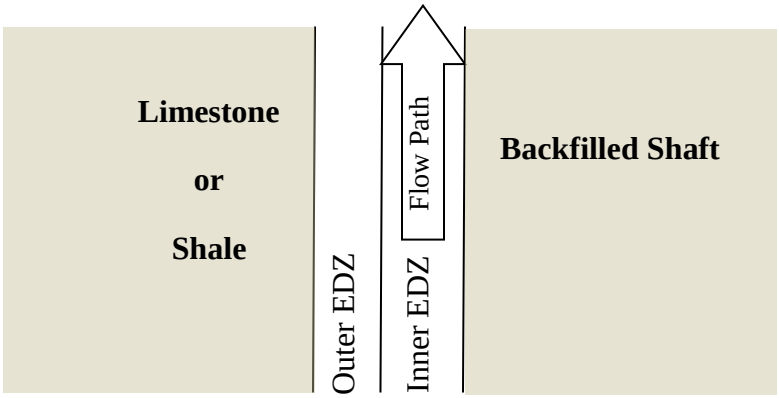

The above discussion of the EDZ is considered in the sensitivity analysis of the deterministic dose calculation as discussed in Section 4.0.

3.5 Comparison between SOAR and NWMO

The following sections examine the releases from the different components within SOAR and compared against those results from NWMO (2013a).

3.5.1 Release from the Waste Package

The NWMO discussion regarding release from the waste package focussed on four radionuclides: Cs-135; I-129; U-234; and U-238. The release rates from the waste package presented by the NWMO are shown in Figure 3.11.

Through the development of the SOAR model, it was determined that the method by which the degradation of the waste form was incorporated affected the release of Cs-135 and I-129. The release of U-234 and U-238 was limited by the solubility.

Figure 3.11 – NWMO predicted radionuclide release from waste package (NWMO, 2013a)

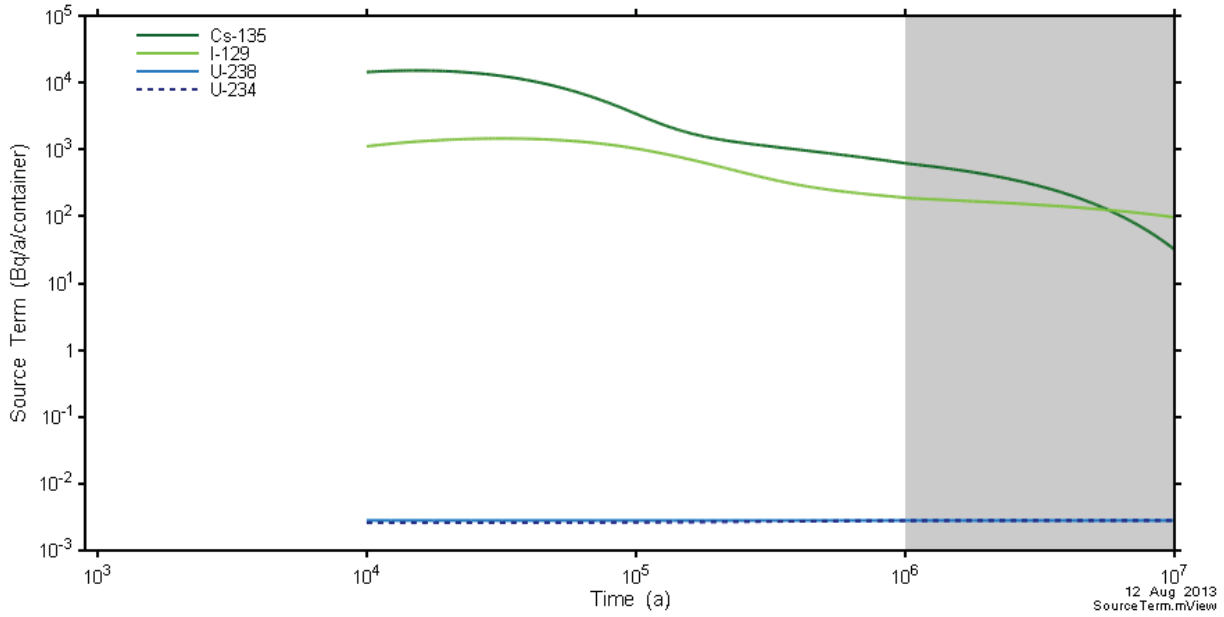

The waste form degradation was calculated from the dissolution model presented by NWMO (2013b) as presented in Section 3.4.1.3. The values of the degradation rate vary over four orders of magnitude, from 10^{-4} 1/yr at early times to 10^{-8} 1/yr at later times. The manner in which GoldSim accounts for model degradation within the Source element states that no degradation occurs until package breach. In the scenario presented by NWMO, it takes 10,000 years for sufficient water to be present for transport out of the package through the undetected defects. To model this within SOAR, the breach of the waste package was set to 10,000 years, which does not account for any degradation that would occur in any water present prior to this time. Therefore, if the degradation rate was defined as declining over time according to Table 3.9, degradation rates greater than 10^{-6} 1/yr were ignored. As the higher degradation rates were neglected it was expected that the releases would be lower. Therefore, accounting for degradation rate in this manner does not correspond with that in the SYVAC3-CC4 model. It was not possible to model the degradation or dissolution in SOAR as was done in SYVAC3-CC4 due to constraints of how GoldSim accounts for degradation. Accordingly, the incorporation of degradation rates was conducted in different ways to observe the effects.

The four methods by which the degradation was accounted for was through constant values of 10^{-4} 1/yr, 10^{-5} 1/yr and 10^{-7} 1/yr and declining over time according to Table 3.9. SOAR was run using each of these methods, and the results are shown in Figures 3.12 – 3.15.

Figure 3.12 – Waste package release using degradation rate of 10^{-4} 1/yr (SOAR)

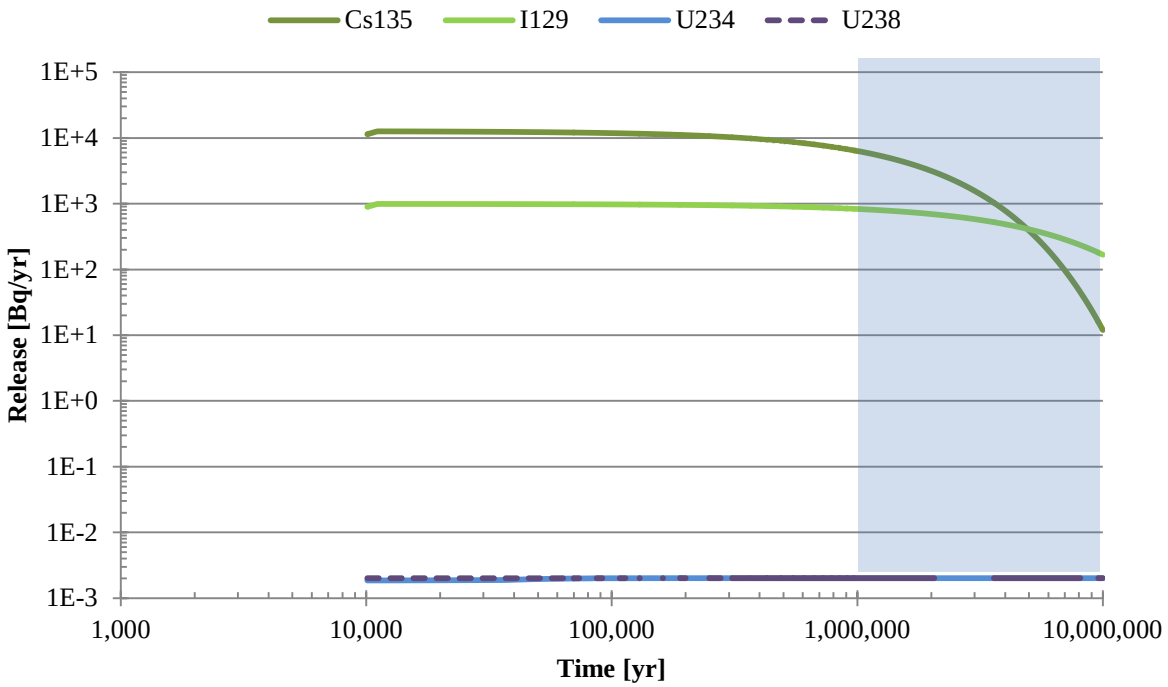

Figure 3.13 – Waste package release using degradation rate of 10^{-5} 1/yr (SOAR)

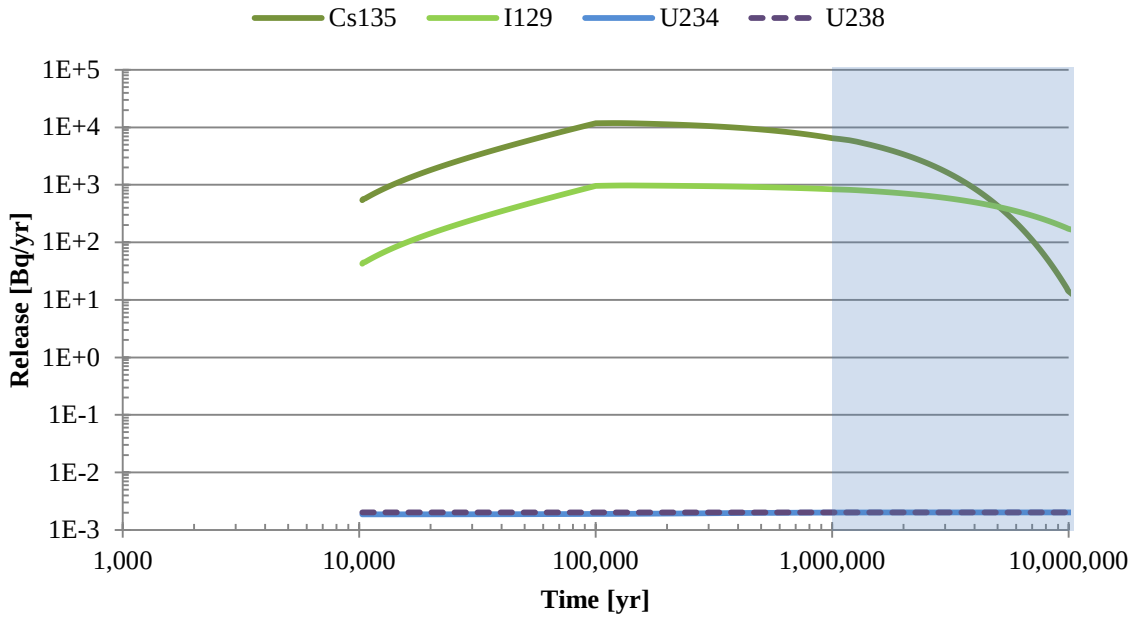

Figure 3.14 – Waste package release using degradation rate of 10^{-7} 1/yr (SOAR)

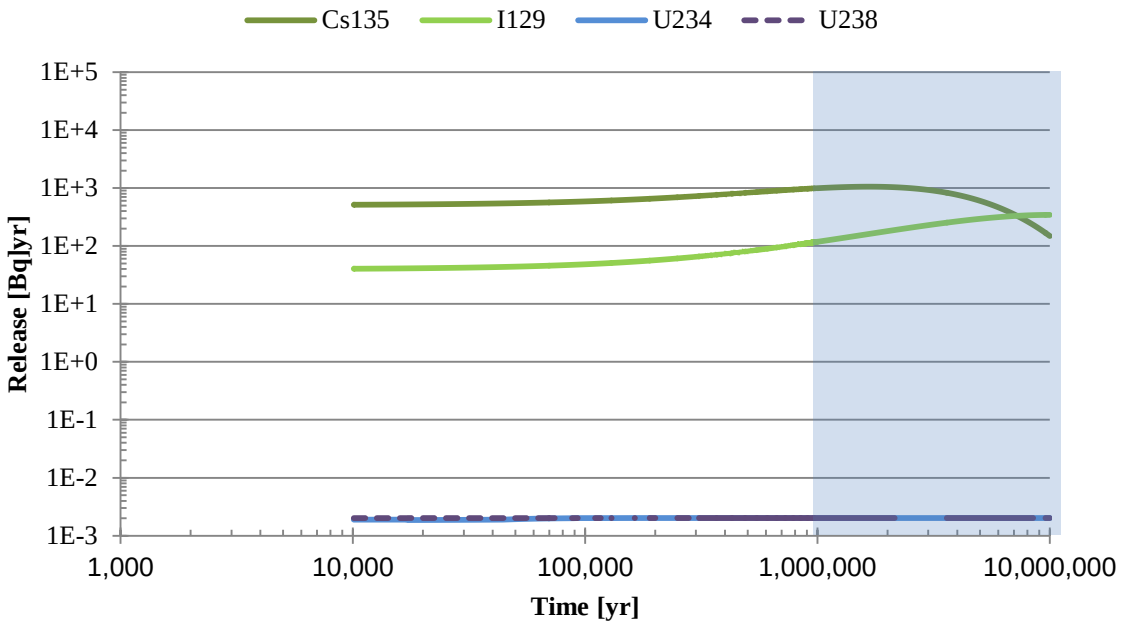

Figure 3.15 – Waste package release using degradation rate changing with time (SOAR)

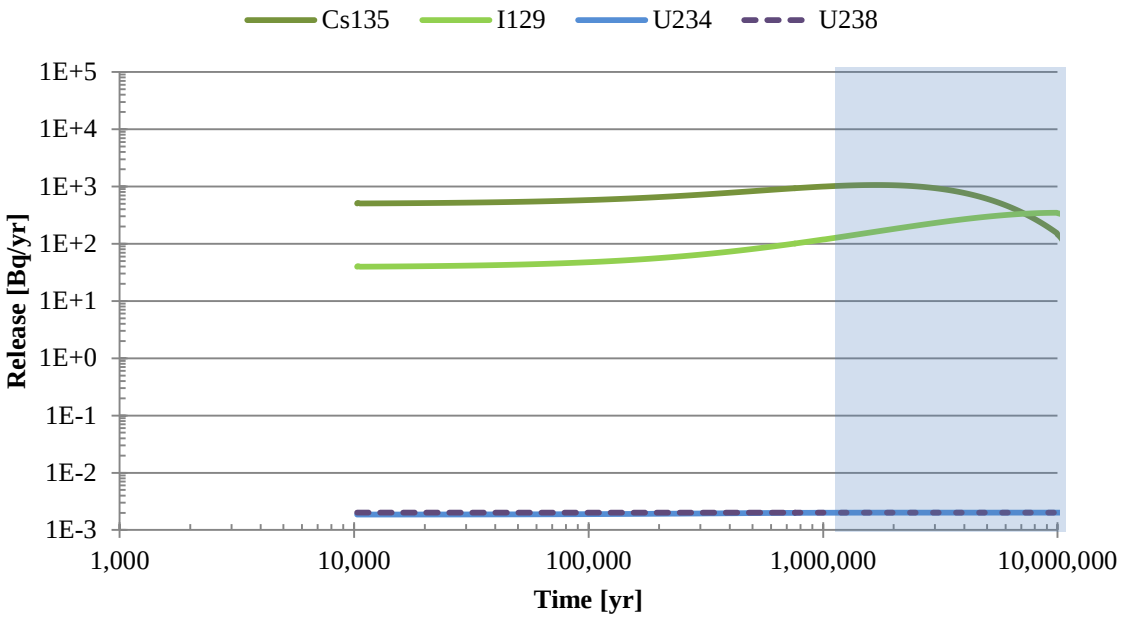

In all cases, the release commences at 10,000 years, which is the time required for water to create a transport pathway out of the package. As stated previously, the release of U-234 and U-238 is dependent on the solubility limit and therefore does not change with the varying methods of

incorporating degradation rate. For Cs-135 and I-129, the release rate increases to a maximum and then decreases over time. Initially, for all cases, the release rate for Cs-135 is greater than that for I-129 and then the release rate for Cs-135 decreases to below that of I-129 at later times. The maximum release rate and time of occurrence for Cs-135 and I-129 for each incorporated degradation method are presented in Table 3.23.

Table 3.23 – Maximum release rates from waste package and time of occurrence for select radionuclides using different waste degradation methods (used in SOAR)

Nuclide	Waste Form Degradation Method							
	10^{-4} 1/yr		10^{-5} 1/yr		10^{-7} 1/yr		Decreasing over time	
	Max Release Rate [Bq/yr]	Time of Occurrence [yr]	Max Release Rate [Bq/yr]	Time of Occurrence [yr]	Max Release Rate [Bq/yr]	Time of Occurrence [yr]	Max Release Rate [Bq/yr]	Time of Occurrence [yr]
Cs-135	12,580	11,260	12,027	101,170	1056	1.65×10^6	1061	1.67×10^6
I-129	991	11,260	981	101,260	344	9.97×10^6	347	9.89×10^6

From the model results with different degradation rates, it was evident that the higher the degradation rate the higher the maximum release and earlier it occurred. The run with the degradation rate decreasing over time had similar results to the run with constant degradation equal to 10^{-7} 1/yr. The reason for this similarity is that only degradation rates after 10,000 years were considered, ranging between 10^{-6} 1/yr and 10^{-8} 1/yr. The runs with higher degradation rates (10^{-4} 1/yr and 10^{-5} 1/yr) reached similar maximum release rates, which were similar to the results predicted by SYVAC3-CC4. The releases from the run with decreasing degradation rates and that from constant degradation rate equal to 10^{-7} 1/yr were too low and therefore were not considered in the remaining discussion.

Due to the differences between how the SOAR and SYVAC3-CC4 models accounted for release of the bound waste form approximations had to be made within SOAR. The best comparison between the SOAR and SYVAC3-CC4 predicted results from the waste package occurred when SOAR assumed a constant degradation rate of 10^{-4} 1/yr and 10^{-5} 1/yr. One possibility may be to determine the SOAR degradation rate which optimizes the comparison to the SYVAC3-CC4 predictions. This degradation rate would be within these higher rates as previously shown as these provided the most similar results to SYVAC3-CC4. As will be shown in the Sensitivity Analysis section, the model runs conducted with degradation rates equal to 10^{-4} and 10^{-5} 1/yr provided similar results indicating that within this range the degradation rate did not affect the results. Therefore, determining the optimum total dose rate to match the waste package releases was not deemed necessary.

3.5.2 Release from the Near Field

Once radionuclides exit the waste package, they are transported through the buffer material of the Near Field before releasing to the Far Field. The release rates from the Near Field to Far Field obtained from the modelling conducted by NWMO (2013a) are presented in Figure 3.16 for Cs-135 and I-129. The solid lines represent the results from SYVAC3-CC4 and the dashed lines the results from the FRAC3DVS-OPG. In all cases, the release begins at 10,000 years increases to a maximum and then declines over time.

Figure 3.16 – Near field release to the Geosphere (NWMO, 2013a)

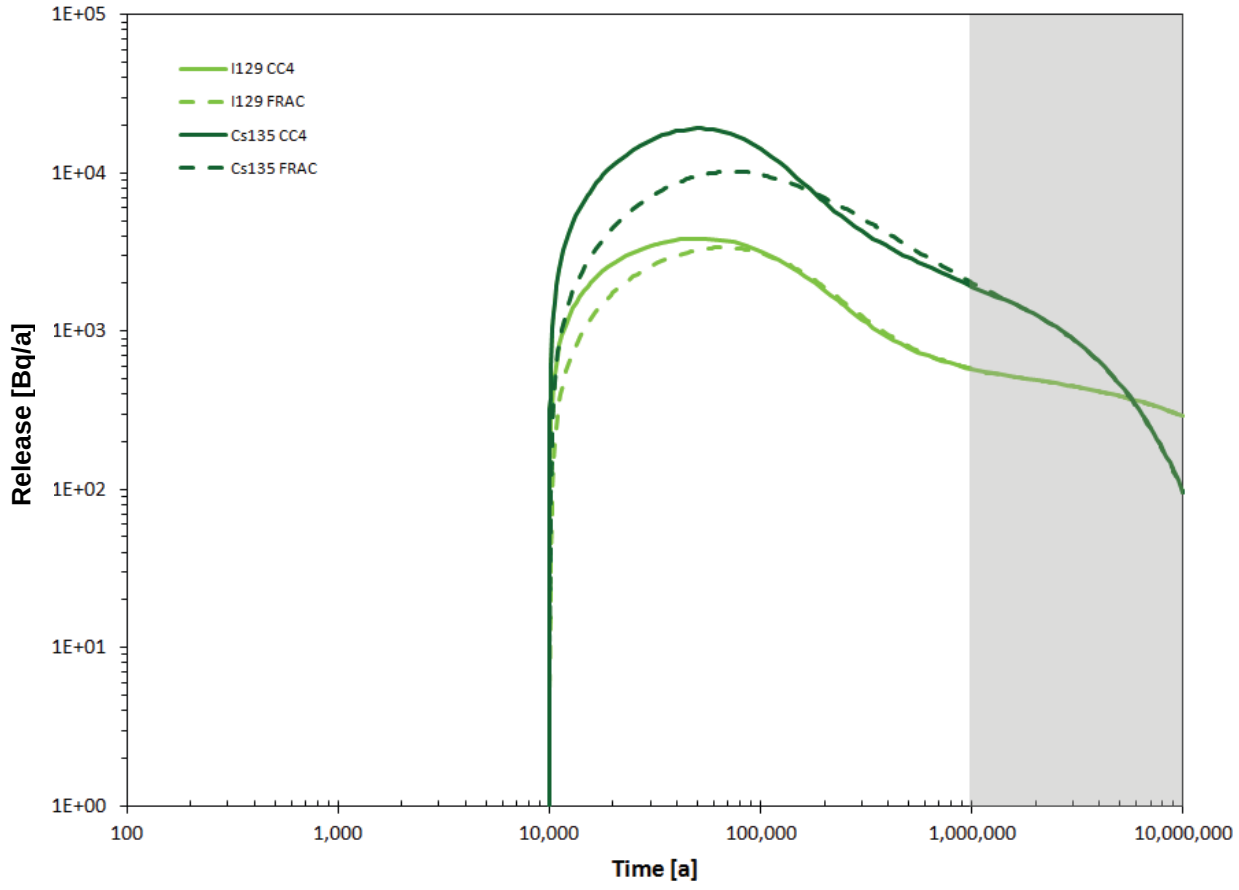

The release from the Near Field was determined from the SOAR modelling results using a degradation rate equal to 10^{-4} 1/yr (solid lines) and 10^{-5} 1/yr (dashed lines) (see Figure 3.17). The purpose of using the two different degradation rates was to evaluate the effect on the release from the Near Field.

The results from using the two different degradation methods provided slightly altered results. At 10,000 years, release from the Near Field began in both cases and increased to a maximum and then declined over time. The results from the higher degradation rate increases to the

maximum release rate faster for both Cs-135 and I-129. At approximately 100,000 years the release rates from both degradation rates meet and follow the same path for the remaining simulation time. This indicates that at later times, the release from the Near Field was not affected by the choice of one of these degradation rates. Both have a plateau after the increase which may be due to the constant degradation rate.

The releases of U-234 and U-238 were also examined. The modelling results presented by NWMO are shown in Figure 3.18. FRAC3DVS-OPG predicted the same releases for both radionuclides. SYVAC3-CC4 also predicted approximately the same releases for both radionuclides, however these occurred earlier than those from the FRAC3DVS-OPG.

Figure 3.17 – Near field release from SOAR model

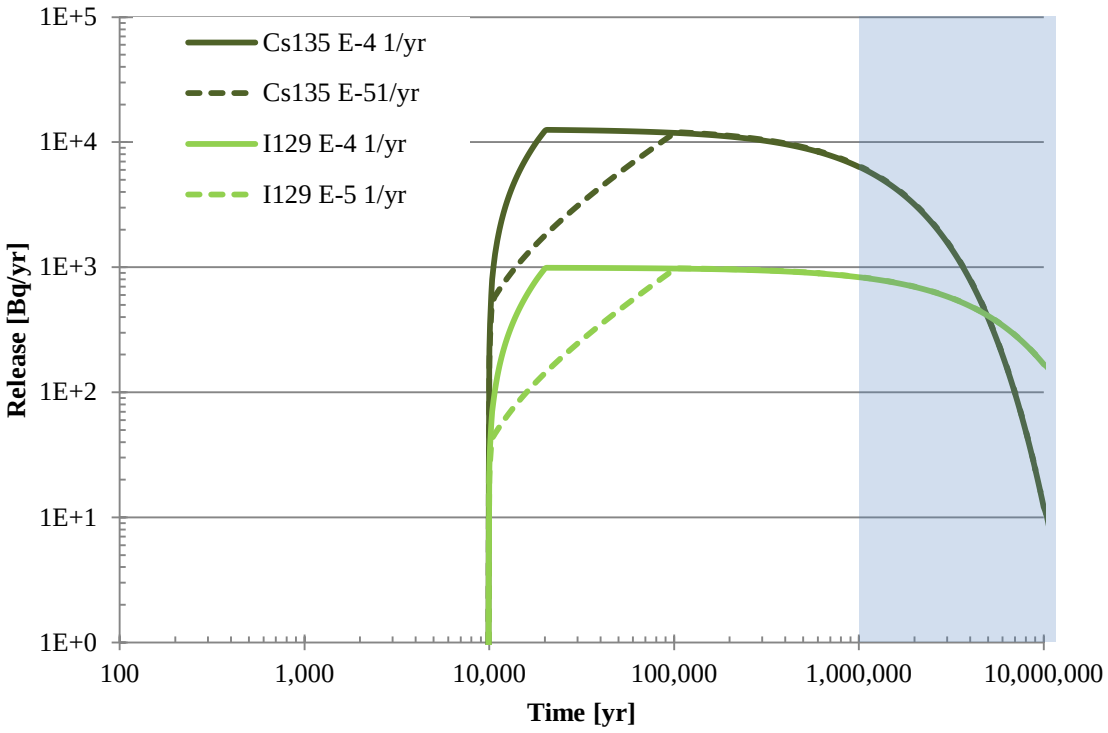

The Near Field releases from SOAR for U-234 and U-238 are presented in Figure 3.19. The releases of U-234 and U-238 are higher than those from the NWMO study and occur earlier. This difference may be due to how the waste package configuration varied and manner in which bound waste form was released.

The maximum release rate and time of occurrence for Cs-135, I-129, U-234 and U-238 predicted by SYVAC3-CC4 from the NWMO study and those from SOAR are presented in Tables 3.24 and 3.25, respectively. For all radionuclides, the maximum release rate predicted for both SOAR runs are within the ratio of 1.08 or less. Therefore, the use of these two degradation rates did not greatly affect the value of the maximum release rate. Comparing the maximum release between

SOAR and SYVAC3-CC4 for Cs-135 and I-129 were approximately within the same order of magnitude. The maximum releases of U-234 and U-238 predicted by SOAR were much greater than those by SYVAC3-CC4.

The time of maximum release for all radionuclides occurred earlier for the higher degradation rate. This result is as expected as the higher degradation rate indicates that the radionuclides would be released faster from the waste form. Comparing the results between SOAR and SYVAC3-CC4 for Cs-135 and I-129 had time of maximum release within an order of magnitude. For the remaining development of the SOAR model, a degradation rate of 10^{-5} 1/yr was used. Within the Sensitivity Analysis section, the impact on the total dose rate due to choice of degradation rate is examined. Investigation of U-234 and U-238, SOAR predicted earlier time of maximum release. Further examination as to how the buffer is treated within both models may be required to determine the cause of this difference.

Figure 3.18 – NWMO Near field releases for U-234 and U-238 (NWMO, 2013a)

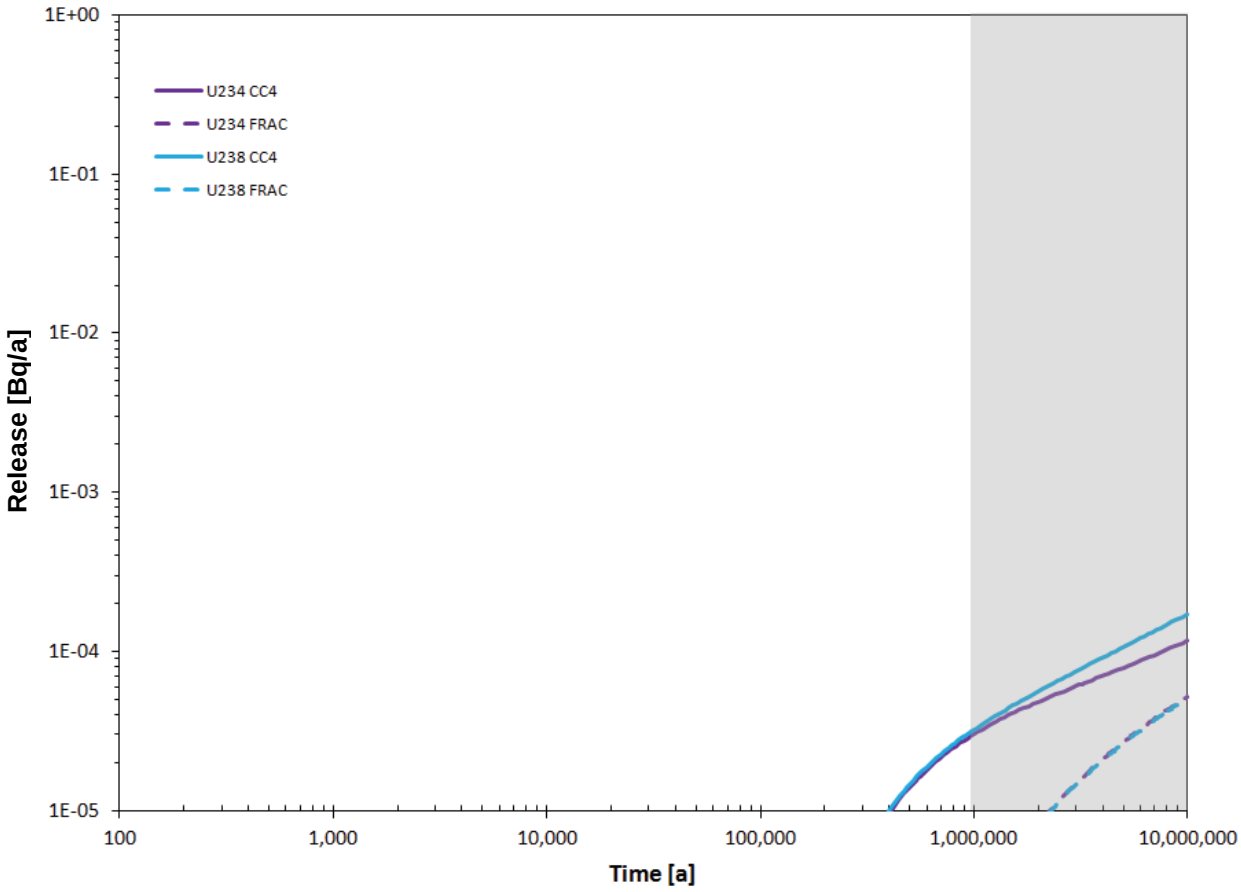

Figure 3.19 – Near field releases for U-234 and U-238 generated from SOAR

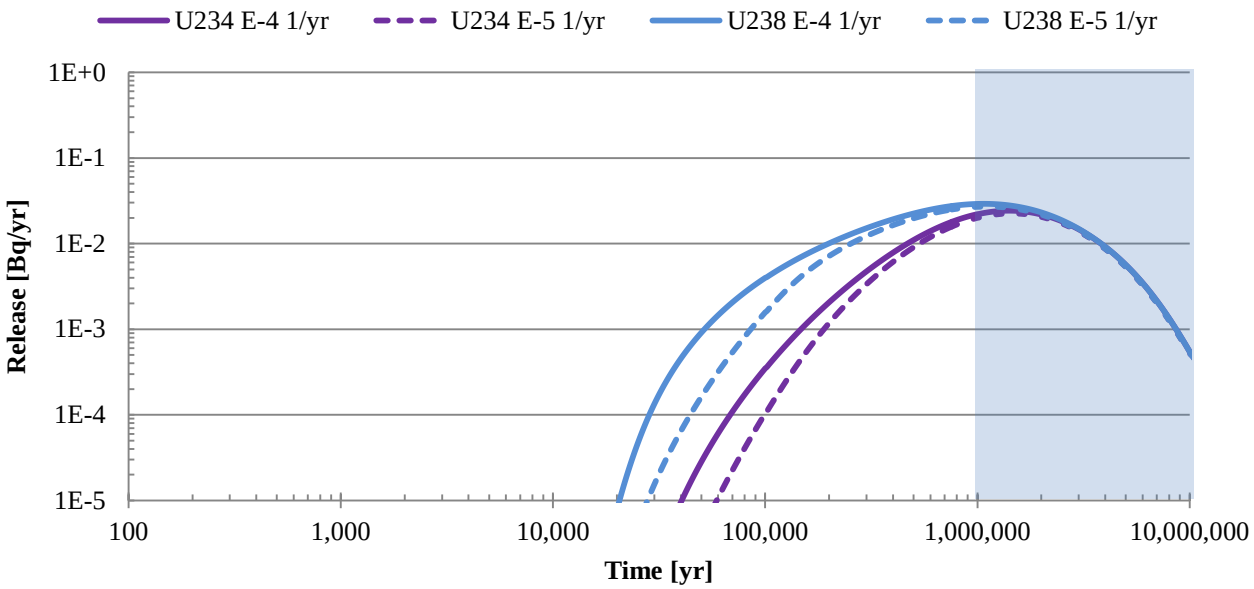

Table 3.24 – Maximum release rates from Near Field for comparison of SOAR and SYVAC3-CC4

Radionuclide	SOAR Maximum Release [Bq/yr]			SYVAC3 Maximum Release [Bq/yr]	Ratio[2]
	Degradation Rate		Ratio[1]		
	10^{-4} 1/yr	10^{-5} 1/yr			
Cs-135	$1.25x10^{4}$	$1.20x10^{4}$	1.04	1.91×10^{4}	0.65
I-129	$9.90x10^{2}$	$9.81x10^{2}$	1.01	3.86×10^{3}	0.26
U-234	$2.42x10^{-2}$	$2.25x10^{-2}$	1.08	1.16×10^{-4}	209
U-238	$2.91x10^{-2}$	$2.70x10^{-2}$	1.08	1.72×10^{-4}	169

1. Ratio is SOAR 10^{-4} 1/yr divided by SOAR 10^{-5} 1/yr.
2. Ratio is SOAR 10^{-4} 1/yr divided by SYVAC3.

Table 3.25 – Time of maximum release for comparison of SOAR and SYVAC3-CC4

Radionuclide	SOAR Time of maximum release [yr]			SYVAC3 Time of maximum release [yr]	Ratio[4]
	Degradation Rate		Ratio[3]		
	10^{-4} 1/yr	10^{-5} 1/yr			
Cs-135	2.05×10^{4}	1.04×10^{5}	0.20	5.26×10^{4}	0.39
I-129	2.08×10^{4}	1.05×10^{5}	0.20	4.98×10^{4}	0.42
U-234	1.41×10^{6}	1.45×10^{6}	0.9	1×10^{7}	0.14
U-238	1.07×10^{6}	1.11×10^{6}	0.96	1×10^{7}	0.11

3. Ratio is SOAR 10^{-4} 1/yr divided by SOAR 10^{-5} 1/yr.
4. Ratio is SOAR 10^{-4} 1/yr divided by SYVAC3.

3.5.3 Releases in Far Field

3.5.3.1 Natural Geosphere

The releases in the Far Field were examined by NWMO (2013a). The results for I-129 and Cs-135 exiting the Cobourg Formation, the Georgian Bay Formation and to the well from the NWMO analysis are presented in Figure 3.20. The release from the Cobourg Formation of Cs-135 was higher and occurred earlier than that of I-129. Cs-135 is a weakly sorbing radionuclide and therefore no release was observed within the modelling time from other layers in geosphere. I-129 is a non-sorbing radionuclide and therefore the releases from the other units occurred at later times and have a lower maximum release as would be expected. The highly sorbing radionuclides U-234 and U-238 had zero release from all formations.

The SOAR model was run and the releases from the formations were examined for I-129, Cs-135, U-234 and U-238 to compare against those results from NWMO. SOAR was run using degradation rates equal to 10^{-4} 1/yr and 10^{-5} 1/yr and was found to give essentially the same releases in the Far Field. Therefore, the remaining releases presented in this report used a degradation rate of 10^{-5} 1/yr.

Similar to the NWMO results, the releases for U-234 and U-238 were zero from all formations for the entire modelling time. The results for I-129 and Cs-135 are presented in Figure 3.21.

Figure 3.20 – Far field releases predicted in NWMO Fifth Case Study (NWMO, 2013a)

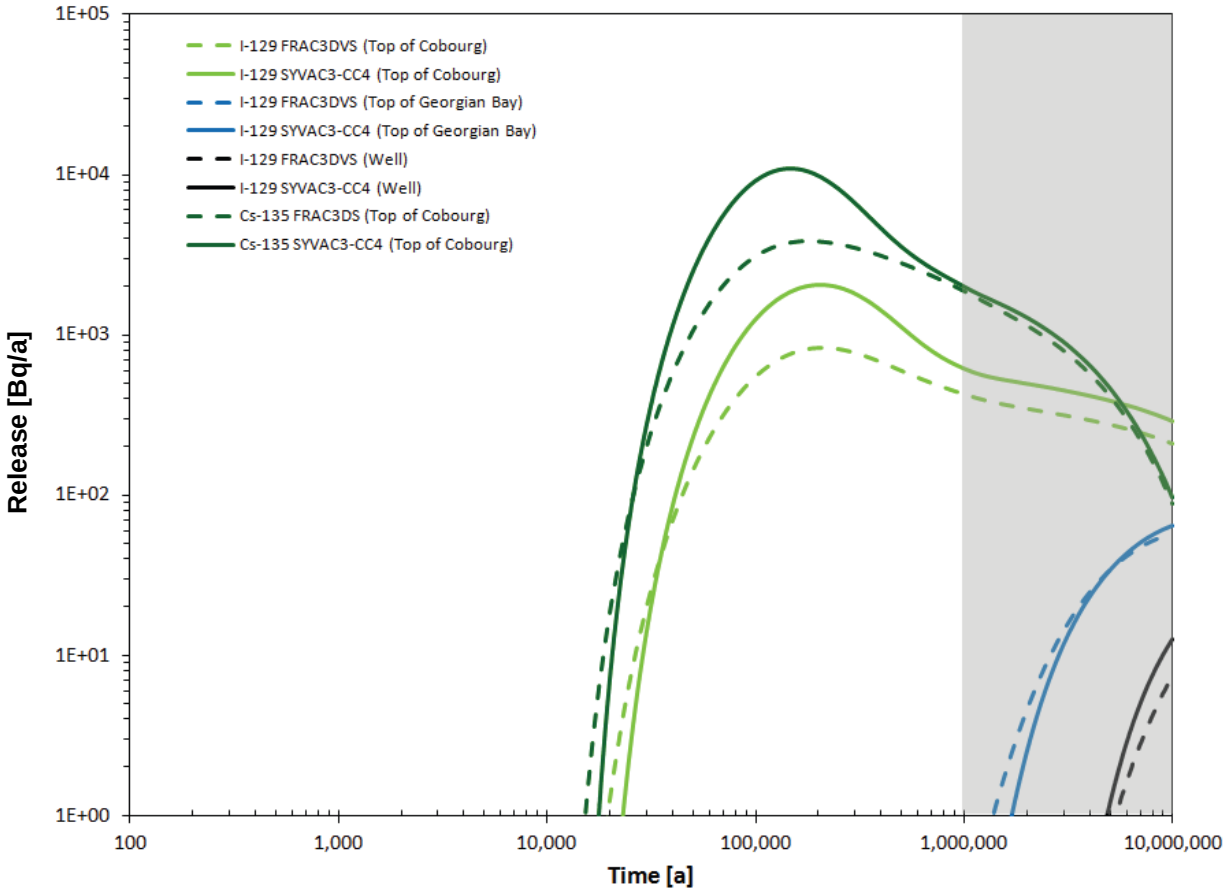

The maximum release of Cs-135 from the Cobourg Formation as predicted by SOAR is 864 Bq/yr which is below that predicted by SYVAC3-CC4 in the NWMO analysis (see Table 3.26). The time of occurrence of this maximum release predicted by SOAR occurs about one order of magnitude later. The SOAR model predicted no release of Cs-135 from the subsequent formations, which is in agreement with the SYVAC3-CC4 model results. Cs-135 is weakly sorbing, which explains no further release within the geosphere. It should be recalled that within SYVAC3-CC4, the repository was divided into five waste vaults and had five separate pathways through the Cobourg Formation before being combined into one pathway through the remainder of the geosphere. Within SOAR, the repository was not divided and only one pathway was modelled through the Cobourg Formation which accounts for the observed difference of release from this formation. However, as both models predict no release from the remaining formations, the difference in release from the Cobourg Formation does not affect the results.

Figure 3.21 – Release rates in the geosphere predicted by SOAR

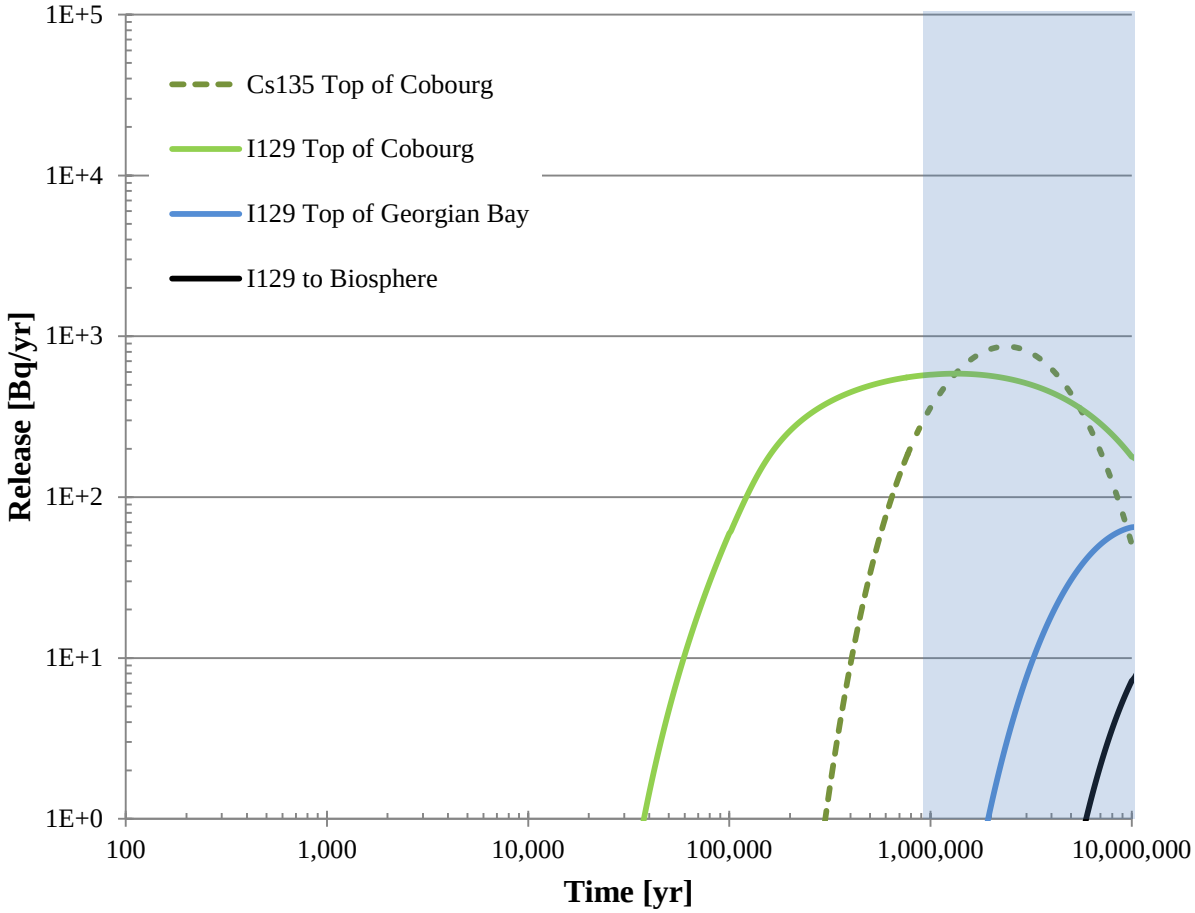

Table 3.26 – Maximum release rates and time of occurrence in geosphere

Nuclide	Layer	Maximum Release Rate [Bq/yr]			Time of Occurrence [yr]		
		SOAR	SYVAC3	Ratio	SOAR	SYVAC3	Ratio
I-129	Cobourg	$5.87x10^{2}$	$2.06x10^{3}$	0.28	$1.32x10^{6}$	$2.05x10^{5}$	6.44
	Georgian Bay	$6.49x10^{1}$	$6.45x10^{1}$	1.01	$1x10^{7}$	$1x10^{7}$	1
	Biosphere	$7.19x10^{0}$	$1.28x10^{1}$	0.56	$1x10^{7}$	$1x10^{7}$	1
Cs-135	Cobourg	$8.64x10^{2}$	$1.09x10^{4}$	0.08	$2.33x10^{6}$	$1.49x10^{5}$	15.6

The maximum release of I-129 from the Cobourg Formation as predicted by SOAR was slightly below that predicted by SYVAC3-CC4 and occurred later. The predicted release of I-129 from the top of the Cobourg Formation differed between these two models. Again, this may be a result of the differences in the representation of the repository and the pathways through the Cobourg Formation. The maximum releases of I-129 from the Georgian Bay Formation and to the biosphere as predicted by SOAR and SYVAC3-CC4 are approximately within the same order of magnitude, occur at the same time and both have not reached maximum at 10,000,000 years. At this point within both models, only one pathway is being represented through the geosphere.

For both Cs-135 and I-129, the predicted releases from the Cobourg Formation were not in agreement between the two models, which may be due to the representation of the waste package or how the buffer was treated in both models. NWMO divided the waste into five vaults and five pathways through the Cobourg Formation, resulting in five releases. Each waste package with a defect was randomly assigned to a waste vault. Each pathway through the Cobourg Formation varied according to the location within the repository. SOAR was modelled with all defect waste packages in one repository with one pathway through buffer and one release from Cobourg Formation possibly causing this observed difference. Differences were also observed in the releases from the Near Field and may be due to the treatment of the buffer zone within the models. Therefore, further investigation into the treatment of this zone within each model may be required.

The predicted releases from the remaining formations and to the biosphere were much better showing better agreement between the models. Within these two models, both represent the transport through these formations using one single pathway. This agreement between models provides confidence in both models results.

3.5.3.2 Shaft

Similar to the natural geosphere path, the releases from the shaft path were examined from the SOAR results. For Cs-135 and I-129, the releases predicted from SOAR are presented in Figure 3.22. Within the shaft units, the sorption coefficient was set to zero for all units due to lack of data for this parameter as presented by NWMO (2013 a, b). Therefore, releases of Cs-135 from Leg 6 were observed since as defined earlier NWMO assumed no sorption within these units.

Figure 3.22 – Cs-135 and I-129 releases in shaft as predicted by SOAR

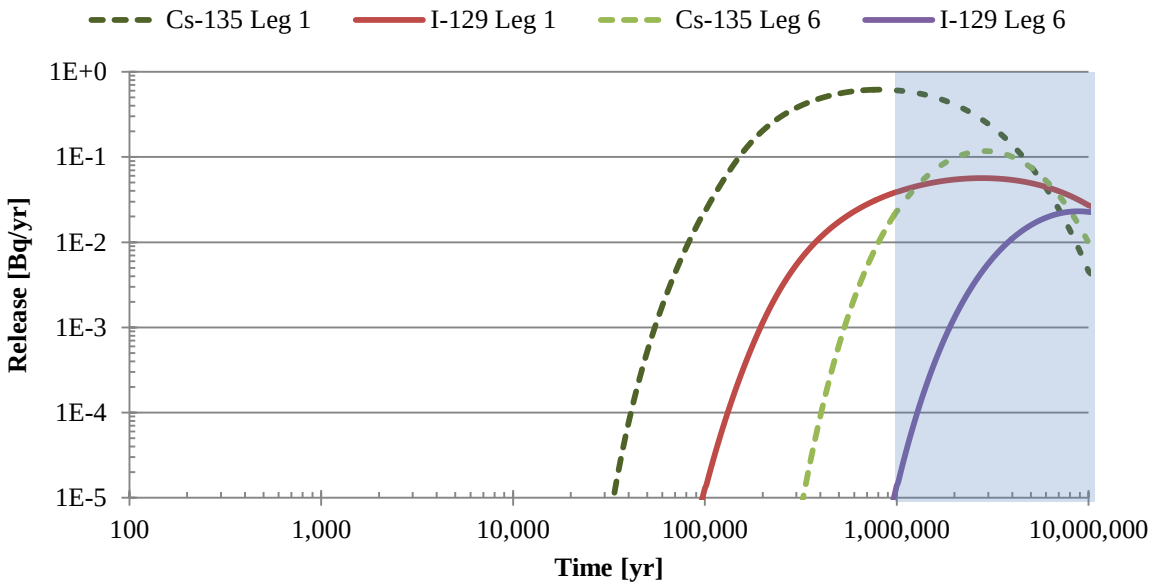

The maximum releases of Cs-135 and I-129 in the shaft are lower than that in the natural geosphere. This result was as expected as only a portion from the Near Field is released to the shaft as assumed by the NWMO in their analyses.

The releases of U-234 and U-238 as predicted by SOAR are presented in Figure 3.23. The maximum releases of U-234 and U-238 in the shaft are lower than that of Cs-135 and I-129 as these are limited by the solubility.

Figure 3.23 – U-234 and U-238 releases in shaft as predicted by SOAR

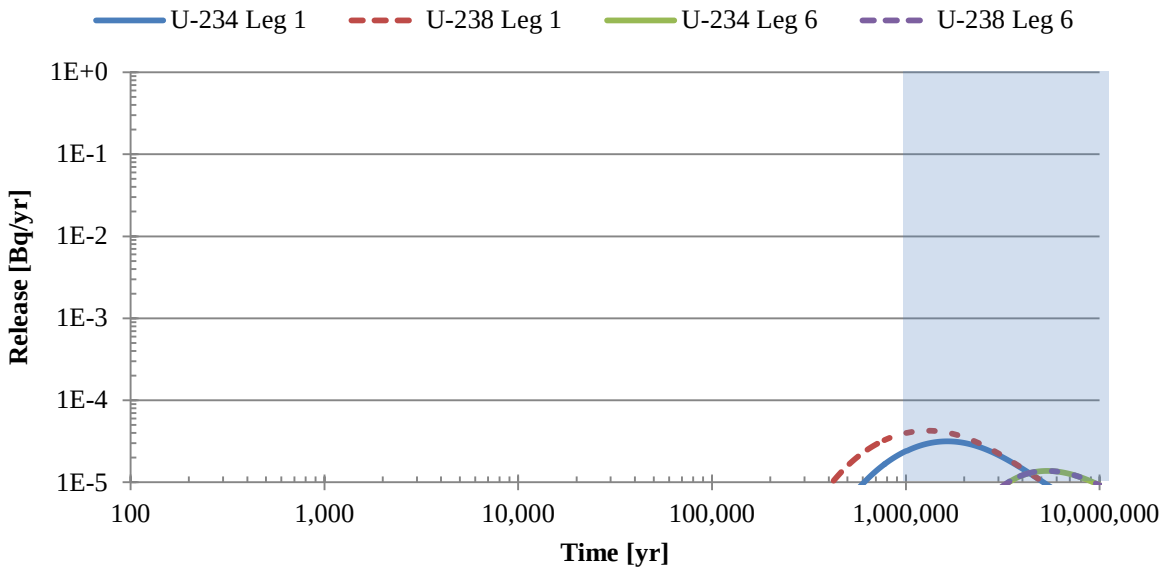

Within the natural geosphere, no release of U-234 and U-238 occurred, due to high sorption of U within the limestone and shale units. However, since sorption is neglected in the shaft units, release of U-234 and U-238 were observed in this pathway.

3.5.3.3 Summary of Far Field Releases

To summarize the releases within the Far Field in the natural geosphere and shaft pathways, I-129 was examined. The time of maximum release and time of 0.1% of maximum release exiting each leg of the pathways as predicted by SOAR are presented in Table 3.27. The release times predicted by SYVAC3-CC4 are also presented for comparison. The release times from the Cobourg Formation as predicted by SOAR occur at later time than predicted by SYVAC3-CC4. This difference may be due to the waste package configuration employed in the two models. As the transport progresses through the formations, the times of occurrence as predicted by SOAR and SYVAC3-CC4 compare better and are on the same order of magnitude. The releases from Cabot Head and Fossil Hill are same to two significant digits.

The releases from the shaft units as predicted by SOAR are in general later than those predicted by SYVAC3-CC4. This difference may be due to the NWMO dividing the repository into five waste vaults and the release to the shaft being from the fifth waste vault. However, in SOAR this configuration is not possible and the repository was considered as one unit.

Table 3.27 – Time of maximum release of I-129 in natural geosphere and shaft materials

Layer	**SYVAC3-CC4**		**SOAR**	
	Time of Maximum Release [year]	**Time of 0.1% of Maximum Release [year]**	**Time of Maximum Release [year]**	**Time of 0.1% of Maximum Release [year]**
Natural Geosphere				
Cobourg	205,000	25,000	1,320,000	34,600
Georgian Bay	15,200,000	1,190,000	11,500,000	1,810,000
Queenston	18,500,000	2,290,000	16,840,000	2,404,000
Manitoulin	19,100,000	2,590,000	18,360,000	2,800,000
Cabot Head	19,600,000	2,780,000	19,120,000	2,998,000

Fossil Hill	20,000,000	3,010,000	20,064,000	3,358,000
Shaft Pathway (0.015% of Near Field Releases)				
Bentonite/Sand	685,000	72,000	2,782,000	15,400
Degraded concrete	691,000	74,000	2,872,000	128,800
Bentonite/Sand	1,400,000	118,000	3,754,000	202,600
Asphalt	2,810,000	264,000	7,174,000	767,800
Bentonite/Sand	5,600,000	410,000	8,776,000	1,054,000
Degraded concrete	5,900,000	418,000	8,812,000	1,072,000

3.6 Summary

The SOAR model was developed using the parameters and concepts presented by the NWMO as used in the SYVAC3-CC4 model. The main differences in how the SOAR model was developed were with the waste package configuration, the method by which the bound waste form was released, the number of radionuclides and that only one exposure pathway was used for dose calculation.

Within SYVAC3-CC4 a dissolution model was used to define how bound waste form was released. For the SOAR model, the degradation rate was accounted for through different degradation rates as well as decreasing over time similar to that conducted in SYVAC3-CC4. The scenario that was presented by NWMO was that three packages were placed within the repository with undetected defects and that it would take 10,000 years for satisfactory water to be present to provide a transport pathway out of the package. The method by which this was modelled within SOAR was to set the breach time at 10,000 years. The issue that arose with using the degradation rates decreasing with time was that SOAR only considered degradation rates after breach occurred thereby neglecting any higher degradation rates occurring before this time. The SYVAC3-CC4 model had degradation occurring from the beginning of the model simulation but travel out of the package did not occur until 10,000 years. As the SOAR model neglected the earlier degradation rates, the release from the waste package was lower.

Other degradation rates were considered that were constant throughout the model simulation. As would be expected, the higher the degradation rate the higher the maximum release rate and earlier the maximum was achieved. Using degradation rates of 10^{-4} 1/yr and 10^{-5} 1/yr in SOAR predicted waste package releases in the same order of magnitude as that predicted by SYVAC3-CC4.

The waste package was represented differently within the two models. In SYVAC3-CC4 the repository was represented using five waste vaults followed by five separate pathways through the Cobourg Formation. After the Cobourg Formation, a single pathway was implemented through the remaining natural geosphere units. The packages with undetected defects were randomly assigned to a specific vault. SOAR does not explicitly model waste package configuration and therefore the repository was represented as one unit and had one pathway through all the natural geosphere units including the Cobourg Formation. These differences are the most probable reason why the two models have different predictions of the release from the Cobourg Formation. However, the releases of I-129 from the Georgian Bay Formation and to the biosphere compare well as this is where both the SYVAC3-CC4 and SOAR models represented the system as a single pathway.

4.0 Deterministic Dose Calculation using SOAR

The SOAR model as developed to model NWMO's Fifth Case Study as presented in the previous section was used to calculate the dose using deterministic parameters. Within this section the method by which the dose is calculated within the SOAR model is discussed. The SOAR model was initially used to determine the dose for the "Reference Case", which used the deterministic parameters as defined by NWMO (2013a and b).

In regards to the predicted total dose rates, the NWMO (2013a) defined an acceptance criterion as 3×10^{-4} Sv/yr, where any dose rate exceeding this value would be deemed unacceptable. A threshold value was also identified as 1×10^{-9} Sv/yr where dose rates below this value were found to be negligible.

It should be recalled that SOAR utilizes a different manner of accounting for degradation of the bound waste form than that by NWMO in the SYVAC3-CC4 model. It was not possible to account for degradation decreasing with time as the releases were underestimated since the higher degradation rates were neglected prior to package breach. Also, SOAR represents the waste package as one unit and one pathway through all the natural geosphere units. This representation differs from that conducted by NWMO using SYVAC3-CC4 in which the repository was divided into five waste vaults, with five pathways through the Cobourg Formation to a single pathway through the remaining units. The aforementioned differences may result in alterations to the releases.

The SOAR model only considers 14 of the 37 radionuclides modelled in SYVAC3-CC4 by the NWMO. The main contributor, I-129, to the total dose is considered in SOAR. The impact of the absence of those not considered by SOAR will be assessed.

The SOAR model was then used to evaluate the sensitivity of the model to several parameters. These included changes to hydraulic conductivity, including the incorporation of the EDZ and changes to the chemical and physical barrier properties.

4.1 Dose Calculation

Within the SOAR model, the dose calculation only considers ingestion of drinking water. The release rate in g/yr predicted within the Far Field Component is passed to the Biosphere Component to determine the dose using the following methodology.

First the mass concentration in g/L of radionuclides entering the well was calculated using equation 4.1. The capture fraction in this equation represents the amount of release that travels to the well. For the Fifth Case Study, the capture fraction was given in the NWMO report from three-dimensional modelling as 93.7% (NWMO, 2013a). The water flow to biosphere is a flow rate from the Far Field to the Biosphere and is equal to the well pumping rate of 1307 m^3/yr (NWMO, 2013a).

$$\textbf{mass concentration } \left[\frac{g}{L}\right] = \frac{\textbf{Capture Fraction} * \textbf{Release}[\frac{g}{yr}]}{\textbf{Water Flow to Biosphere } [\frac{L}{yr}]} \qquad \textbf{4.1}$$

The activity concentration is then calculated using equation 4.2 using the specific activity values given in Table 4.1.

$$\textbf{activity concentration } \left[\frac{Bq}{L}\right] = \textbf{mass concentration } \left[\frac{g}{L}\right] * \textbf{specific activity } \left[\frac{Bq}{g}\right] \qquad \textbf{4.2}$$

Table 4.1 – Specific activities and ingestion dose coefficients of radionuclides

Species	Specific Activity [Bq/g]	Ingestion Dose Coefficient [Sv/Bq]
C-14	1.6576×10^{11}	5.8×10^{-10}
Cs-135	4.26×10^{7}	2×10^{-9}
I-129	6.531×10^{6}	1.1×10^{-7}
Np-237	2.6031×10^{7}	1.1×10^{-7}
Pu-238	6.3372×10^{11}	2.3×10^{-7}
Pu-239	2.2955×10^{9}	2.5×10^{-7}
Pu-240	8.4002×10^{9}	2.5×10^{-7}
Pu-242	1.4634×10^{8}	2.4×10^{-7}
Se-79	5.6757×10^{8}	2.9×10^{-9}
Tc-99	6.3292×10^{8}	6.4×10^{-10}
U-232	8.1682×10^{11}	3.3×10^{-7}
U-233	3.5659×10^{8}	5.1×10^{-8}
U-234	2.3025×10^{8}	4.9×10^{-8}
U-235	7.9975×10^{4}	4.7×10^{-8}
U-236	2.3932×10^{6}	4.7×10^{-8}
U-238	1.2439×10^{4}	4.5×10^{-8}

The dose was then calculated using equation 4.3 and the ingestion dose coefficients given in Table 4.1. The water consumption rate used by the NWMO in their analysis was 0.84 m^3/yr (NWMO, 2013a).

$$\boldsymbol{Dose}\left[\frac{\boldsymbol{Sv}}{\boldsymbol{yr}}\right] = \boldsymbol{activity\ concentration}\left[\frac{\boldsymbol{Bq}}{\boldsymbol{L}}\right] * \boldsymbol{Ingestion\ Dose\ Coefficient}\left[\frac{\boldsymbol{Sv}}{\boldsymbol{Bq}}\right] * \boldsymbol{water\ consumption\ rate}\left[\frac{\boldsymbol{m^3}}{\boldsymbol{yr}}\right] \qquad \textbf{4.3}$$

Using this methodology, SOAR calculates the dose rate for each radionuclide as well as the total dose rate.

4.2 Dose from Reference Case

The NWMO in their analyses calculated the total dose rate for the "Reference Case" over time (see Figure 4.1). On the figure, the times greater than 1,000,000 years and dose rates below the threshold level are shaded to depict times and dose rates that are out of range or minimal.

Figure 4.1 – Reference case total dose rate as predicted by SYVAC3-CC4 (Taken from NWMO (2013a))

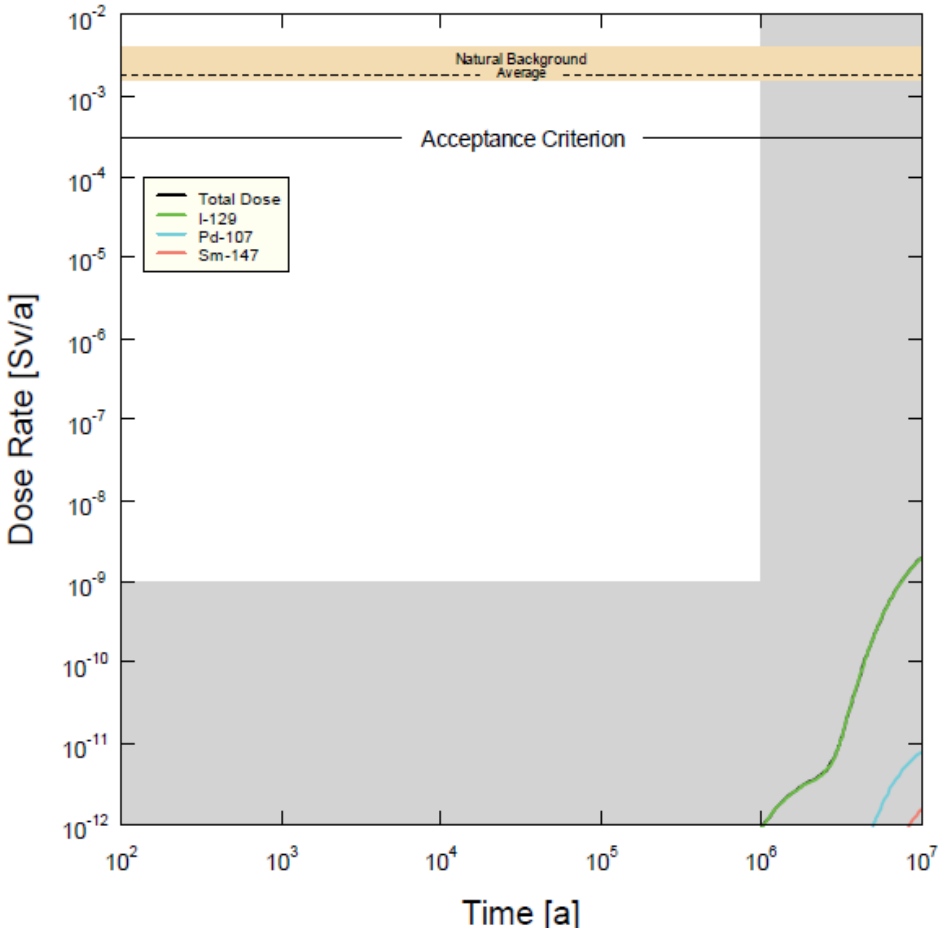

The dose rates were predicted by SYVAC3-CC4. At 1,000,000 years, the observable dose was 10^{-12} Sv/yr and increased to approximately 2 x 10^{-9} Sv/yr at 10,000,000 years. The maximum dose rate was not reached within the modelling time of 10,000,000 years. Within the first

1,000,000 years the predicted total dose rate was below the threshold level and below the acceptance criterion at all times.

The pathways for this Reference Case as presented by NWMO are presented in Table 4.2. The main contributor to the total dose rate was I-129 with 99.5% contribution to the total dose. The input from I-129 is through an internal dose with almost equal contributions between food ingestion and water ingestion and a much smaller contribution due to external dose. Lesser contributions from Pd-107 (0.4% of total) and Sm-147 (0.1%) were observed. SOAR does not consider Pd-107 and Sm-147 in the prediction, however as the contributions are so low this absence was not an issue.

Table 4.2 – Radionuclide Dose Pathways for the SYVAC3-CC4 Reference Case (taken from NWMO (2013a))

Element	Internal Dose [Sv/yr]	% of total Internal Dose	Primary Pathways	%	External Dose [Sv/yr]	Primary Pathways	%
I-129	2×10^{-9}	99.5	Food Ingestion	54	6.4×10^{-14}	Groundshine	86
			Water Ingestion	46		Water Immersion	13
Pd-107	7.9×10^{-12}	0.4	Food Ingestion	90	0	None	0
			Water Ingestion	8			
Sm-147	1.6×10^{-12}	0.1	Food Ingestion	57	0	None	0
			Air Inhalation	34			

The SYVAC3-CC4 predication had an internal dose from I-129 which had approximately equal contribution via ingestion of food and water. The SOAR model only considers ingestion of water in the calculation of the total dose in the biosphere model. Due to the difference in ingestion pathways, it would be expected that the predicted dose by SOAR would be approximately half that predicted by SYVAC3-CC4.

The SOAR model was run for the Reference Case and the results are presented in Figure 4.2. As with the SYVAC3-CC4 model prediction, I-129 was the main contributor. The time to reach a total dose rate of 10^{-12} Sv/yr as predicted by SOAR was later than that predicted by SYVAC3-CC4 (see Table 4.3). The maximum total dose rate as predicted by SOAR was lower than SYVAC3-CC4 as expected. The reason for SOAR having different dose rates were variations in bound waste release, waste package configuration and only one exposure pathway. At all times the total dose rate as predicted by SOAR was well below the threshold level and over five orders of magnitude below the acceptance criterion.

Within the SYVAC3-CC4 model, the repository was divided into five waste vaults and those containers with defects were randomly assigned to a waste vault. It was assumed that 0.015% release from the fifth waste vault was sent to the shaft. As stated previously, to account for this

within SOAR, 0.015% of the Near Field release was sent to the shaft pathway. An alternative method would be to use one fifth of the Near Field release multiplied by 0.015% to be sent to the shaft. Using the initial method the model was run for the Reference Case. Investigation of the results illustrated that the shaft pathway contributed 0.31% of the total dose rate. As this quantity is minimal, the assumption does not greatly impact the results.

Figure 4.2 – Reference case total dose rate as predicted by SOAR

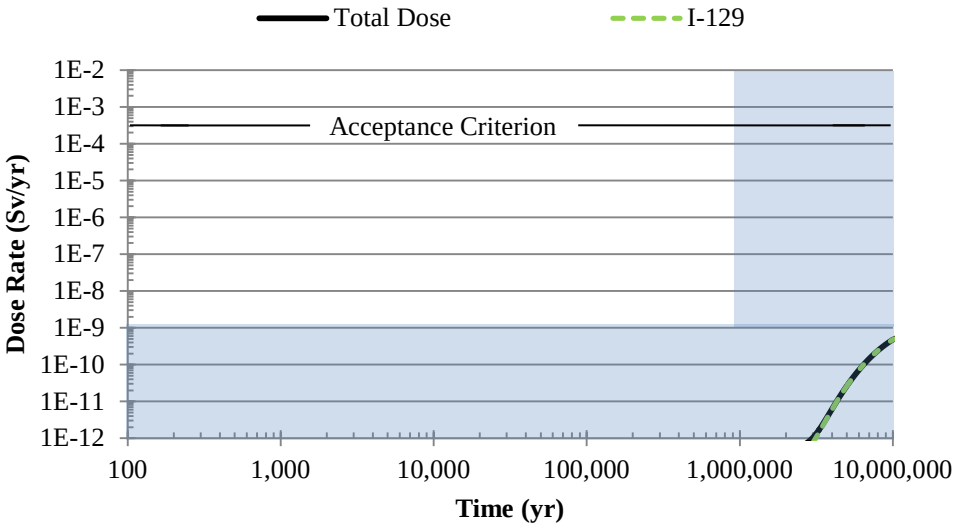

Table 4.3 – Comparison between SOAR and SYVAC3-CC4 dose rates for Reference Case

Parameter	SYVAC3-CC4	SOAR
Time to reach 10^{-12} Sv/yr (yr)	1,000,000	2,980,000
Maximum total dose rate (Sv/yr)	2×10^{-9}	5×10^{-10}
Time to reach maximum (yr)	10,000,000	10,000,000

4.3 Sensitivity Analysis

The total dose rate predicted by SOAR was subject to many different parameters, such as hydraulic conductivity, physical barrier properties and chemical barrier properties. Sensitivity analyses were conducted by changing parameters individually while maintaining all other parameters the same as the Reference Case. The model was run with the altered parameter and then compared against the Reference Case.

4.3.1 Sensitivity to Hydraulic Conductivity

The SOAR model used the hydraulic conductivity to calculate the steady-state flow rate by which the radionuclides were transported through the geosphere. To assess the sensitivity to hydraulic conductivity, three different scenarios were considered. The first scenario was to increase the hydraulic conductivity of each leg within the Far Field component. The second and third scenarios were to consider the EDZ along the natural geosphere and shaft pathways and how this would affect the flow rate and transport to the biosphere. The sensitivity analyses considered in these cases are as follows:

- Increased hydraulic conductivity by 10 times
- Inclusion of EDZ along the natural geosphere path
- Consideration of EDZ along the shaft path

4.3.1.1 Increased Hydraulic Conductivity in the Far Field

Hydraulic conductivity affects flow rate and hence transport. However, in the Reference Case the hydraulic conductivity was sufficiently low that advective transport was negligible and was diffusion dominated. To determine how sensitive the predicted total dose rates were to the hydraulic conductivity, the value defined for each leg in the natural geosphere and shaft pathways were increased by a factor of 10. The model was run and the total dose rate is presented in Figure 4.3.

The increase in hydraulic conductivity resulted in an increase in the model predicting an earlier release and increased total dose at earlier times. At later times, the model predictions follow a similar pattern to the Reference Case. The increased total dose rate was a result of increased flow rate.

Figure 4.3 – SOAR predicted total dose rates with hydraulic conductivity increased by a factor of 10

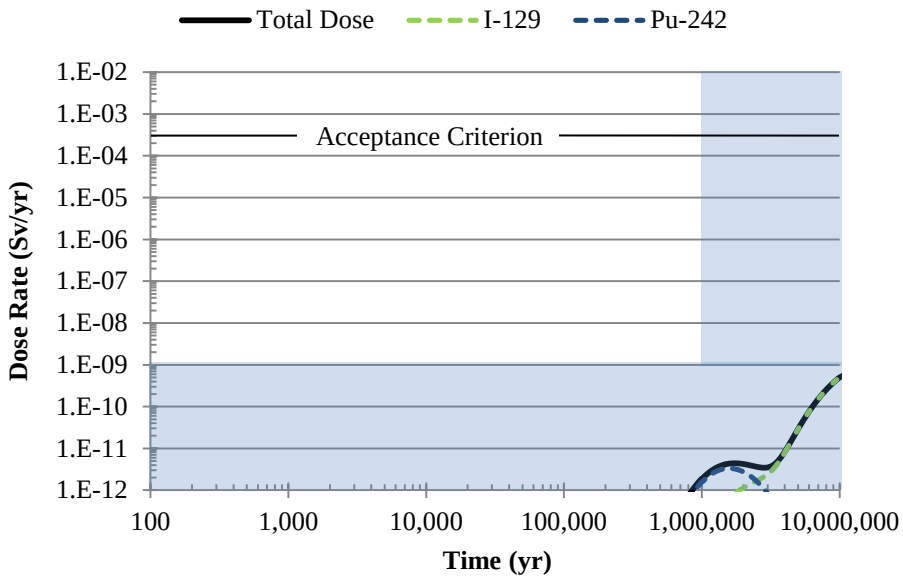

4.3.1.2 EDZ along natural geosphere pathway

The method by which the EDZ along the natural geosphere pathway was modelled within SOAR was discussed in Section 3.4.6. The SOAR model was run with the consideration of the EDZ through the natural geosphere path and the dose rates were calculated (see Figure 4.4).

The total dose rate reached 10^{-12} Sv/yr at approximately 3,000,000 years and increased to a maximum of 5×10^{-10} Sv/yr at 10,000,000 years. There is not a large difference between the consideration of the EDZ along the natural geosphere path and the Reference Case. This was most likely a result that the problem was only considered in one dimension. Whereas in actuality the flow that would occur in this particular EDZ would be perpendicular to the considered flow direction as it would be along the placement room walls. Therefore, this problem would be better considered in two or three dimensions.

Figure 4.4 – Total dose rate considering EDZ in natural geosphere pathway

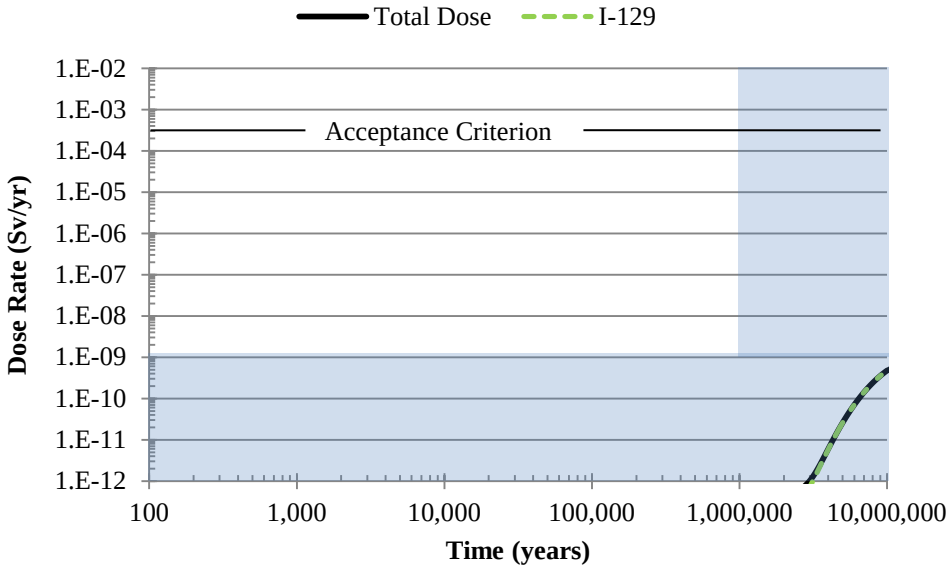

4.3.1.3 EDZ along shaft pathway

For the shaft pathway, the EDZ transport direction would be parallel to that within the backfilled shaft materials as discussed in Section 3.4.6. The model altered to account for the EDZ along the shaft pathway and was run and the total dose rate was calculated (see Figure 4.5).

Figure 4.5 – Total dose rate considering EDZ in shaft pathway

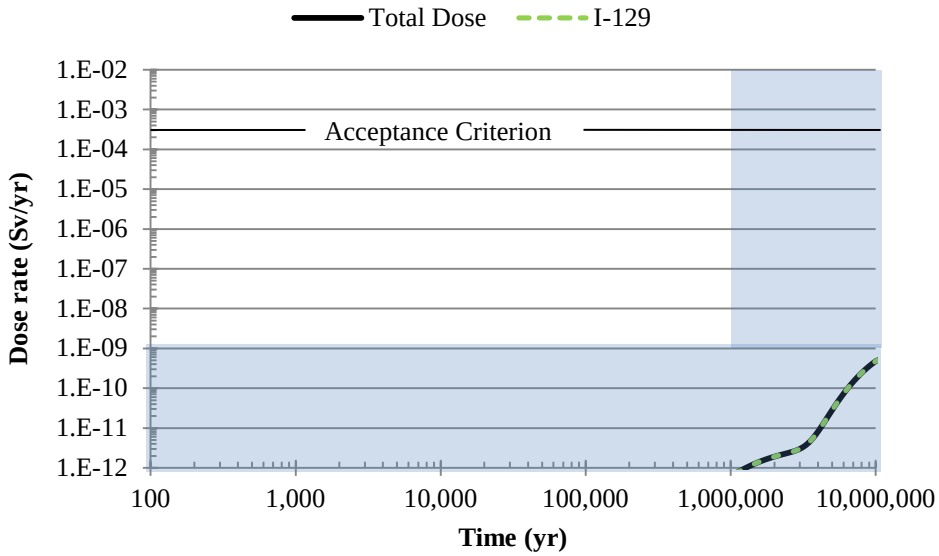

When considering the EDZ along the shaft pathway, the SOAR model predicted that 10^{-12} Sv/yr would be reached at 1,290,000 years. The maximum total dose rate was higher at 5 x 10^{-10} Sv/yr, which was reached at 10,000,000 years. The total dose rate was higher for times less than approximately 3,000,000 years then followed the same rates as predicted for the Reference Case.

4.3.1.4 Summary

In order to examine the effects of the different changes in hydraulic conductivity or incorporation of the EDZ, the total dose rates were plotted against those from the Reference Case (Figure 4.6) and times of occurrence were compared (Table 4.4). The increase in hydraulic conductivity had the most significant effect as it resulted in higher flow rate and therefore increased transport and ultimate dose. The consideration of the EDZ along the shaft path also resulted in an increase in total dose rate. In modelling this scenario, the blocks that would be keyed in to stop preferential flow along the EDZ were not considered. Accounting for the EDZ along the natural geosphere pathway did not result in a large change from the Reference Case. The EDZ along this pathway would be better represented by a two- or three-dimensional model. For all cases, the total dose rate within the first one million years is below the threshold level and is below the acceptance criterion at all times.

Figure 4.6 – Sensitivity of SOAR to hydraulic conductivity changes

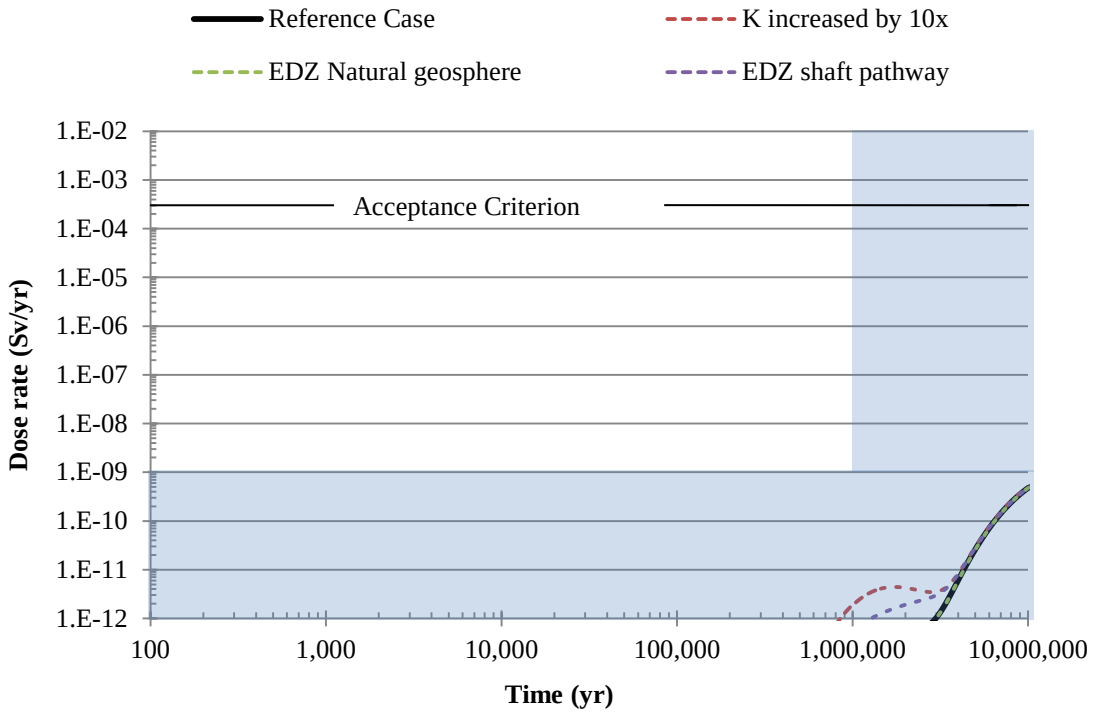

Table 4.4 – Sensitivity to hydraulic conductivity changes

Parameter	Reference Case	K increased 10x	EDZ along natural geosphere pathway	EDZ along shaft pathway
Time to reach 10^{-12} Sv/yr (yr)	3,000,000	852,400	3,000,000	1,290,000
Maximum total dose rate (Sv/yr)	5×10^{-10}	5×10^{-10}	5×10^{-10}	5×10^{-10}
Time to reach maximum (yr)	10,000,000	10,000,000	10,000,000	10,000,000

4.3.2 Sensitivity to a Degraded Physical Barrier

The NWMO in their analysis investigated the sensitivity of the SYVAC3-CC4 model results to parameters related to the physical barrier as follows:

- Increase the degradation rate by one order of magnitude (10^{-4} 1/yr)
- Decrease the degradation rate by two orders of magnitude (10^{-7} 1/yr)
- Increase the defect area by an order of magnitude
- Increase instant release of all radionuclides to 10%
- Increase the diffusion coefficient by one order of magnitude

The results of these sensitivity analyses as predicted by SYVAC3-CC4 for the NWMO analyses are presented in Figure 4.7 and Table 4.5. The different sensitivity cases were compared against the total dose rate of the Reference Case. From this figure, it was determined that the instant release fraction and defect area did not have a large effect on the total dose rate from the Reference Case. The increase in fuel dissolution, or degradation rate, increased the total dose rate at all times, indicating that this parameter had more effect. The higher diffusivity values in the geosphere had the largest impact on the resulting total dose rate. For this case, the release was observed at earlier times and had a larger maximum. For all cases at all times the total dose rate was below the acceptance criterion.

These same sensitivity cases were analysed for the SOAR model to ascertain the sensitivity to these different parameters and to compare against the NWMO results.

Figure 4.7 – Sensitivity to a Degraded Physical Barrier using SYVAC3-CC4 (taken from NWMO, 2013)

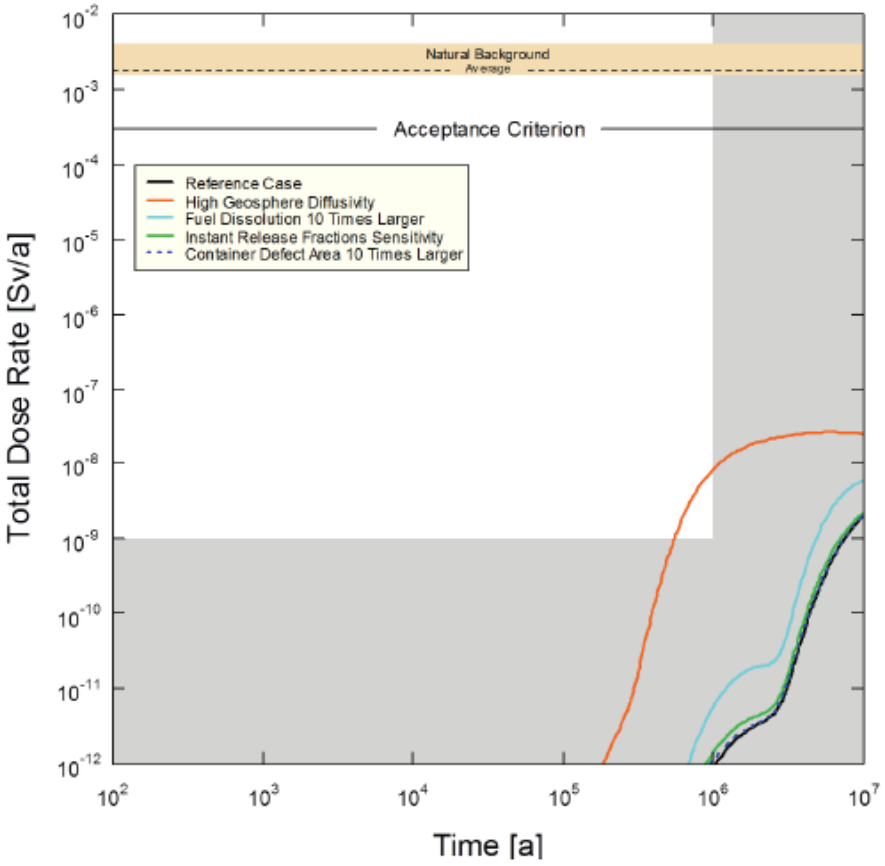

Table 4.5 – Sensitivity to physical barrier changes as predicted by SYVAC3-CC4 (values are approximate)

Parameter	Reference Case	Increased degradation rate	Increased defect area	Instant release fraction of 10%	Increased diffusivity
Time to reach 10^{-12} Sv/yr (yr)	1,000,000	700,000	1,000,000	1,000,000	200,000
Maximum total dose rate (Sv/yr)	2×10^{-9}	8×10^{-9}	2×10^{-9}	2×10^{-9}	2×10^{-8}
Time to reach maximum (yr)	10,000,000	10,000,000	10,000,000	10,000,000	10,000,000

4.3.2.1 Degradation Rate Sensitivity

The waste form in the deep geological repository would be encased by a buffer material. Once water reaches the waste form a portion would be released instantly and the remaining waste would be released over time. The rate at which waste was released in the SYVAC3-CC4 model was defined by a dissolution model in mol/yr. However, the SOAR model required a degradation rate in 1/yr. In the NWMO sensitivity analysis, the dissolution rates from the model were increased by a factor of 10. For the SOAR model, the degradation rate was also increased by a factor of 10. The degradation was also decreased by a factor of 10^2 to observe the effects.

The degradation rate that was used for the Reference Case was 10^{-5} 1/yr. For this sensitivity case, the degradation rates were increased to 10^{-4} 1/yr for one simulation and then decreased to 10^{-7} 1/yr for another. All other parameters were kept the same and the model was run to ascertain the sensitivity to degradation rate and the dose rate was calculated (see Figures 4.8 and 4.9).

Figure 4.8 – SOAR prediction with increased degradation rate to 10^{-4} 1/yr

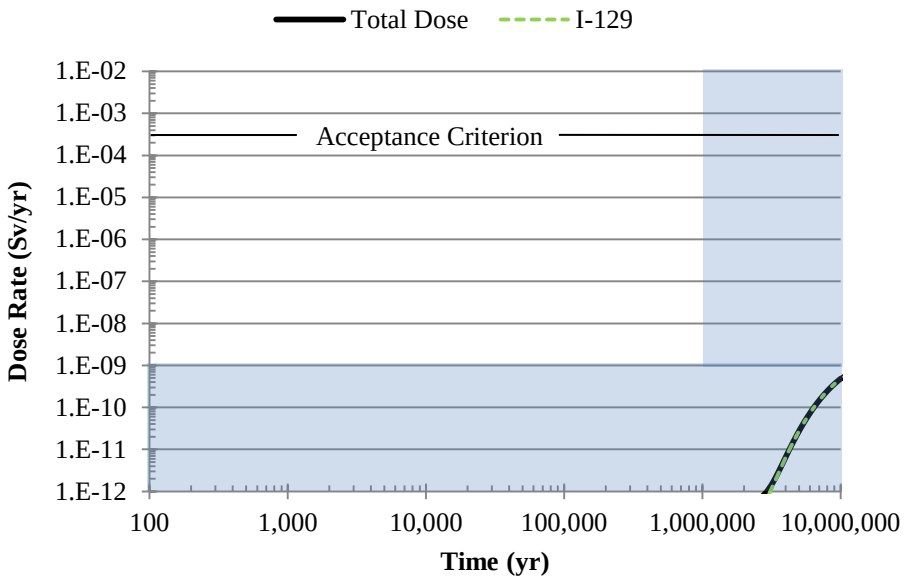

Figure 4.9 – SOAR prediction with increased degradation rate to 10^{-7} 1/yr

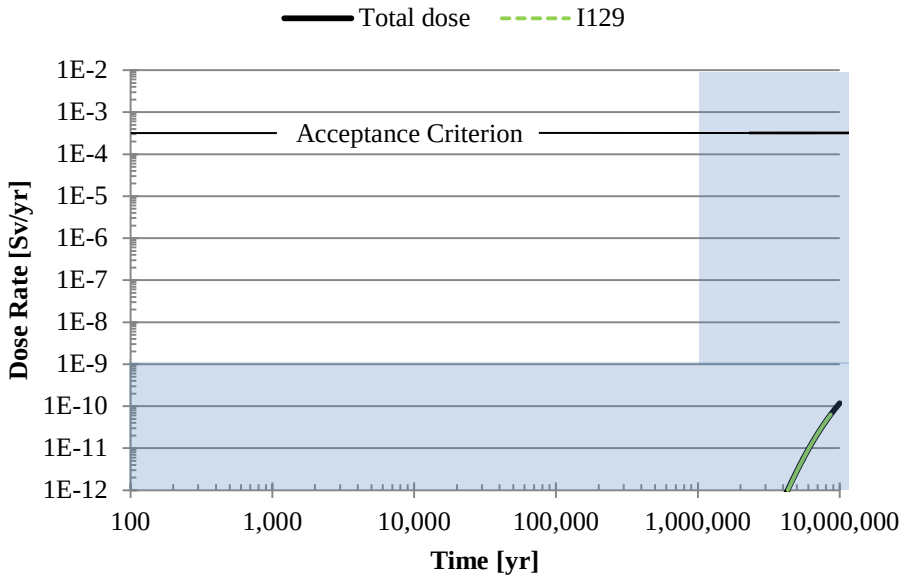

Comparing the case of increased degradation rate against the Reference Case in Figure 4.2 indicates that this change resulted in no large difference from the Reference Case. The release began slightly earlier, with a total dose rate reaching 10^{-12} Sv/yr at 2,930,000 years and reaching 4.8×10^{-10} Sv/yr at 10,000,000 years.

The NWMO sensitivity analysis with respect to fuel dissolution rate resulted in a large impact on the total dose rate. In the NWMO's case, the fuel dissolution rates that varied over time were increased by one order of magnitude. The SOAR model utilized a constant degradation rate and therefore an order of magnitude increase was not an equivalent comparison resulting in the observed differences in impact. This order of magnitude increase in degradation rate did not have a large impact on the SOAR predicted total dose.

To further observe the effects of the degradation rate on total dose rate, a run was conducted with the degradation decreased by two orders of magnitude. As expected the total dose rate occurred later and had a lower maximum total dose rate. The total dose rate reached 10^{-12} Sv/yr at 4,300,000 years and had a maximum total dose of 1.2×10^{-10} Sv/yr.

4.3.2.2 Defect Area Sensitivity

The SOAR model was developed with three packages containing defects with radius of 1 mm. The radionuclides escape the packages through these defects to the Near Field. By increasing the

size of the defect it was expected that the total dose rate would increase. To examine the sensitivity, the defect area was increased by one order of magnitude, while maintaining all other parameters the same as the Reference Case. The SOAR model was run and the dose rates were predicted (see Figure 4.10).

Figure 4.10 – SOAR prediction with increased defect area

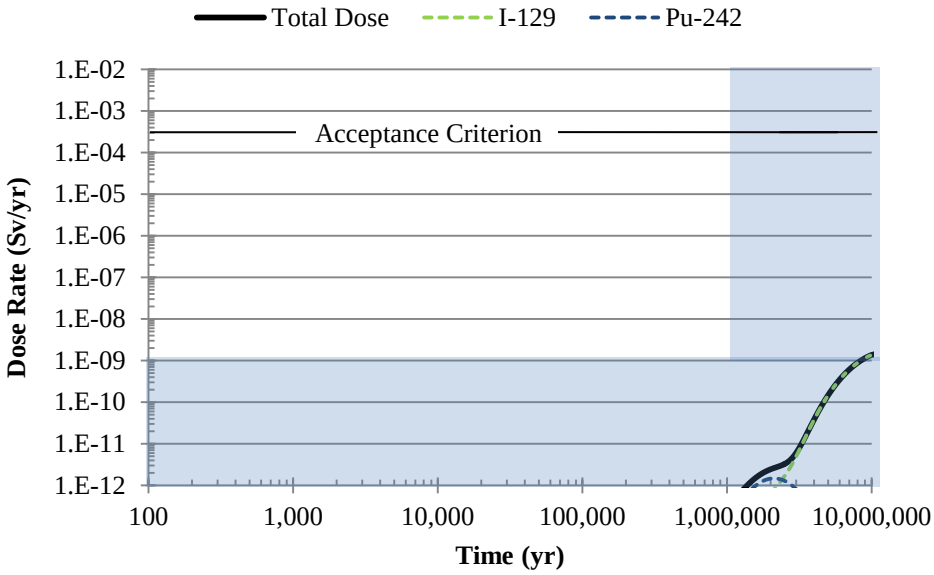

The increase in defect area resulted in a slightly larger dose rate predicted by SOAR. The dose rate was predicted to reach 10^{-12} Sv/yr at 1,380,000 years which was earlier than that of the Reference Case. Also, the maximum total dose rate was higher at a level of 1.4×10^{-9} Sv/yr occurring at 10,000,000 years. As with the Reference Case, the main contributor was I-129. For the NWMO analysis, the defect area did not result in a large change in the predicted total dose rate by SYVAC3-CC4.

4.3.2.3 Instant Release Sensitivity

The instant release fraction is that component of waste that would release instantaneously once the waste form comes into contact with water. For this scenario, the instant release fraction for all radionuclides was increased to 10%. The SOAR model was run with all remaining parameters the same as the Reference Case. The total dose rate was predicted by the SOAR model and is presented in Figure 4.11.

Figure 4.11 – SOAR prediction with instant release fraction of 10%

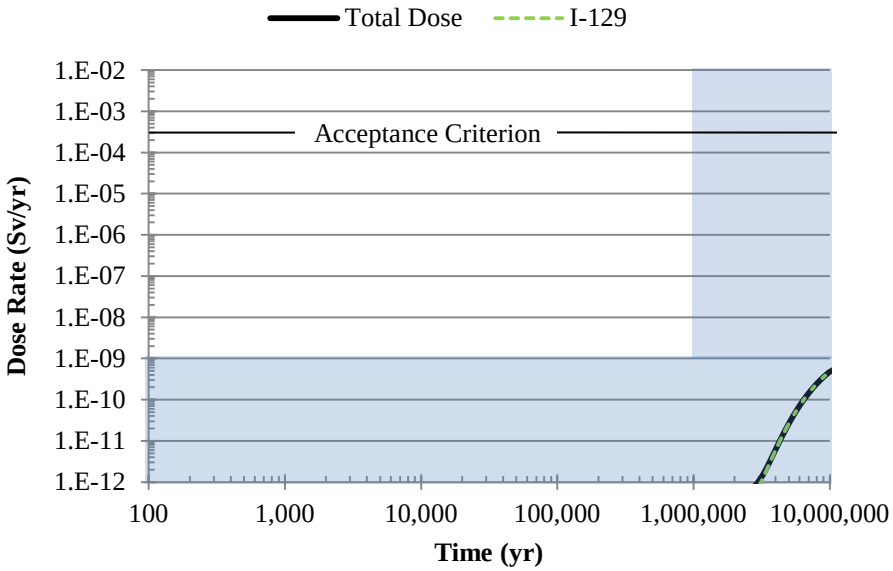

By investigation of the total dose rate with increased instant release fractions to the Reference Case in Figure 4.2, very little differences were observed. Therefore, the model was not overly sensitive to the instant release fraction, which was similar to that predicted in the NWMO analysis.

4.3.3 Diffusivity Sensitivity

The sensitivity of the SOAR model to the diffusivity was evaluated by increasing the values by an order of magnitude. The SOAR model was run by increasing the free-water diffusivity by an order of magnitude. As the free-water diffusivity was used to calculate the diffusion coefficient, this corresponds to a one order of magnitude increase. The total dose rate was predicted by SOAR and is presented in Figure 4.12.

By increasing the diffusivity by one order of magnitude, the total dose rate was increased. The dose rate reached 10^{-12} Sv/yr at approximately 240,400 years, and reached a maximum of 1.1 x 10^{-8} Sv/yr at 5,790,000 years. Therefore, the total dose rate increased faster and occurred at earlier times than that of the Reference Case. The NWMO analysis using SYVAC3-CC4 also predicted a larger change in the predicted total dose rate with an increase in the diffusivity.

Figure 4.12 – SOAR prediction with diffusivity increased by one order of magnitude

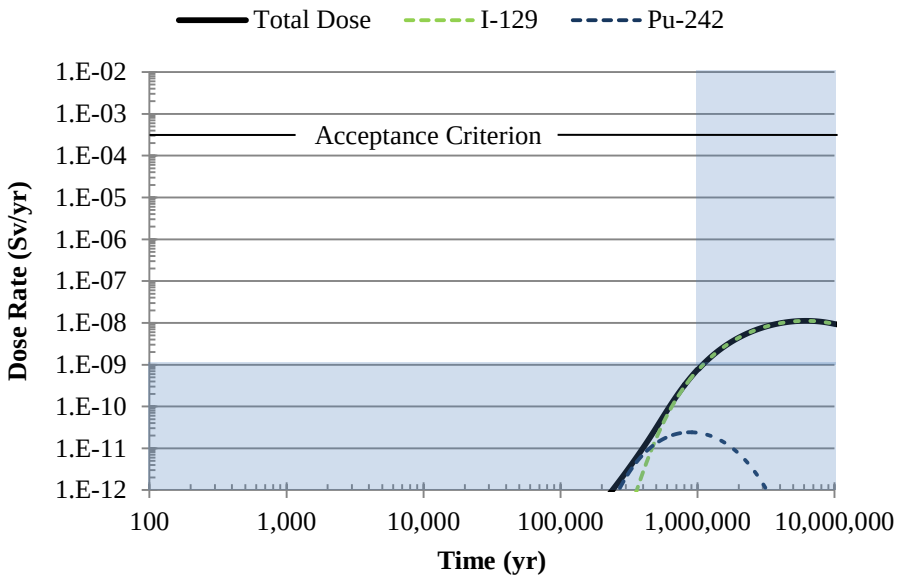

4.3.3.1 Summary

The total dose rates predicted for each scenario were plotted on a graph with the Reference Case for comparison (see Figure 4.13) and times of occurrence are compared in Table 4.6. From the graph and table it was evident that the instant release fraction had little to no effect on the predicted total dose rate which agreed with the results from the NWMO.

Increasing the degradation rate resulted in a slightly higher total dose rate at earlier times as predicted by SOAR. The NWMO analysis showed a larger impact by increasing the dissolution rate. SYVAC3-CC4 used a dissolution model and SOAR used a degradation rate. A one order magnitude increase in the dissolution model does not equate to one order magnitude increase in degradation rate. This difference accounts for the variation in the observed sensitivity. The SOAR model run with a decrease in degradation rate resulted in a lower total dose rate as would be expected.

The increased defect area when used in SOAR resulted in earlier and higher total dose rate release as compared to the Reference Case. For the SYVAC3-CC4 the increase in defect area did not result in a large change in predicted dose rates. The reason that these models had different sensitivity to this parameter is unknown.

The run with the increased diffusivity resulted in the earliest release and highest maximum total dose rate. This result illustrated the impact of the diffusivity on the time and magnitude of the release.

In all the sensitivity cases the total dose rate was below the threshold level within the first one million years. For the increase in diffusion coefficient and defect area, the total dose increased above the threshold level after one million years. At all times, for all the physical barrier sensitivity cases, the predicted total dose rate was below the acceptance criterion by more than four orders of magnitude for the worst case.

Figure 4.13 – Sensitivity to degraded physical barrier

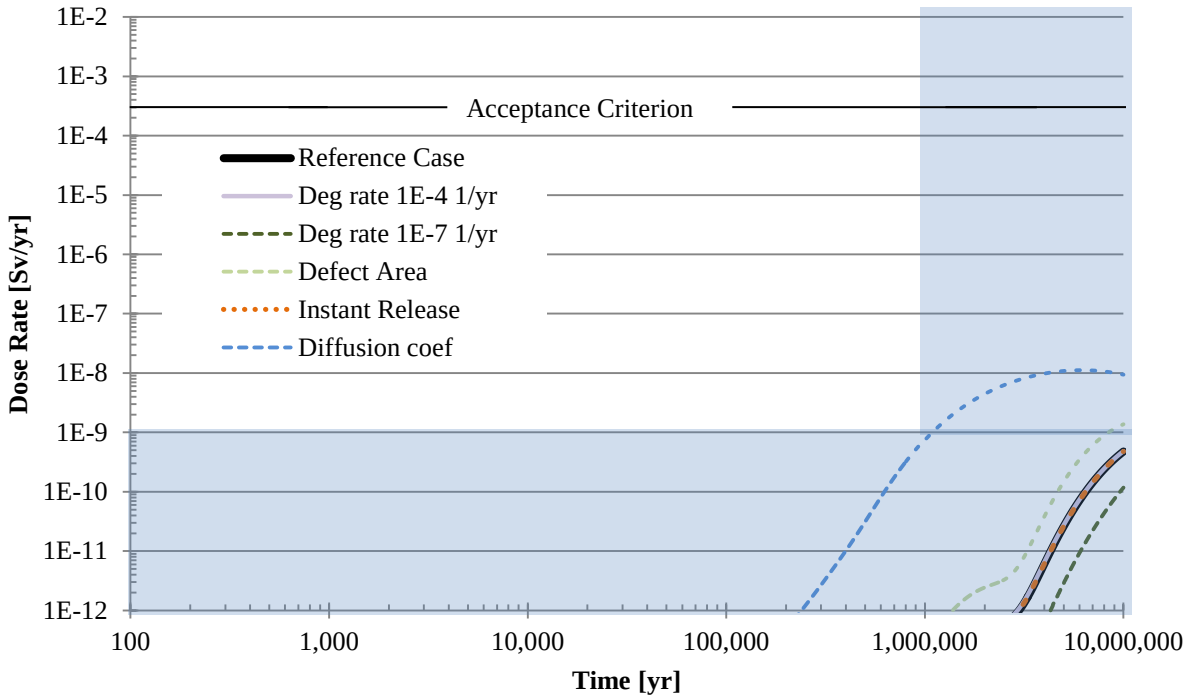

Table 4.6 – Sensitivity to physical barrier changes

Parameter	Reference Case	Degradation rate		Increased defect area	Instant release fraction of 10%	Increased diffusivity
		10^{-4} 1/yr	10^{-7} 1/yr			
Time to reach 10^{-12} Sv/yr (yr)	3,000,000	2,930,000	4,300,000	1,380,000	2,980,000	240,400
Maximum total dose rate (Sv/yr)	5×10^{-10}	5×10^{-10}	1.2×10^{-10}	1.40×10^{-9}	5×10^{-10}	1.1×10^{-8}
Time to reach maximum (yr)	10,000,000	10,000,000	10,000,000	10,000,000	10,000,000	5,790,000

4.3.4 Sensitivity to a Degraded Chemical Barrier

The NWMO performed different sensitivity analyses with respect to the performance of the chemical barrier. The parameters that were altered for the current sensitivity analyses are as follows:

- Removal of sorption in the geosphere
- Remove all solubility limits
- Ignore sorption in the buffer material

The NWMO results of the aforementioned sensitivity analyses are presented in Figure 4.14 and Table 4.7. By ignoring the solubility limits, the predicted total dose rate had little to no change when compared against the Reference Case. The run that was conducted with no sorption in the geosphere predicted a slightly earlier release and a higher total dose rate in the mid 10^{-9} Sv/yr range at 10,000,000 years. The largest impact was observed by eliminating the sorption within the backfill or buffer material. This resulted in an earlier release and a total dose rate in the higher 10^{-9} Sv/yr at 10,000,000 years. In all cases, the total dose rate was below the threshold value in the first 1,000,000 years, which was the time-scale of interest. The total dose rate exceeded this threshold value prior to the 10,000,000 year modelling time but was well below the acceptance criterion at all times.

4.3.4.1 No Sorption in the Geosphere

The sorption in the geosphere slows down the movement of radionuclides as they are adsorbed to the soil particles. The rate which individual radionuclides adsorb is defined by the sorption parameter, K_d. The higher the K_d value, the higher the sorption. Some radionuclides are non-sorbing such as I-129 and have a K_d of zero. To evaluate the SOAR model sensitivity to sorption, K_d was set to zero for all radionuclides. With this setting, no radionuclides would adsorb and should move farther in the two geosphere pathways and it was expected that the total dose rate should increase. The SOAR model predicted total dose rates are presented in Figure 4.15.

Figure 4.14 – Summary of chemical barrier sensitivity using SYVAC3-CC4 (taken from NWMO (2013a))

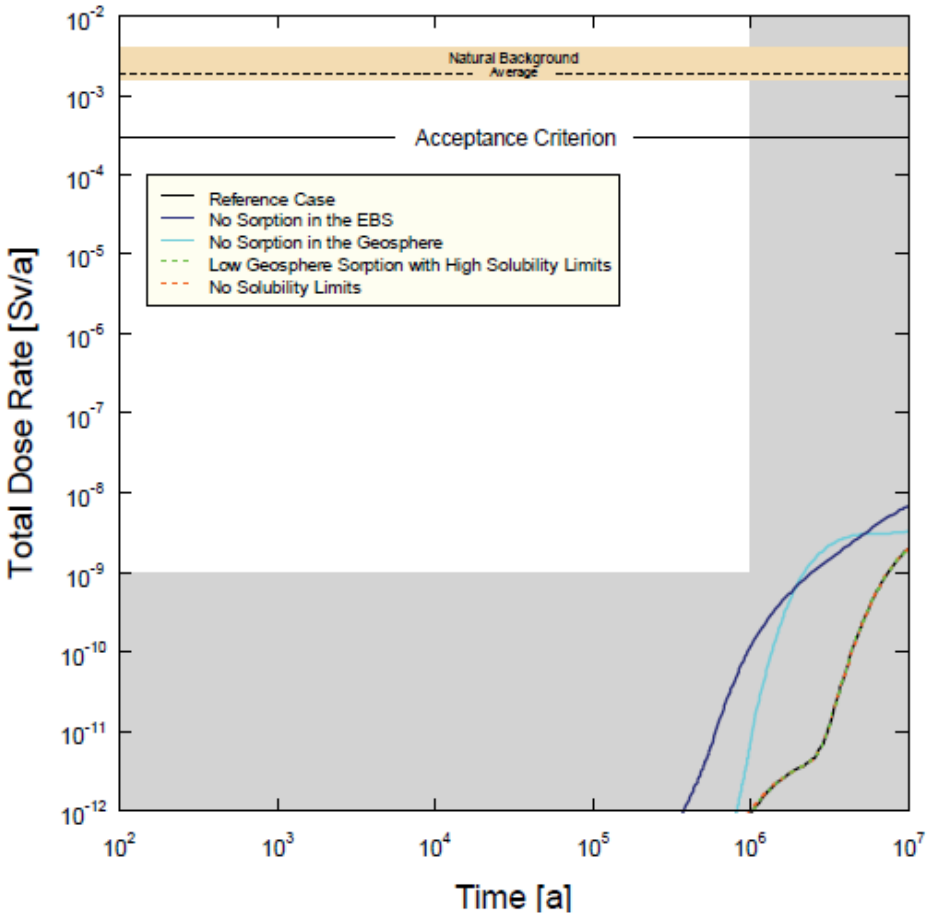

Table 4.7 – Sensitivity to chemical barrier changes as predicted by SYVAC3-CC4 (values are approximate)

Parameter	Reference Case	No sorption in the geosphere	No solubility limits	No sorption in the buffer
Time to reach 10^{-12} Sv/yr (yr)	1,000,000	900,000	1,000,000	300,000
Maximum total dose rate (Sv/yr)	2×10^{-9}	3×10^{-9}	2×10^{-9}	8×10^{-9}
Time to reach maximum (yr)	10,000,000	10,000,000	10,000,000	10,000,000

Figure 4.15 – SOAR prediction with no sorption in the geosphere

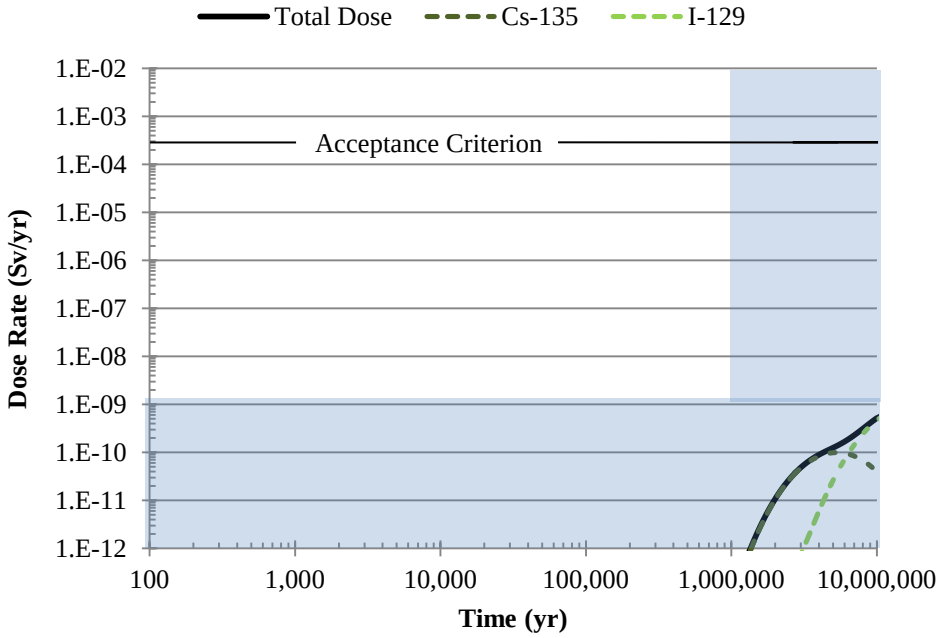

By ignoring sorption in the geosphere, the SOAR model predicted a total dose rate reaching 10^{-12} Sv/yr at an earlier time of 1,360,000 years than that from the Reference Case. The maximum total dose rate reached 5.2 x 10^{-10} Sv/yr at 10,000,000 years. The contribution from I-129 remains the same as the Reference Case as it was always a non-sorbing radionuclide. Cs-135 is a weakly sorbing radionuclide and by removing the sorption showed a larger impact.

With the removal of sorption the total dose rate did not exceed the threshold value of 10^{-9} Sv/yr at all times.

4.3.4.2 Solubility limit neglected

The solubility limit determines the amount of radionuclides that can become soluble in water. Certain radionuclides such as I-129 have no solubility limit. However, other radionuclides have limits that depict the amount of the release. In this sensitivity scenario, the solubility limit of all radionuclides was neglected. Within the SOAR model, this was done by setting the solubility limit to "-1", which indicates to GoldSim that there is no limit. By neglecting the solubility limit, it was expected that the total dose rate would be higher as a larger amount of radionuclides would be released. The SOAR model was run to predict the total dose rate with no solubility limit (see Figure 4.16).

By ignoring the solubility limit the total dose rate reach 10^{-12} Sv/yr at 2,280,000 years which was slightly earlier to that of the Reference Case. The maximum total dose rate was 5.4 x 10^{-10} Sv/yr

and occurred at 10,000,000 years, which was slightly higher than the Reference Case. As I-129 does not have a solubility limit, its contribution was unchanged from the Reference Case. Other radionuclides such as U-234, U-236 and U-238 made smaller contributions which were not observed in the Reference Case. These contributions were not large enough to impact the total dose rate. The SYVAC3-CC4 model in the NWMO analysis showed minimal sensitivity to the solubility limit. This was similar to the results observed in this current study using SOAR.

Figure 4.16 – SOAR prediction with no solubility limit

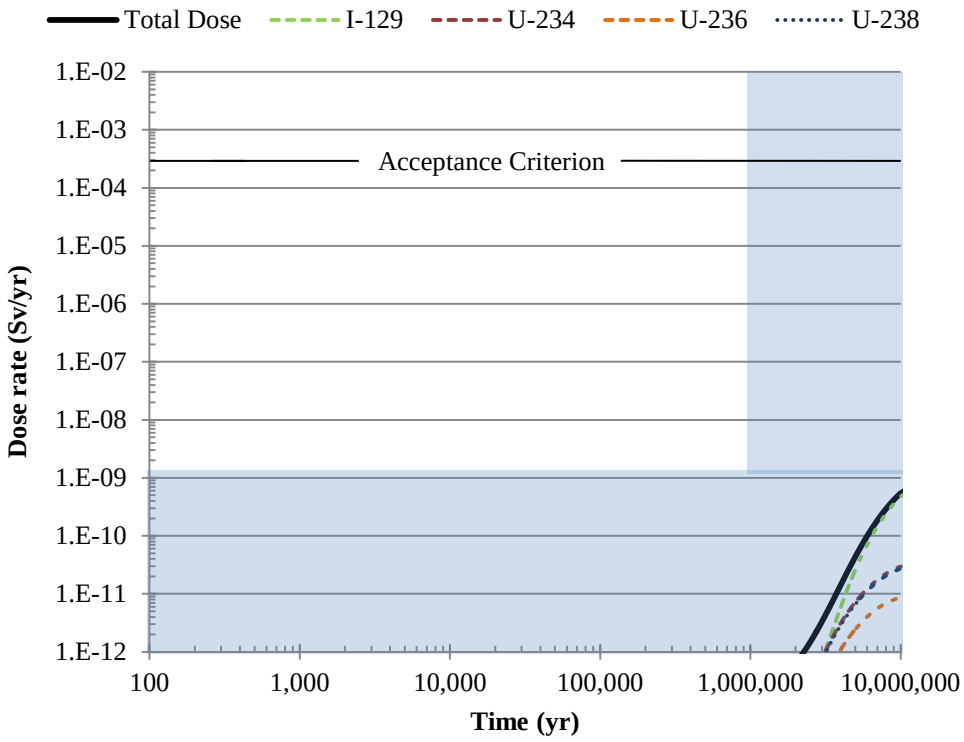

4.3.4.3 No Sorption in the Buffer Material

As in the geosphere, sorption also occurs within the buffer material of the Near Field. By neglecting sorption in the buffer material it was expected that the total dose rate would increase. The SOAR model was run with all the K_d values set to zero within the Near Field component and the total dose rate was predicted (see Figure 4.17).

The total dose rate predicted with no sorption in the buffer material resulted in little to no change from the Reference Case. The time to reach a dose rate of 10^{-12} Sv/yr was earlier than the Reference Case, and the maximum total dose rate was slightly higher.

The SYAC3-CC4 modelling conducted by NWMO showed the highest sensitivity to the removal of sorption in the buffer material. Whereas for the SOAR model, little change in total dose rates were observed for this parameter. This difference may be a result of variations in the waste package representation or how the buffer is treated in both models. Further examination into how both models treat the buffer or Near Field may be required.

Figure 4.17 – SOAR prediction with no sorption in the Near Field

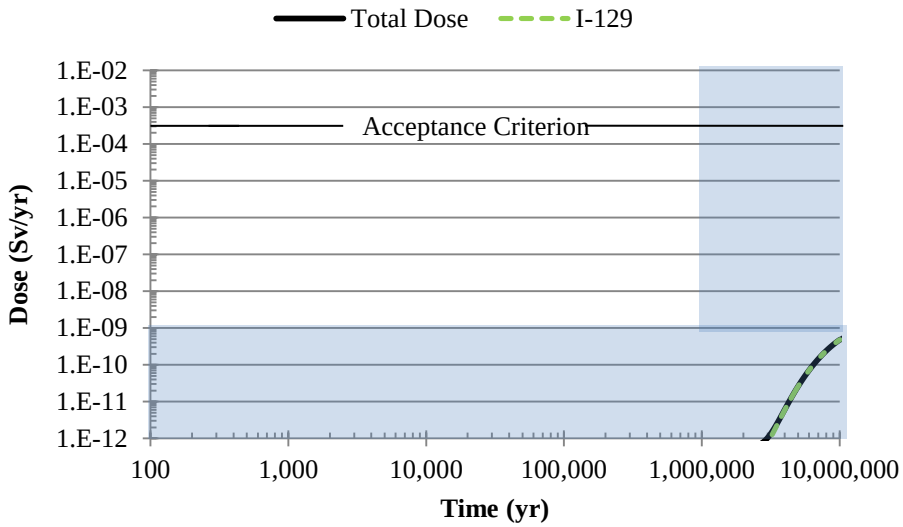

4.3.4.4 Summary

A series of sensitivity analyses were conducted with respect to the chemical barrier. A graph of the total dose rate from each sensitivity case and the Reference Case was constructed for comparison purposes (see Figure 4.18) and times of occurrence are presented (Table 4.7). In all cases, the time to reach a dose rate of 10^{-12} Sv/yr and the maximum total dose rates were approximately the same.

As stated previously, removal of sorption in the buffer material did not change the total dose rate to any extent as predicted by SOAR. This result was different than that observed in the NWMO analysis where removal of sorption in the buffer material resulted in earlier release of total dose rate and a higher maximum. This difference may be due to how the waste package was accounted for in the two models.

For the case of no solubility limits the SOAR model showed a slight increase in total dose rate at some times during the model simulations. The NWMO analysis predicted that the solubility limit had little to no effect on the total dose rate. The results for this sensitivity scenario from both models were similar as both show minimal changes.

Figure 4.18 – Sensitivity to the Chemical Barrier

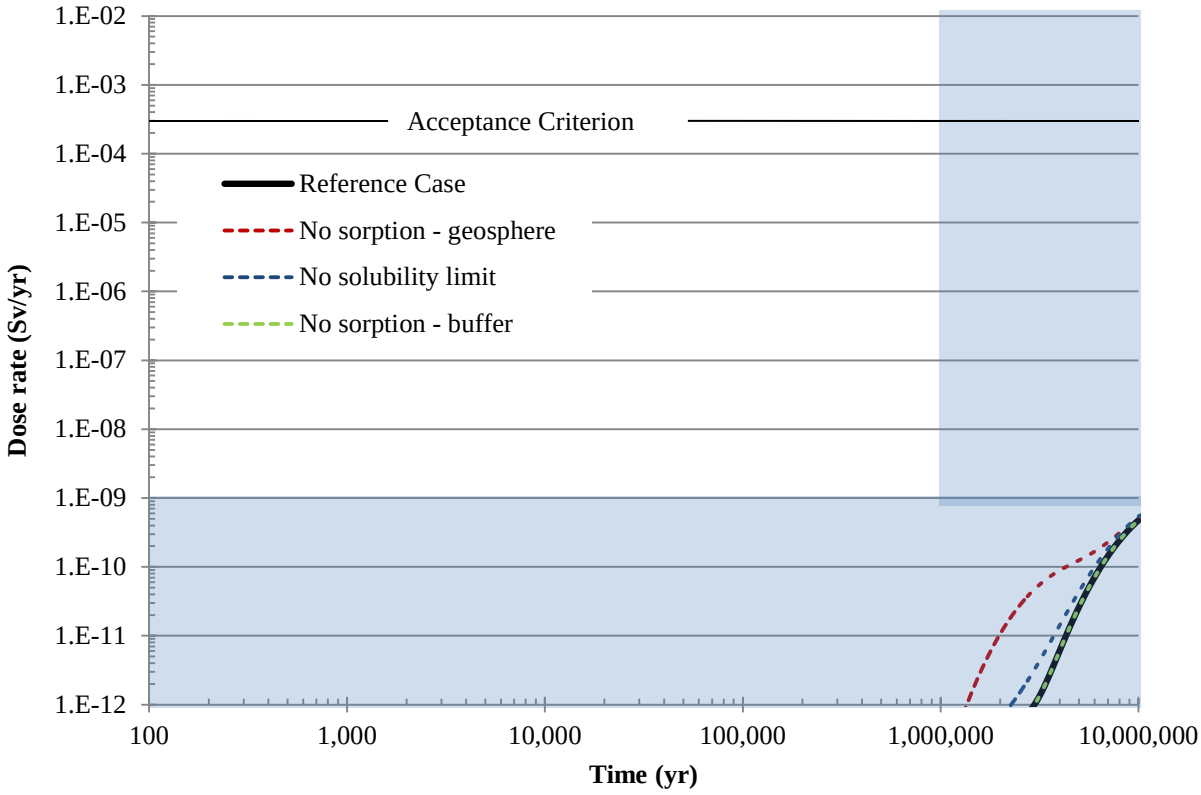

Table 4.8 – Sensitivity to chemical barrier changes

Parameter	Reference Case	No sorption in geosphere	Solubility limit ignored	No sorption in backfill material
Time to reach 10^{-12} Sv/yr (yr)	3,000,000	1,360,000	2,280,000	2,980,000
Maximum total dose rate (Sv/yr)	5×10^{-10}	5.2×10^{-10}	5.4×10^{-10}	5×10^{-10}
Time to reach maximum (yr)	10,000,000	10,000,000	10,000,000	10,000,000

The removal of sorption in the geosphere resulted in the largest chemical barrier change in total dose rate as predicted by the SOAR model. The total dose rate was higher than the Reference

Case at times between one and ten million years. The NWMO analysis neglecting the sorption in the geosphere also resulted in higher dose rates over time.

In all chemical barrier cases, the total dose rate was below the threshold level prior at all times modelled and therefore also below the acceptance criterion.

4.4 Summary

The SOAR model was adapted and parameterized to predict total dose rates for the NWMO`s Fifth Case Study. Initially, a Reference Case was evaluated and compared. The development of the SOAR model had several limitations and differences from the NWMO's SYVAC3-CC4 model.

The first difference is that the NWMO divided the repository into five waste vaults in the SYVAC3-CC4 model. Five separate pathways were considered from each waste vault through the Cobourg Formation. Subsequently a single pathway was modelled through the remaining natural geosphere units. This representation was not possible within SOAR and a simplified waste package was considered. When comparing the releases from the Cobourg Formation from both models, differences were observed which may be due to waste package configuration. However, the releases further along the natural geosphere units compared better.

A second difference is that the SOAR model only considered 14 of the 37 radionuclides modelled in SYVAC3-CC4. The element that was found to have the most significant contribution by SYVAC3-CC4 was I-129 (99.5% of internal exposure) through approximately equal pathways of food and water ingestion. SOAR does consider I-129 in the model and as this element is by far the largest contributor the absence of the other radionuclides in the calculation did not have a large impact.

For the dose calculation in SOAR, the only exposure pathway considered was through ingestion of water. The SYVAC3-CC4 considered other exposure pathways and for the Reference Case had I-129 as the major contributor through ingestion of food and water. The model predicted approximately equal contribution to the total dose through these two pathways. Therefore, it would be expected that the SOAR results would be approximately half that of the SYVAC3-CC4 results as a result of this difference.

The final difference in the development of SOAR from that of SYVAC3-CC4 was in how the bound waste form was released over time. Within SYVAC3-CC4 a dissolution model was used that had numerous parameters and the rate declined over time. This model produced a dissolution rate in mol/yr that defined the rate at which the waste was released over time. For SOAR a degradation rate in 1/yr was used to define the rate of release. The dissolution model was transferred into degradation rates, with highest rates of 10^{-4} 1/yr at early times to 10^{-8} 1/yr at later times. It should also be noted that the degradation was only considered within SOAR once the waste package was breached. To incorporate the 10,000 years for adequate water to be available for transport as set in the NWMO analysis, the package was set to breach at this time

within SOAR. Therefore, the higher degradation rates prior to 10,000 years were ignored resulting in lower predicted releases when the rate was varied over time as was done in the SYVAC3-CC4 model. In the SOAR model three different constant degradation rates and that decreasing over time were considered. The higher constant degradation rates compared well with the results from SYVAC3-CC4.

Considering the aforementioned differences, the predicted results of the Reference Case from both models were compared. In the NWMO analysis, the SYVAC3-CC4 model predicted a maximum total dose rate of approximately 2×10^{-9} Sv/yr (NWMO, 2013a). The maximum total dose rate as predicted by SOAR was 5×10^{-10} Sv/yr which was slightly less than half the dose predicted by SYVAC3-CC4. The general shapes of the total dose rate relationship over time were similar in that it increased and had not yet reached a maximum at 10,000,000 years.

The results as predicted by the SOAR model and the SYVAC3-CC4 model both showed I-129 as a major contributor. The SYVAC3-CC4 prediction also showed minor contributions from Pd-107 (0.4%) and Sm-147 (0.1%). Since the contributions from these were not through water ingestion and were low, the absence of these within the SOAR model was not thought to adversely affect the results.

Sensitivity analyses were conducted investigating the effects of hydraulic conductivity, physical and chemical barrier parameters on the predicted total dose rates. In the hydraulic conductivity cases the total dose rate was affected by increased hydraulic conductivity in the geosphere and the inclusion of the EDZ in the shaft pathway. The predicted increase in total dose rate was due to higher flow rates from the increased hydraulic conductivity. The total dose predicted with the EDZ accounted for in the natural geosphere pathway resulted in little change from the Reference Case. This scenario would be better modelled in two or three dimensions.

The sensitivity to the physical barriers such as degradation rate, defect area, instant release fractions and diffusivity were investigated. The instant release fractions did not affect the total dose rate as predicted by SOAR, which agrees with the SYVAC3-CC4 results.

The defect area in the NWMO analysis did not show a change from the Reference Case however SOAR predicted an increase in total dose rate. This indicates that the SOAR model was more sensitive to the defect area than it was for SYVAC3-CC4.

The increase in degradation rate did not affect the SOAR model predictions as much as that of the SYVAC3-CC4 model. An order of magnitude increase in the dissolution model was not equivalent to an order of magnitude increase in degradation rate. The increased degradation or dissolution rate indicates that the waste breaks down faster and exits the waste package faster and should result in a larger total dose rate. Only a small change was observed in that predicted by SOAR in that the total dose rate started increasing at an earlier time. The decrease in the degradation rate by two orders of magnitude resulted in a decline in predicted total dose rate as would be expected.

The increase in diffusivity resulted in the largest change in predicted total dose rate as predicted by the SOAR and SYVAC3-CC4 models. As the transport is diffusion dominated, changes in

the diffusion greatly affected the resulting total dose rate as would be expected. The maximum total dose rate as predicted by SOAR was 1.1×10^{-8} Sv/yr.

The parameters affecting the chemical barrier were also evaluated. For the sensitivity case with no solubility limits considered, the SOAR model predicted a slight increase in the total dose rate at some times. However, the SYVAC3-CC4 model did not predict any observable change. Neither model was very sensitive to this parameter.

Removal of sorption in the geosphere had an effect on total dose rate. By removing the sorption, larger contributions were observed from Cs-135 which is normally a weakly sorbing radionuclide. Even with this increase the contribution from Cs-135 did not greatly affect total dose rate. The SYVAC3-CC4 model predicted an increase in the total dose rate when sorption in the geosphere was neglected, agreeing with the SOAR results.

The removal of sorption in the buffer material did not change the total dose rate as predicted by SOAR. However, for the SYVAC3-CC4 model, this change had the largest impact on the predicted total dose rate. This observed difference may be a result of how the waste package was incorporated in the two models.

The total dose rates as predicted by SOAR with consideration of the chemical barrier parameters did not exceed the threshold value in the 10,000,000 years. The case of neglecting sorption in the geosphere had the largest impact on total dose rate.

The overall performance of the SOAR model showed that for all cases considered, the total dose rate are below the acceptance criterion at any time by at least 4 orders of magnitude, similar to that predicted by SYVAC3-CC4. The sensitivity case due to increased diffusion resulted in the largest change to the predicted total dose rate according to the SOAR model. This scenario resulted in the largest maximum dose of 1.1×10^{-8} Sv/yr occurring at the earliest time of 5,610,000 years. In most cases, the results between the SOAR and SYVAC3-CC4 models showed similar sensitivity to parameters.

The SOAR model was used to provide predictions of the scenario presented by the NWMO. When comparing the results with those from SYVAC3-CC4 the aforementioned differences should be recalled. Even with these differences the model results compared well.

5.0 Probabilistic Dose Calculation using SOAR

In the previous section, the Reference Case was evaluated using deterministic parameters. However, in general some parameters are uncertain and are better defined by a range of possible values represented by a PDF. If some or all parameters are defined by a PDF, then probabilistic modelling can be conducted to determine the PDF of the results.

5.1 NWMO parameters and results

The NWMO conducted probabilistic modelling using the Monte Carlo technique with random sampling. The Monte Carlo method involves running the model for many simulations. For each simulation, values are obtained for each parameter from the respective PDF and the model is run. Each simulation represents one possible realization or outcome. The results from all simulations are compiled and used to determine possible range of outcomes. The Monte Carlo technique's underlying principle is that when a large number of simulations are conducted, an improved statistical representation of all possible outcomes is achieved. For the NWMO's probabilistic analysis 120,000 simulations were conducted.

In the NWMO analysis, parameters that affect the groundwater flow rate were not varied as the transport is diffusion dominated (NWMO, 2013a). The PDFs for most parameters as defined by the NWMO analysis were presented in Section 3.0 which described the model development.

The number of defective containers within the repository for the deterministic Reference Case was set to three. For the probabilistic analysis, the number of defective containers was defined by a binomial distribution characterized by the probability of a container having a defect and the total number of packages. The probability of a container having a defect was defined through a lognormal distribution with geometric mean equal to 2×10^{-4}, a geometric standard deviation equal to 2 and bounds set as 10^{-4} and 10^{-3} (NWMO, 2013a). For each simulation, the number of defective containers was determined and randomly placed within the repository. The number of container failures for each simulation from NWMO's probabilistic analysis is presented in Figure 5.1. The results show that the highest number of defective containers in a simulation was 12 and this occurred for only one simulation. For approximately 8% of the simulations (9259 simulations) zero containers had defects.

Figure 5.1 – Number of defective containers/simulation (taken from NWMO (2013a))

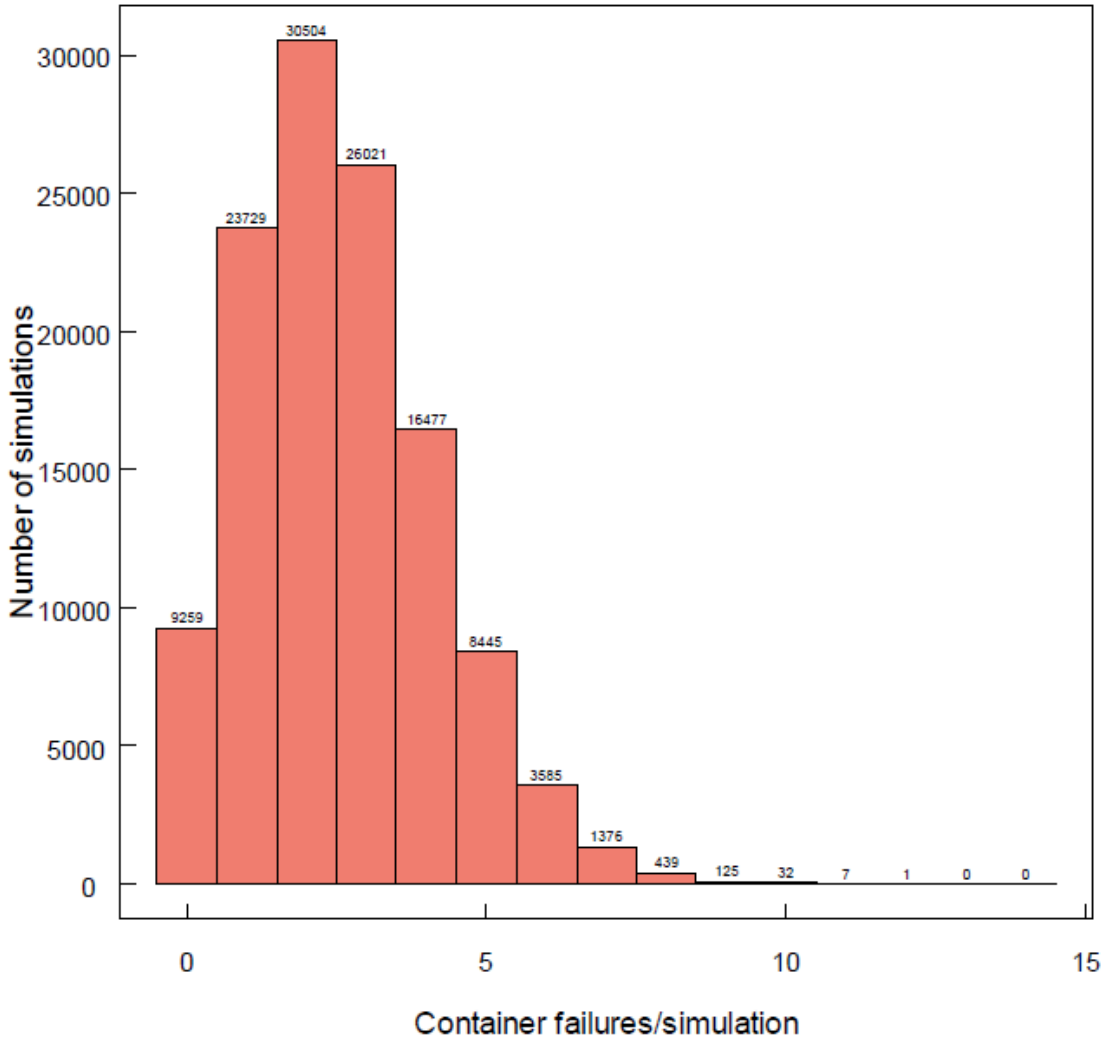

The maximum total dose rate, with at least one defective container as predicted by the probabilistic modelling using SYVAC3-CC4 is presented in Figure 5.2. The maximum total dose rate is defined as the maximum at any point in the 10,000,000 year simulation time. The average of the maximum values is also presented on Figure 5.2 as the vertical blue line at 1.6 x 10^{-8} Sv/yr. For the Reference Case using deterministic values the maximum dose rate predicted by SYVAC3-CC4 was equal to 2.0 x 10^{-9} Sv/yr. The probabilistic modelling results in a higher average maximum total dose rate as many scenarios were evaluated. The statistics of the maximum total dose rates from the probabilistic modelling are presented in Table 5.1.

The dose rates for individual radionuclides are presented in Table 5.2. As for the Reference Case, I-129 is the dominant contributor to the maximum total dose rate (96%). Smaller contributions were made by Pd-107 (3.1%), Sm-147 (0.56%) and Cl-36 (0.26%), which were not radionuclides considered by SOAR. However, the contributions were orders of magnitude below

that of I-129 and therefore the fact that SOAR did not consider these should not have a large impact.

Figure 5.2 – Distribution of the maximum dose rate for simulations with at least one defective container (taken from NWMO (2013a))

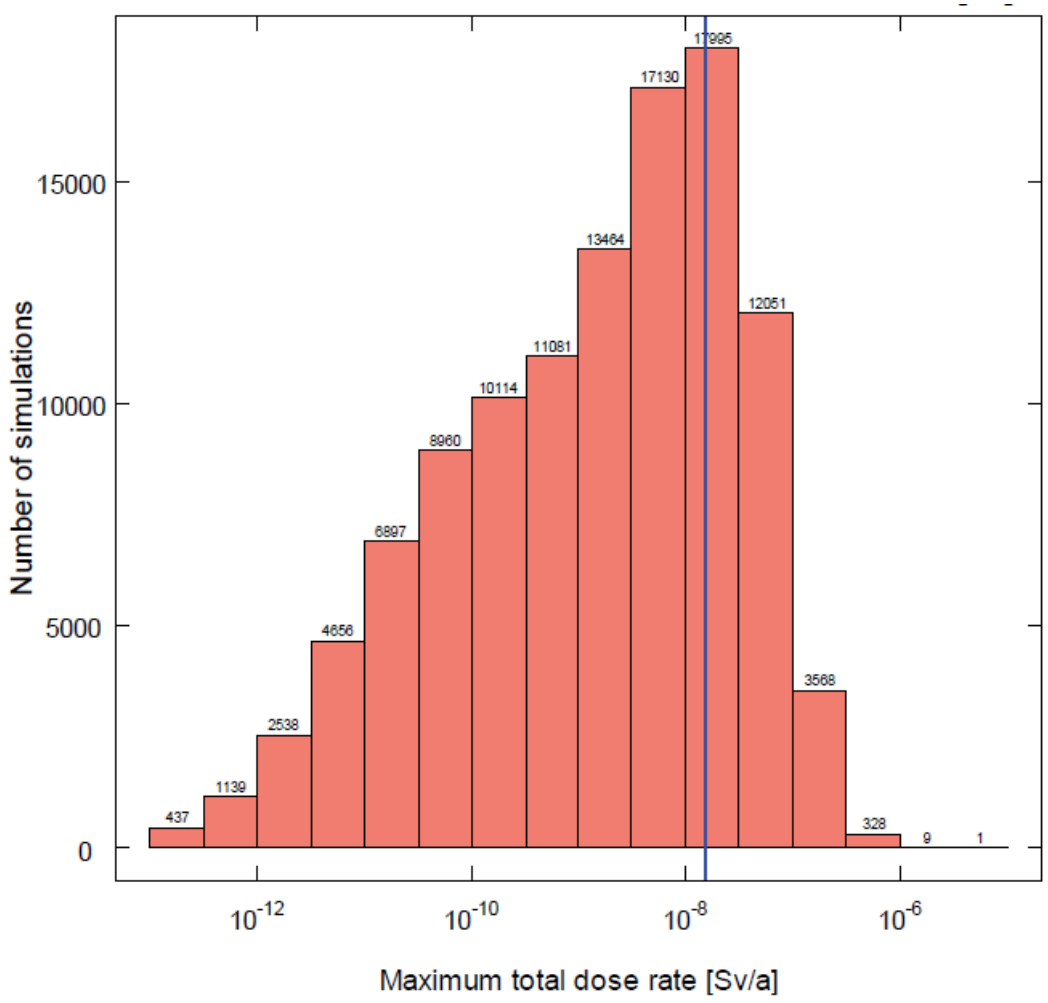

Table 5.1 – Statistics of maximum total dose rate from probabilistic modelling using SYVAC3-CC4 (taken from NWMO (2013a))

Statistic	Value
Average (Sv/yr)	1.55×10^{-8}
95th Percentile (Sv/yr)	7.46×10^{-8}
99th Percentile (Sv/yr)	1.82×10^{-7}
Probability of exceeding 3.0×10^{-4} Sv/yr	0
Median (Sv/yr)	1.52×10^{-9}

Table 5.2 – Average and median maximum dose rates for individual radionuclides from SYVAC3-CC4 (taken from NWMO (2013a))

Radionuclides	Average		Median
	Value	% of total	
I-129	1.50×10^{-8}	96	1.00×10^{-9}
Pd-107	4.49×10^{-10}	3.1	4.10×10^{-12}
Sm-147	8.68×10^{-11}	0.56	1.10×10^{-12}
Cl-36	4.10×10^{-11}	0.26	
Cs-135	2.19×10^{-11}	0.14	
Se-79	1.08×10^{-11}	0.07	
Tc-99	6.93×10^{-13}	0.004	
Total	1.57×10^{-8}		

- Values cut-off at 10^{-14} Sv/yr

The percentile bands as determined by the probabilistic modelling conducted by NWMO are presented in Figure 5.3. The percentile bands provide information on ranges of possible outcomes. The maximum for the 99th percentile band was 1.8×10^{-7} Sv/yr. Whereas the maximum dose rate predicted for the 25th percentile band was in the 10^{-10} Sv/yr range. This result shows over a three order of magnitude difference between predicted maximum total dose rate values. The 50th percentile band had a maximum total dose rate was 1.5×10^{-9} Sv/yr, which was in the same order of magnitude as that predicted in the Reference Case. In all scenarios evaluated through the Monte Carlo technique the dose rate did not exceed the acceptance criterion defined by the NWMO as 3×10^{-4} Sv/yr.

5.2 Probabilistic modelling using SOAR

The SOAR model was parameterized with the PDFs for all applicable parameters as defined previously within Section 3.0 of this report. As discussed earlier, there were several differences in how the SOAR and SYVAC3 models were developed. One variation was the method by which the bound waste form was released. In the SYVAC3 model, a dissolution model represented by numerous parameters, eight of which were defined by a PDF, was used to define the release of bound waste. In the sensitivity analysis using SYVAC3-CC4 a one order of magnitude increase in the dissolution rates resulted in a higher dose rate at all times. Therefore, changes in the dissolution model parameters could result in an increase in total dose rate for a particular simulation in the probabilistic modelling.

Figure 5.3 – SYVAC3-CC4 - Dose rate percentile bands (taken from NWMO (2013a))

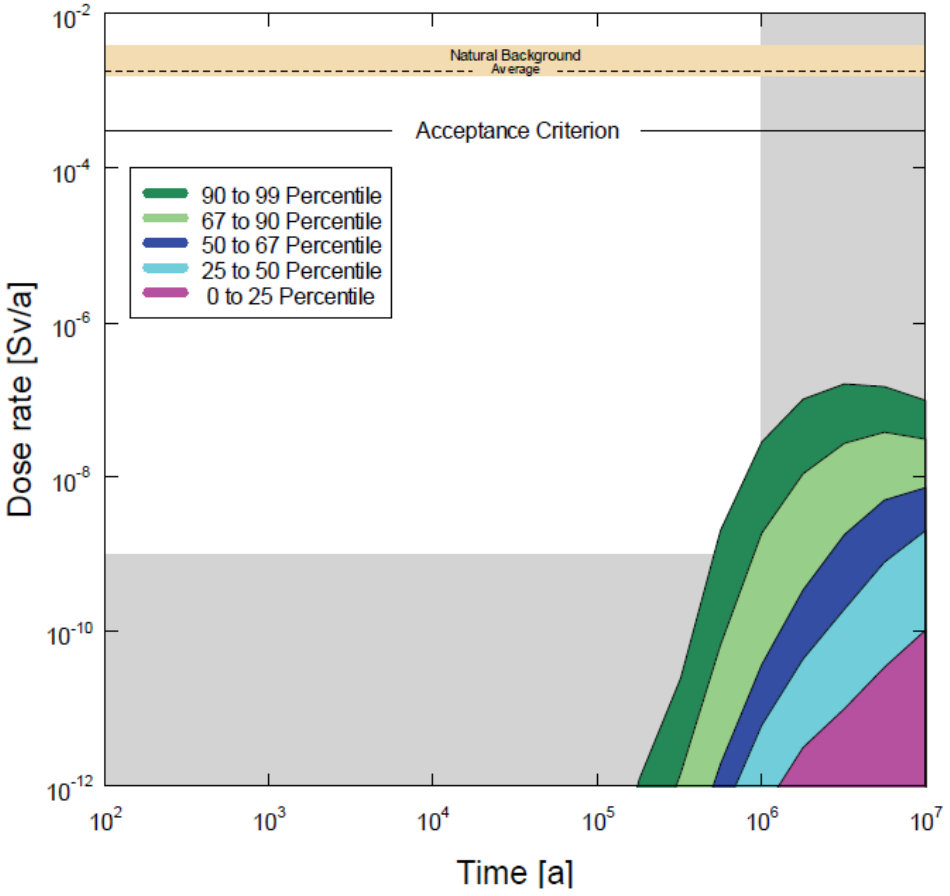

Representing the release from the bound waste form in SOAR using this same dissolution model was not possible. Within SOAR the release was described by a degradation rate that was found to range between 10^{-4} 1/yr and 10^{-8} 1/yr. As discussed in Section 3, better results were obtained when a constant degradation rate was used throughout a simulation. For the probabilistic analysis the degradation rate was set to a loguniform PDF with upper and lower bounds equal to 10^{-4} 1/yr and 10^{-8} 1/yr, respectively.

In the sensitivity analysis conducted using SOAR an increase of degradation rate from 10^{-5} 1/yr of the Reference Case to 10^{-4} 1/yr had little effect on the resulting total dose. This differs from the SYVAC3-CC4 model where an increase in the dissolution rates did raise the total dose rate. Therefore, within the probabilistic modelling using SOAR, the predicted total dose rates would not increase for any simulation due to increased degradation rate, but could decrease due to a reduction in degradation rate. For this reason the SOAR model should result in lower predicted total dose rates for the probabilistic model.

The second difference in the model development was the number of exposure pathways considered. SYVAC3-CC4 took into account numerous exposure pathways and SOAR only incorporated exposure through drinking water. For the Reference Case using SYVAC3-CC4, the NWMO found that I-129 was the major contributor with 54% through food ingestion and 46%

through water ingestion. Therefore, for the deterministic case the SOAR results were expected to be approximately half that predicted by SYVAC3-CC4.

For the probabilistic modelling within SYVAC3-CC4, it may have been possible that these proportions from different exposure pathways differ from that of the Reference Case. A SYVAC3-CC4 simulation in which the relative contribution due to drinking water decreased would result in larger difference to that of SOAR. For this reason, the SOAR probabilistic results should be lower than those from SYVAC3-CC4.

The third difference in the development of the models is the number of radionuclides that were accounted for in each model. The SYVAC3-CC4 model incorporated more radionuclides than SOAR in the modelling exercise. However, in both models the total dose rates were greatly dominated by the impact of I-129 (>99%). Therefore the absence of a selection of radionuclides in SOAR was not thought to greatly affect the probabilistic results.

The final difference was the representation of the repository. In SYVAC3-CC4, the repository was divided into five waste vaults with five pathways through the buffer and Cobourg Formation. In SOAR this was not possible and it was configured into one unit. In the model development this difference was found to affect releases from the waste form, Near Field and from the top of the Cobourg Formation. However, where both models were represented by a single pathway, the predicted results were similar and as such this difference was not thought to greatly impact the final total dose rates.

Within the SOAR model, Monte Carlo probabilistic modelling was conducted, however Latin Hypercube rather than random sampling was used. Latin Hypercube is a method of sampling each distribution which ensures that all areas of the PDF are sampled. For this method, each parameter with a probability distribution function is divided into equal probability sections. The number of sections is equal to the number of Monte Carlo iterations that would be conducted. From each section, a value of the parameter is chosen, resulting in one value for each Monte Carlo simulation. As this is conducted for all uncertain parameters, one value from each is used per simulation. During the Monte Carlo simulations all of the values for each uncertain parameter are used. This sampling method results in each uncertain parameter having values taken from every portion of the PDF, even the extremes. Therefore since Latin Hypercube Sampling has been shown to be more precise than random sampling, fewer iterations or simulations need to be conducted.

For the probabilistic modelling conducted using SOAR two runs were conducted with different number of Monte Carlo simulations for comparison. One run was conducted with 40,000 simulations and the other with 60,000 both using Latin Hypercube sampling. The purpose of conducting two Monte Carlo runs was to examine any differences between the runs with different number of simulations. If the observed differences were small between the two cases then the number of simulations was satisfactory. It should be noted that it was not possible to perform 120,000 iterations, as was done in NWMO analysis due to technical difficulties within the SOAR model in terms of unsatisfactory data storage. However, since Latin Hypercube sampling was used it was possible to run the model with fewer simulations.

For the run conducted with 60,000 simulations using SOAR, the distribution of defective containers per simulations is presented in Figure 5.4. The maximum number of containers with a defect in any run was 25 and only one run had this value. The mean number of defects for all the simulations was 3.5.

Figure 5.4 – Number of defective containers/simulation for run with 60,000 iterations

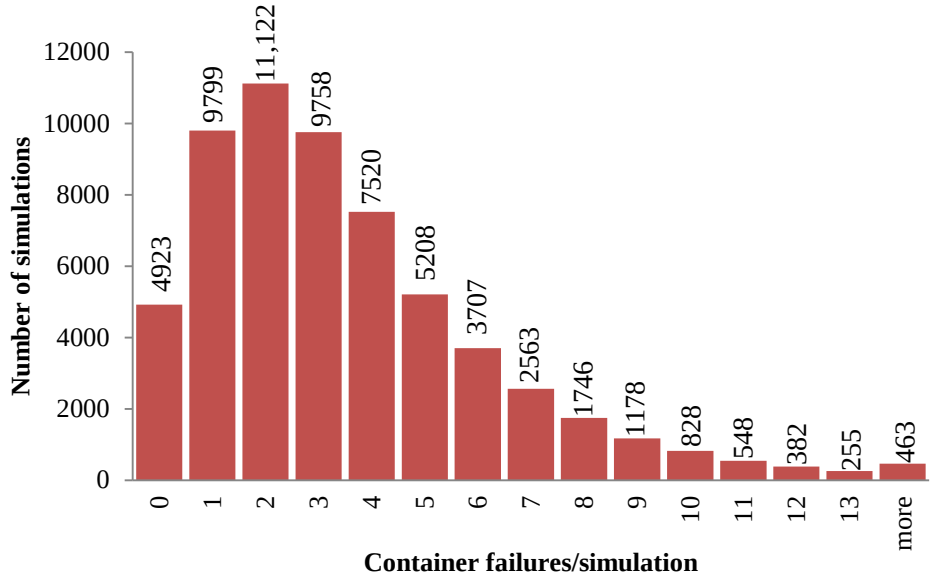

A comparison of the number of defects between the two different runs is presented in Table 5.3. The cumulative probability was used for comparison as the total number of simulations differed. These probabilities were compared and it was determined that the results were the same to at least two significant digits. This agreement was one indication that there was not a large difference between the two runs with different number of simulations. Therefore, adding confidence that the fewer runs conducted in the SOAR probabilistic modelling as compared to NWMO's analyses was not an issue.

Table 5.3 – Cumulative probability of number of defective containers/simulation from SOAR with 40,000 and 60,000 iterations

Number of defects	Cumulative probability	
	60,000 iterations	40,000 iterations
0	0.08205	0.082475
1	0.24537	0.24632
2	0.43073	0.4313
3	0.59337	0.59347
4	0.7187	0.72018
5	0.8055	0.8072
6	0.86728	0.86767
7	0.91	0.91005
8	0.9391	0.939
9	0.95873	0.95857
10	0.97253	0.97193
11	0.98167	0.98152
12	0.98803	0.98808
13	0.99228	0.99238
More	1	1

In the NWMO's probabilistic modelling, approximately 8% of the simulations had zero containers with defects. The scenario with two containers having undetected defects had the largest number of occurrences. The largest number of containers with undetected defects was 12 and that occurred in only one simulation. The SOAR PDF modelling also had approximately 8% of the simulations with no defects. Also in agreement with the NWMO analysis is that the largest number of simulations had two containers with undetected defects. However, the SOAR model had a larger number of simulations with increased number of defects as compared to the NWMO analyses. In the SOAR modelling, 1.2% of the simulations had 12 or more containers with defects. As the same PDFs were used to define the number of defects, it was thought that the reason for this difference was the variation in how the sampling was conducted for the Monte Carlo simulations. For the NWMO's analysis random sampling was conducted, however within SOAR Latin Hypercube sampling was conducted. It should be recalled when examining the probabilistic results that the SOAR model had larger number of simulations with increased number of packages with defects.

The distribution of maximum total dose rate for SOAR run with 60,000 iterations is presented in Figure 5.5. The average maximum total dose rate of 7.23×10^{-10} Sv/yr is shown on the figure with a vertical line. The results show that the maximum total dose rates with at least one defect are between approximately 3.8×10^{-15} Sv/yr and a maximum of 6.2×10^{-8} Sv/yr.

The statistics of the SOAR results for the two runs with different number of simulations are presented in Table 5.4. Comparing the statistics between the two runs showed that these values are essentially the same, generally to within two significant digits. The fact that the runs with 40,000 and 60,000 simulations had very similar statistics indicates that there was not a large difference with the larger number of simulations. Therefore, additional simulations to the Monte Carlo runs would not have changed the results and the run with 60,000 simulations was deemed adequate.

The contribution to the total dose from individual radionuclides is presented in Table 5.5. As with the SYVAC3-CC4 model, the main contributor to the total dose rate was I-129. Smaller contributions by orders of magnitude were observed by Cs-135, Tc-99 and Se-79.

Comparison of the statistics shows that the SOAR predictions were lower than those from the SYVAC3-CC4 predictions. The previously described differences in the model development specifically the method by which the bound waste form was released and the exposure pathways would result in SOAR having lower predicted dose rates.

Figure 5.5 – Distribution of the maximum dose rate for 60,000 simulations with at least one defective container from SOAR

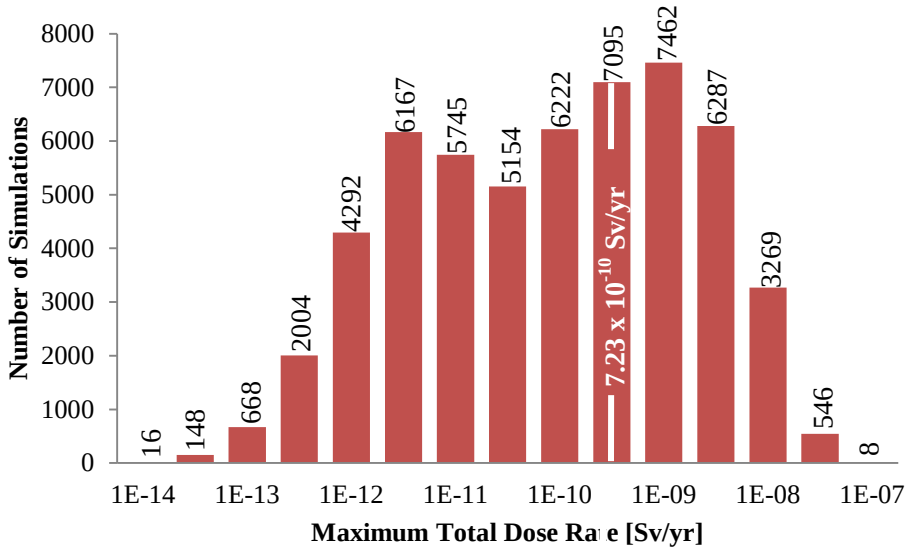

Table 5.4 – Statistics of probabilistic modelling using SOAR

Statistic	60,000 iterations	40,000 iterations
Average (Sv/yr)	7.23×10^{-10}	7.17×10^{-10}
95th percentile (Sv/yr)	3.86×10^{-9}	3.82×10^{-9}
99th percentile (Sv/yr)	9.65×10^{-9}	9.16×10^{-9}
Maximum (Sv/yr)	6.17×10^{-8}	6.17×10^{-8}
Probability of exceeding 3×10^{-4} Sv/yr	0	0
Median (Sv/yr)	3.73×10^{-11}	3.71×10^{-11}

Table 5.5 – Average and median maximum dose rates for individual radionuclides from SOAR

Radionuclide	60,000 iterations Sv/yr		40,000 iterations Sv/yr	
	Mean	Median	Mean	Median
I-129	7.2×10^{-10}	3.7×10^{-11}	7.2×10^{-10}	3.7×10^{-11}
Cs-135	8.8×10^{-14}	3.7×10^{-14}	8.8×10^{-14}	3.7×10^{-14}
Tc-99	4.7×10^{-18}	1.0×10^{-20}	4.2×10^{-18}	1.0×10^{-20}
Se-79	4.6×10^{-17}	1.7×10^{-19}	4.5×10^{-17}	1.7×10^{-19}

The percentiles of the total dose rate as predicted by SOAR using 60,000 iterations are presented in Figure 5.6. In the SOAR results, a Greatest Result curve is presented which illustrates the maximum total dose rates as predicted by SOAR for any simulation that was conducted in the probabilistic analysis. The curve representing the Greatest Result begins at the earliest time of just over 200,000 years and increases to a maximum of 6.2×10^{-8} Sv/yr, which is over three orders of magnitude below the acceptance criterion. None of the percentile bands exceed the threshold level prior to 1,000,000 years.

Figure 5.6 – SOAR (60,000 iterations) – Dose rate percentile bands

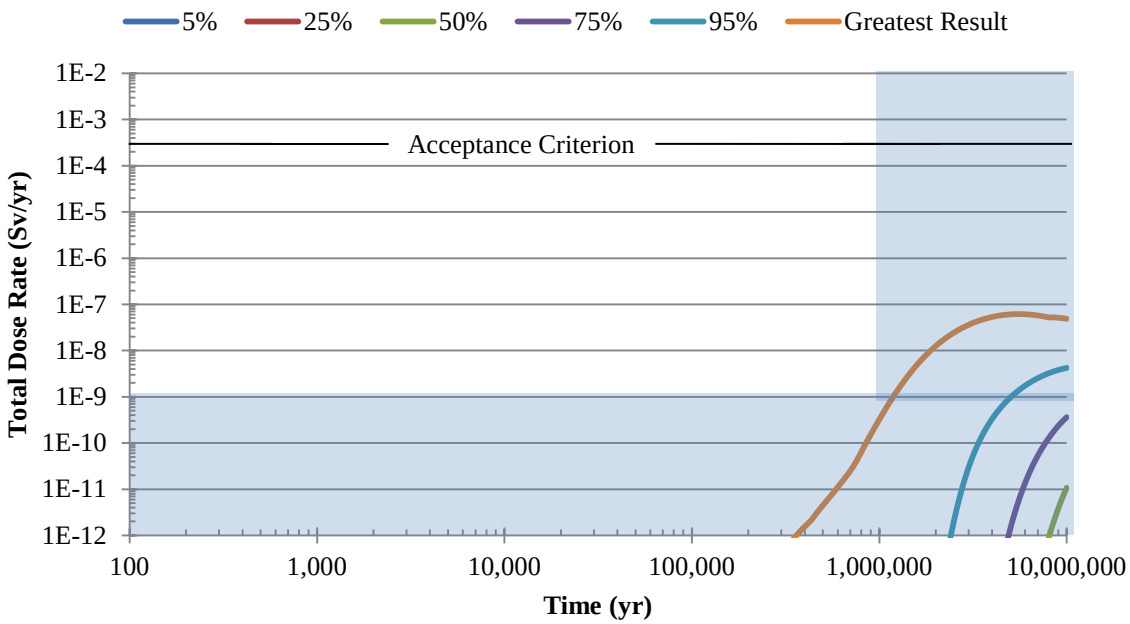

Comparison of the maximums for each percentile as predicted by SOAR and SYVAC3-CC4 are presented in Table 5.6. The percentiles from the probabilistic modelling from SOAR are below those from SYVAC3-CC4. The main differences for the probabilistic modelling in SOAR were how the release from bound waste form was accounted and the number of exposure pathways. These differences in the dose calculation would result in SOAR having predicted lower total dose rates.

Table 5.6 – Maximum total dose rate for probabilistic modelling from SYVAC3-CC4 and SOAR (SYVAC3-CC4 values are approximate)

Percentile	SYVAC3-CC4 [Sv/yr]	SOAR [Sv/yr]
25th	10^{-10}	1.8×10^{-12}
50th	1.5×10^{-9}	3.7×10^{-11}
67th	10^{-8}	2.2×10^{-10}
75th	-	4.7×10^{-10}
90th	7×10^{-8}	2.0×10^{-9}
95th	7.5×10^{-8}	3.9×10^{-9}
99th	1.8×10^{-7}	9.7×10^{-9}
Greatest result	-	6.2×10^{-8}

The maximum values as predicted by both models showed the 99th percentile of 1.8 x 10^{-7} Sv/yr by SYVAC3-CC4 and the greatest result of 6.2 x 10^{-8} Sv/yr by SOAR. This greatest result as predicted by SOAR is approximately half that of the 99th percentile by SYVAC3-CC4, which could be explained by the differences in exposure pathways.

The percentiles and statistics as predicted by SOAR and SYVAC3-CC4 provided information on all possible outcomes. The 99th percentile total dose rate as predicted by SYVAC3-CC4 was the highest value and was more than three orders of magnitude below the acceptance criterion.

5.3 Summary

Probabilistic modelling was conducted to account for uncertainties in the model parameters. The modelling time that was considered by both models was 10,000,000 years. The NWMO's analysis involved using the SYVAC3-CC4 model and applying the Monte Carlo technique with 120,000 simulations using random sampling. The SOAR model was also used for probabilistic modelling using the Monte Carlo technique. The difference being that Latin Hypercube sampling was used resulting in the requirement of fewer simulations. In this case 60,000 simulations were used and was deemed satisfactory.

Probabilistic modelling using the SOAR model resulted in a larger number of simulations with increased packages with defects as compared to SYVAC3-CC4. The SOAR model had 1.2% of simulations with 12 or more containers with defects. Whereas, SYVAC3-CC4 only had 1 simulation with 12 packages containing defects and no simulations with more. The difference in these values is thought due to the varying sampling techniques used.

Investigation of contribution from individual radionuclides indicated that I-129 was the largest contributor by both the SYVAC3-CC4 and SOAR models. The SYVAC3-CC4 had lower contributions from Pd-107, Sn-147 and Cl-36, which were radionuclides not considered by SOAR. However, the contributions from these radionuclides were two to three orders of magnitude lower than that from I-129 and were therefore not deemed an issue. Both the SOAR and SYVAC3-CC4 models predicted much smaller contributions by Cs-135, Tc-99 and Se-79.

Statistics of the maximum total dose rates were compared and the average predicted by SYVAC3-CC4 was 1.55 x 10^{-8} Sv/yr. However, that predicted by SOAR was 7.23 x 10^{-10} Sv/yr, which was below that of SYVAC3-CC4. The percentile bands from the SOAR probabilistic modelling were also lower than those from SYVAC3-CC4. The reason that the SOAR results were lower was due to differences in exposure pathways considered and the method by which the bound waste form was released.

In SYVAC3-CC4 the bound waste form release was set through a dissolution model with eight parameters defined by a PDF and dissolution rates that decline over time. It was shown in the SYVAC3-CC4 sensitivity analysis that an increase in the dissolution rates resulted in an increase in predicted total dose rate. Within SOAR, the bound waste form was released through a constant degradation rate throughout the simulation. This degradation rate was set a loguniform

PDF. For the SOAR sensitivity analysis it was shown that an order of magnitude increase in degradation rate from the Reference Case did not raise the total dose rate. However, a lower degradation rate would decrease the resulting total dose rate. This difference in the release of the bound waste form would result in SOAR having lower predicted total dose rates and therefore account for the lower percentile bands.

The second main difference that would result in SOAR having lower predicted total dose rates was that the SYVAC3-CC4 model considered numerous exposure pathways and SOAR only one through ingestion of drinking water. It was shown that for the Reference Case using SYVAC3-CC4 that the main exposure pathways with almost equal impact were through ingestion of food and water. As SOAR only considers ingestion of water, it was expected that the SOAR deterministic results should be approximately half those of SYVAC3-CC4. For the probabilistic case, the impact of the individual exposure pathways may differ in the SYVAC3-CC4 analysis. In a scenario where other exposure pathways other than water ingestion increase, the relative difference to the SOAR results would also increase. This difference in exposure pathways could possibly result in the SOAR model predictions to below those of SYVAC3-CC4.

6.0 Summary

The NWMO prepared a report on the post-closure safety assessment of the disposal of spent nuclear waste in a hypothetical DGR located at 500 m depth within a limestone formation in the Fifth Case Study (NWMO, 2013a and b). The report included modelling the DGR at several different scales and using different numerical codes to determine groundwater flow regime, contaminant transport and also the potential dose to humans over the next 1,000,000 years. The Site Scale modelling that was conducted in one dimension using SYVAC3-CC4 was the focus for this current report.

Within this report, an alternate model, the SOAR model was applied to the NWMO's Fifth Case Study using the data and information provided in the NWMO's reports (NWMO, 2013a and b). The purpose was to assess the applicability of both the SYVAC3-CC4 and SOAR models to this problem.

The SOAR model was developed by the US NRC as a flexible tool to assess different disposal options. The SOAR model is coded in GoldSim and contains a one dimensional steady state groundwater flow and contaminant transport code that can predict contaminant movement and the total dose. The SOAR model was applied to the NWMO's Fifth Case study using the data and information provided in the NWMO's reports (NWMO, 2013a and b). The SOAR model was parameterized and the code altered in order to model the NWMO's Fifth Case Study.

6.1 SOAR applicability

The SOAR model was developed by the US NRC as a tool to assess different disposal options. The SOAR model was coded in a commercially available coding platform called GoldSim. GoldSim is composed of many elements that can be used to simulate many different problems. A Contaminant Transport module was used for the development of SOAR, which contains elements such as Sources, Pipe Pathways and Cell Pathways. The advantage of this software is that these elements have been verified by GoldSim and that the software has been commercially available for 20 years.

Another advantage of GoldSim is that it is possible to conduct deterministic modelling or probabilistic modelling using the Monte Carlo method. With ease, parameters can be defined by a deterministic value or through a PDF and the simulations conducted.

SOAR contains a one-dimensional groundwater flow and contaminant transport model that can be used to investigate different disposal options of nuclear waste. The model allows for the input of different types of waste, additional waste over time, different methods of package breach including localised and general corrosion as well as forced breach and establishment of different types of geosphere.

The SOAR model can be used at three different levels depending on the problem being considered. The first level uses the free GoldSim player and the user can make changes through a series of dashboards representing the different components. This level allows for the assessment of options at a high level where the user can input amount of waste, package dimensions and Near Field and Far Field lengths without any knowledge of coding in GoldSim. However, the user would be limited in which parameters could be varied.

The second and third levels of SOAR require the full version of GoldSim Version 10.50. The second level allows the user to change a larger array of parameters through a parameter MS Access database that can then be uploaded to SOAR. The user could still change parameters through the dashboards and the model could be run. The final and most detailed version of SOAR, the user can alter the code to represent a more specific situation. This level requires knowledge of GoldSim to make the required changes. Also at this level the user can directly input the parameters and associated distributions directly into the code.

One attractive feature of GoldSim is that the coding environment is visual with windows and drop down menus to add in equations and features. As such, this visual environment makes the learning curve of GoldSim and SOAR much quicker. Another advantage of GoldSim is the provision of an excellent environment for viewing the results of the model at intermediate points and also the final results in both tabular and graphic format.

6.2 Strong/weak points of SOAR

The strength of SOAR is that it was modelled within the GoldSim environment, which is software that has been commercially available for twenty years. The different elements used to develop the SOAR model within GoldSim, such as Pipe and Cell Pathways, have been verified providing more confidence in the model.

A main strong point is that SOAR has flexibility in terms of the types of disposal problems modelled beyond the Fifth Case Study examined here. The user can define the material used for construction of the waste package and have failure occur due to localized corrosion, general corrosion or defined to occur at a specific time. Combinations of all these failure modes can be used and examined. Also, the SOAR model allows for four different types of waste to be present in the repository. The user can define the initial inventory, the age of the waste and have further waste added to the repository over time. These aforementioned features can be conducted at a high level without the requirement of altering the SOAR code itself.

Another strong point of SOAR is that it is possible to make alterations to the code at a more detailed level to model more varied problems. These changes may include such variations as the addition or removal of Pipe Pathways in the Far Field in the representation of the geology. The changes need to be conducted in such a manner as to not affect the verification of the code.

The weak points of SOAR were more related to issues in accounting for certain parameters in the same method that NWMO accounted for them in SYVAC3-CC4. These differences resulted in

alterations between the development of SOAR and SYVAC3-CC4 to represent the NWMO's Fifth Case Study.

SOAR allowed for only a simple waste package configuration. In SYVAC3-CC4, the waste was divided into five vaults with five individual pathways through the Cobourg Formation to a single pathway through the remaining natural geosphere pathways. It was not possible to represent the waste repository in this manner within SOAR. Within SOAR more flexibility within the waste package configuration would be beneficial to allow for more complex arrangements.

The NWMO considered 37 radionuclides within the SYVAC3-CC4 model. Investigation of the SYVAC3-CC4 results showed that I-129 was the major contributor (99.5%) with approximately equal contributions through food and water ingestion. SOAR only considers 16 radionuclides within the model, one of which is I-129. The absence of the other radionuclides used by NWMO did not affect the results in SOAR. However, the inclusion of additional radionuclides to the SOAR model would be beneficial even though the impact observed in this case was minimal.

Within SOAR, the only exposure pathway considered was ingestion of water. The SYVAC3-CC4 model considered other pathways such as food ingestion and air inhalation amongst others. The main contributor for the Reference Case of the Fifth Case Study as predicted by SYVAC3-CC4 was I-129 through exposure via almost equal contributions from water and food ingestion. The SOAR model would benefit from a more comprehensive biosphere model that considers other exposure pathways other than water ingestion.

Within SOAR the release of contaminants from the waste repository was represented through a Source element. Within this Source element, the bound waste form was released through a degradation rate. Within SYVAC3-CC4, the release of the bound waste form was established through a more complex dissolution model. It was not possible to represent the release in this manner within SOAR.

Overall, the SOAR model is a robust assessment tool that is flexible and applicable to a variety of disposal options. The model was coded in GoldSim using Contaminant Transport module elements providing more confidence in the model. Even with the aforementioned differences between the SOAR and SYVAC3-CC4 model development, the results from SOAR agreed well with those from SYVAC3-CC4.

6.3 SYVAC3-CC4 Highlights

The SYVAC3-CC4 model was developed by the NWMO and the theory is presented in NWMO (2012). The verification and validation of the model is presented by Garisto and Gobien (2013). Whereas the SOAR model was developed in a more flexible manner to make predictions for various disposal options, the SYVAC3-CC4 model was developed for the Fifth Case Study Scenario.

One key feature of the SYVAC3-CC4 model is that it allows for multiple sector repositories, as was observed in modelling the Fifth Case Study, in that the repository was divided into five waste vaults. The model also contains a more complex biosphere model for calculating the total dose rate. The model calculates field concentrations, well water concentrations and assumes discharge to a surface water body. As a result the dose to a self-sufficient human household was calculated by the model considering such pathways as ingestion of well water, locally grown crops and food animals amongst others. The SYVAC3-CC4 model accounts for release of the bound form through the dissolution model used in the Fifth Case Study.

6.4 Summary of SOAR as applied to Fifth Case Study

The SOAR model was parameterized and altered to provide predictions for the Fifth Case Study and to compare against the results that the NWMO conducted using the SYVAC3-CC4 model. The SOAR model used the same parameters and accounted for the development in the same manner. The differences in SOAR, as previously mentioned, were the number of radionuclides considered, the exposure pathways, the waste package configuration and the release of the bound waste form.

The waste repository within SOAR was represented as a single unit with one pathway through the Near Field and through the Cobourg Formation and remaining formations. However, in SYVAC3-CC4, the repository was divided into five waste vaults with five pathways through the Near Field and Cobourg Formation. Subsequently, a single pathway was used to model the transport through the remaining formations. Due to these differences, the releases from waste package, Near Field and from the Cobourg Formation between the two models varied. However, releases further along the natural geosphere pathway, where both were represented by a single pathway, compared well.

The dominant contributor as predicted by SYVAC3-CC4 was I-129 through ingestion of water and ingestion of food. These two exposure pathways had approximately equal contributions to the total dose rate. Therefore, the absence of ingestion of food in the dose calculation would decrease the SOAR predicted total dose rate.

The release of the bound waste form in SYVAC3-CC4 was defined through a dissolution model that had many parameters, eight of which were defined through a PDF for the probabilistic model. The model had dissolution rates that declined over time. In the SOAR model, the release of the bound waste form could not be through this dissolution model and was through a degradation rate instead. Degradation rates were obtained at different times from the dissolution model using deterministic parameters, which ranged from 10^{-4} 1/yr at early times to 10^{-8} 1/yr at later times. The NWMO scenario stated that it would take 10,000 years for sufficient water to be available to provide a transport pathway. To model this within SOAR, the package breach was set to 10,000 years. However, the SOAR model does not consider any degradation prior to package breach, which essentially neglects degradation rates greater than 10^{-6} 1/yr. Therefore, if the degradation rate was directly set within SOAR as declining over time, only the degradation rates post 10,000 years were used resulting in a low predicted release. It was determined that

constant degradation rates in the 10^{-4} 1/yr and 10^{-5} 1/yr used throughout the simulation time compared well with the deterministic results from SYVAC3-CC4. Another SOAR run was conducted with a lower constant degradation rate of 10^{-7} 1/yr which resulted in lower predicted total dose rate.

Recalling these differences, deterministic runs were conducted using the SOAR model. The releases to the waste package and Near Field as predicted by SOAR and SYVAC3-CC4 were similar and on the same order of magnitude for I-129 and Cs-135. The releases of U-234 and U-238 as predicted by SOAR were higher than those predicted by SYVAC3-CC4.

The releases in the Far Field were compared between both models. The release of Cs-135 from the top of the Cobourg Formation as predicted by SOAR occurred later than that predicted by SYVAC3-CC4. However, since Cs-135 is a weakly sorbing radionuclide, neither model showed any release of Cs-135 from the remaining geological formations. The release of I-129 from the top of the Cobourg Formation was similar between the two models. The release occurred slightly later as predicted by SOAR however both increased to a similar order of magnitude and then declined over time. The releases of I-129 from the top of Georgian Bay and to the biosphere were similar between both the SOAR and SYVAC3-CC4 model results.

Investigation of time of maximum release and time of 0.1% maximum release of I-129 as predicted by both SOAR and SYVAC3-CC4 models showed that SYVAC3-CC4 predicted earlier release from the Cobourg Formation. However, as the models progress through the other geological units, the times compare well between the two models.

The total dose rates of the Reference Case of NWMO's Fifth Case Study were compared between SOAR and SYVAC3-CC4. The total dose rates as predicted by SYVAC3-CC4 and SOAR compared well. The SYVAC3-CC4 showed an initial release of 10^{-12} Sv/yr at 1,000,000 years, whereas SOAR was later at 2,980,000 years. For both models, the total dose rate increased and had not reached a maximum at 10,000,000 years. The predicted maximum total dose rates were 2×10^{-9} Sv/yr and 5×10^{-10} Sv/yr, for SYVAC3-CC4 and SOAR respectively. SYVAC3-CC4 had I-129 as a major contributor through both ingestion of food and water. SOAR also had I-129 as the major contributor however the only exposure pathway was ingestion of water and therefore was expected to have a lower predicted total dose rate. Considering the difference in exposure pathways these total dose rates compare well.

Sensitivity analyses were conducted to determine how the different parameters affected the predicted total dose rate. The SOAR model was most sensitive to the diffusivity and increased to the highest total dose of 10^{-8} Sv/yr. The SYVAC3-CC4 model results also showed that increasing the diffusivity resulted in a large impact on the total dose rate and was the only scenario in which the total dose rate exceeded the threshold level prior to one million years. Both models predict that the total dose rate remains below the acceptance criterion at all times.

Probabilistic modelling was conducted using the Monte Carlo method in SOAR, similar to that conducted by NWMO with SYVAC3-CC4. The probabilistic modelling conducted by NWMO used 120,000 Monte Carlo simulations with random sampling. Within the SOAR probabilistic modelling the Monte Carlo simulations were conducted using Latin Hypercube sampling. This method ensures that all areas of the PDF were sampled and therefore required fewer Monte Carlo

simulations. The PDFs as described in NWMO's reports were inputted to SOAR. Two probabilistic modelling scenarios were investigated, one with 40,000 iterations and one with 60,000 iterations. These two scenarios were compared to ensure little to no difference due to smaller number of Monte Carlo iterations. It was found that the results generated by SOAR for these two scenarios were similar and therefore the run with 60,000 iterations was deemed satisfactory for the remaining discussion.

The NWMO used the dissolution model with the parameters defined by PDFs in the SYVAC3-CC4 model. This representation within SOAR was not possible and therefore was defined by a loguniform PDF with limits defined as the maximum and minimum of the calculated degradation rate. Within the Monte Carlo simulations a value of the degradation rate was chosen from the PDF and remained constant throughout the simulation. Simulations conducted with lower degradation rates would result in lower total dose rates. This difference in how the bound waste form was released within the two models is one reason why the SOAR predicted results were below those from SYVAC3-CC4.

The probabilistic modelling conducted by NWMO using SYVAC3-CC4 resulted in an average of the maximum total dose equal to 1.55×10^{-8} Sv/yr and that from SOAR equal to 7.2×10^{-10} Sv/yr. The overall percentile bands generated from SOAR were also below those from SYVAC3-CC4. The most likely difference in the probabilistic results was due to how the degradation rate was incorporated in the probabilistic modelling and due to the consideration of water ingestion as the only exposure pathway. Investigation of the maximums generated by both models showed the Greatest Result from SOAR to be 6.2×10^{-8} Sv/yr, which was approximately half that of the 99th percentile from SYVAC3-CC4, which would be due to the difference in exposure pathways considered.

Despite the differences mentioned above, overall the results between the two models compare well. In all cases considered by both models, none exceeded the acceptance criterion at any time.

6.5 Future Work/Recommendations

The work performed for this has shown that the SOAR model is a viable option for use in assessing different disposal options. Some future work could be conducted to further establish SOAR as related to the Fifth Case Study.

To provide further confidence in the SOAR model, a verification exercise could be completed. This verification would include establishing simple scenarios of the model with known analytical or semi-analytical solutions and comparing the results.

SOAR would benefit from the addition of further exposure pathways within the model. Currently the SOAR model only considers exposure through drinking water in the biosphere component. The NWMO analysis showed that food ingestion was also another dominant

pathway. Modifying the biosphere component within SOAR to include exposure through food ingestion and other exposure pathways would be beneficial.

A main difference in the development of the Fifth Case Study in SOAR as compared to SYVAC3-CC4 was the method by which the bound waste form was released. Further investigation into the SOAR model to determine if the dissolution model used within SYVAC3-CC4 could in some manner be incorporated. If the bound waste form release must be incorporated through the degradation rate in SOAR, then further investigation into the distribution type applied to the probabilistic modelling should be conducted to ascertain if better results can be obtained in relation to the SYVAC3-CC4 results. One possibility may be to maintain the PDF as log uniform but alter the bounds to 10^{-4} 1/yr and 10^{-5} 1/yr.

The SOAR model in the current version only considers 16 radionuclides. In the NWMO's Fifth Case Study I-129 was the dominant element contributing to total dose rate in both the SOAR and SYVAC3-CC4 model. Therefore, the absence of other elements was not thought to affect the Fifth Case Study results. However, addition of further radionuclides in the model would be beneficial in terms of assessing other disposal options. Adding in different radionuclides is possible within SOAR ensuring that this addition is throughout the entire model.

7.0 References

AMEC 2012. ConnectFlow Release 10.2, Technical Summary Document. Didcot, UK: AMEC. AMEC report AMEC/ENV/CONNECTFLOW/15. 24 p.

Andra. 2005. Dossier 2005 Granite Tome Safety analysis of a geological repository, December 2005.

Avila, R., P-A Ekström and P-G Ăstrand. 2010. Landscape dose conversion factors used in the safety assessment SR-Site. TR-10-06.

Bosson, E., M. Sassner, U. Sabel, and L-G Gustafsson. 2010. Modelling of present and future hydrology and solute transport at Forsmark. SR-Site Biosphere. SKB R-10-02, Svensk Kärnbränslehantering AB.

COMSOL, 2012. COMSOL Multiphysics, version 4.3a. Burlington, MA: COMSOL Inc.

Ekström, P-A. 2011. Pandora – a simulation tool for safety assessments. Technical description and user's guide. SR-Site Biosphere. SKB R-11-01, Svensk Kärnbränslehantering AB.

Garisto, F. and M. Gobien. 2013. SYVAC3-CC4 Verification and Validation Summary. Nuclear Waste Management Organization Report NWMO TR-2013-14.

Graham, D.N. and M.B. Butts. 2005. Flexible, integrated watershed modelling with MIKE SHE. In Singh, V.P and D.K Frevert. Watershed models. Boca Raton: CRC Press, 235-272.

GoldSim, 2010. GoldSim contaminant transport manual: http://c0046032.cdn.cloudfiles.rackspacecloud.com/Contaminant_Transport.pdf. Accessed on 27.9.2013

Holmén, J.G. 1992. A three-dimensional finite difference model for calculation of flow in the saturated zone. Department of quaternary geology, Uppsala University, Uppsala, Sweden, ISBN 91-7376-119-2, ISSN 0348-2979.

Holocher, J., G. Mayer, R. Namar, P. Siegel and N. Hubschwerlen. 2008. VPAC – a numerical model for groundwater flow and radionuclide transport. Nagra Working Report NAB 08-05. Nagra, Wettingen, Switzerland.

Joyce, S., D. Applegate, L. Hartley, J. Hoek, D. Swan, N. Marsic and S. Follin. 2010. Groundwater flow modelling of periods with temperate climate conditions – Forsmark. SKB R-09-20, Svensk Kärnbränslehantering AB.

Kärnbränslehantering AB. 2011a. Long-term safety for the final repository for spent nuclear fuel at Forsmark. Main report of the SR-Site project. TR-11-01 Volume I.

Kärnbränslehantering AB. 2011b. Long-term safety for the final repository for spent nuclear fuel at Forsmark. Main report of the SR-Site project. TR-11-01 Volume II.

Kärnbränslehantering AB. 2011c. Long-term safety for the final repository for spent nuclear fuel at Forsmark. Main report of the SR-Site project. TR-11-01 Volume III.

Löfman, J., Keto, V. & Mészáros, F. 2007. FEFTRA(TM). Verification. Espoo, Finland: Technical Research Centre of Finland (VTT). VTT Tiedotteita - Research Notes 2385. 103 p. + app. 4 p. ISBN 978-951-38-6919-9, 978-951-38-6920-5.

Markley, C., O. Pensado, J-P. Gwo, J. Winterle, T. Ahn, R. Benke, T. Cao, H. Gonzalez, A. Gray, X He, R. Janetzke, H. Jung, G. Oerson, P. Shukla, T. Sippel, S Stothoff and L. Tipton, 2011. SOAR: A Model for Scoping of Options and Analyzing Risk Version 1.0 User Guide.

Nagra. 2013. Biosphere Modelling for C-14: Description of the Nagra Model. Nagra Working Report NAB 12-26. Nagra, Wettingen, Switzerland.

Nagra. 2014. Provisional Safety Analyses for SGT Stage 2. Models, Codes and General Modelling Approach. Technical Report 14-09.

NWMO. 2012. SYVAC3-CC4 Theory, version SCC409. NWMO TR-2012-22.

NWMO. 2013a. Adaptive Phased Management. Postclosure Safety Assessment of a Used Fuel Repository in Sedimentary Rock. Pre-Project Report. NWMO TR-2013-07.

NWMO. 2013b. Fifth Case Study: References, Data and Codes. NWMO TR-2013-05.

Painter, S. and J. Mancillas. 2013. MARFA Users Manual: Migration Analysis of Radionuclides in the Far Field. Posiva Oy, Eurajoki, Finland. Posiva Working Report 2013-01.

POSIVA. 2012. Safety case for the disposal of spent nuclear fuel at Olkiluoto - Surface and near-surface hydrological modelling in the biosphere assessment BSA-2012. Eurajoki, Finland: Posiva Oy. POSIVA 2012-30.

POSIVA. 2013. Safety case for the disposal of spent nuclear fuel at Olkiluoto – Models and Data for the Repository System 2012. POSIVA 2013-01

Robinson, P.C. 2013. STMAN: User Guide and Theoretical Background for Version 5.7. Nagra Working Report NAB 08-46. Nagra, Wettingen, Switzerland.

Robinson, P.C. and C. Watson. 2013. PICNIC-TD: User Guide for Version 1.4. Nagra Working Report NAB 13-21. Nagra, Wettingen, Switzerland.

Svensson, U. and S. Follin. 2010. Groundwater flow modelling of the excavation and operation phases – SR-Site Forsmark. SKB R-09-19, Svensk Kärnbränslehantering AB.

Svensson, U., M. Ferry and H-O Kuylenstierna. 2010. DarcyTools version 3.4 – Concepts, methods and equations. SKB R-07-38, Svensk Kärnbränslehantering AB.

Therrien, R., R.G. McLaren, E.A. Sudicky, S.M. Panday, and V. Guvanasen. 2010. FRAC3DVS_OPG: a three-dimensional numerical model describing subsurface flow and solute transport. User's Guide. Groundwater Simulations Group, University of Waterloo, Ontario, Canada.

US NRC and CNWRA. August 2011. SOAR: A MODEL FOR SCOPING OF OPTIONS AND ANALYZING RISK VERSION 1.0 USER GUIDE

Vidstrand, P., S. Follin, N. Zugec. 2010. Groundwater flow modelling of periods with periglacial and glacial climate conditions – Forsmark. SKB R-09-21, Svensk Kärnbränslehantering AB.

Walke, R. and S. Keesmann. 2013. Nagra's Biosphere Assessment Code SwiBAC 1.2: Model Definition. Nagra Working Report NAB 12-27. Nagra, Wettingen, Switzerland.

Wersin, P., Kiczka, M. & Rosch, D. 2013a. Safety case for the disposal of spent nuclear fuel at Olkiluoto: Radionuclide solubility limits and migration parameters for the canister and the buffer. Eurajoki, Finland: Posiva Oy. POSIVA 2012-39. ISBN 978-951-652-219-0.

Wersin, P., Kiczka, M., Rosch, D., Ochs, M. & Trudel, D. 2013b. Safety case for the disposal of spent nuclear fuel at Olkiluoto: Radionuclide solubility limits and migration parameters for the backfill. Eurajoki, Finland: Posiva Oy. POSIVA 2012-40. ISBN 978-951-652-220-6.

World Nuclear Association. 2013. Public comment on French waste disposal. www.world-nuclear-news.org/wr_public_comment_on_french_waste_disposal_16051311.html

World Nuclear Association. 2014a. Nuclear Power in Canada. www.world-nuclear.org/Info/Country-Profiles/Countries-A-F/Canada--Nuclear-Power/

World Nuclear Association. 2014b. Nuclear Power in Finland. www.world-nuclear.org/Info/Country-Profiles/Countries-A-F/Finland

World Nuclear Association. 2015. Nuclear Power in Switzerland. www.world-nuclear.org/Info/Country-Profiles/Countries-O-S/Switzerland.

Appendix A - Numerical Code Summary

Table A.1 – Numerical codes used by SKB to model and predict groundwater flow, transport and biosphere dose.

Code	Description	Reference	Commercially Available (Y/N)
DarcyTools	Modelling groundwater flow. Can generate a discrete fracture network (DFN) that is then represented as an equivalent porous medium (ECPM)	- SKB - Michel Ferry, R & D Consulting (MFRDC) - Computer-aided Fluid Engineering AB (CFE AB) Svensson et al., 2010	N
GEHYCO	Module in DarcyTools that translates DFN into ECPM		N
ConnectFlow	Groundwater flow and transport modelling, including ECPM, DFN or combined	AMEC, 2012	Y
MIKE SHE	Integrated catchment modelling	MIKE by DHI Graham and Butts, 2005	Y
COMSOL Multiphysics	Used within the detailed near-field flow modelling, i.e. to study the flow inside the repository.	COMSOL, 2012 (COMSOL.com)	Y
PHREEQC	Fully coupled chemical mixing and reaction calculations for aqueous geochemical reactions	USGS (described in Wersin et al., 2013 a, b)	Y
Ecolego	Modelling of radionuclides in nearfield, geosphere and biosphere	www.ecolego.facilia.se	Y
Pandora	Biosphere model for safety assessment of HLW repositories.	Facilia AB (described in Ekström 2011)	N

Table A.2 – Numerical codes used by Posiva Oy to model and predict groundwater flow, transport and biosphere dose.

Code	Description	Reference	Commercially Available (Y/N)
GoldSim	Used for all near-field release and transport calculations. Also used for stochastic simulations.	GoldSim, 2010	Y
MARFA	Used to analyse geosphere retention and transport	Painter and Mancillas, 2013	N
ConnectFlow	Groundwater flow and transport modelling, including ECPM, DFN or combined	AMEC, 2012	Y
FEFTRA-FEM	Groundwater flow finite element modelling that applies the ECPM approach to model transient and density-driven flow and heat transfer.	Löfman et al., 2007	
Ecolego	Modelling of radionuclides in nearfield, geosphere and biosphere	www.ecolego.facilia.se	Y
SHYD	Surface and near-surface hydrological model	Posiva, 2012	N
Pandora	Biosphere model for safety assessment of high level waste repositories.	Facilia AB (described in Ekström 2011)	N
PHREEQC	Fully coupled chemical mixing and reaction calculations for aqueous geochemical reactions	USGS (described in Wersin et al., 2013 a, b)	Y

Table A.3 – Numerical codes used by Andra to model and predict groundwater flow, transport and biosphere dose.

Code	Description	Reference	Commercially Available (Y/N)
ConnectFlow	Groundwater flow and transport modelling, including ECPM, DFN or combined	AMEC, 2012	Y
GEOAN	3D Finite difference flow model	Holmén, 1992	N
PORFLOW	Flow and transport code accounting for heat, salinity and phase changes	www.acricfd.com	Y
FracMan and MAFIC	Hydrologic analysis of flow and transport in DFN	www.fracman.com www.fracturedreservoirs.com/SolutionsMM.asp	N
PROPER	Modelling segments in engineered barrier		N
GoldSim	Used for transport modelling	GoldSim, 2010	Y
PathPipe	Used for conversion of network of tubes for transport		N

Table A.4 – Numerical codes used by Nagra to model and predict groundwater flow, transport and biosphere dose.

Code	Description	Reference	Commercially Available (Y/N)
SwiBAC 1.2	Biosphere Model that evaluates the distribution of radionuclides	Walke and Keesmann, 2013	N
NC14M v3	Biosphere Model for C-14. (Newly developed code)	Nagra, 2013	N
PICNIC-TD 1.4	Geosphere Model that models transport of radionuclides along 1D transport path	Robinson and Watson, 2013	N
VPAC 1.1	Versatile Performance Assessment Code that simulated groundwater flow and radionuclide transport in 2D or 3D porous medium.	Holocher et al., 2008	N
STMAN 5.9	A family of 3 codes that model release of radionuclides from different waste forms and subsequent 1D radial transport through engineered barriers.	Robinson, 2013	N

Appendix B – SYVAC3-CC4 GEONET Diagram NWMO (2013b)